Supporting Information:

Supporting Information Corrected January 8, 2015

"Proxy-Phenotype Method Identifies Common Genetic Variants Associated with Cognitive Performance"

This document provides further details about materials, methods and additional analyses to accompany the research report "Proxy-Phenotype Method Identifies Common Genetic Variants Associated with Cognitive Performance."

Contents

Materials and Methods

1. Meta-analyses and selection of education-associated candidate SNPs

The first stage of our two-stage procedure consisted of conducting a GWAS meta-analysis on years of schooling, using the same analysis plan as Rietveld et al. (1) for the years-of-schooling variable (referred to in Rietveld et al. as "EduYears") and the same cohorts, except omitting the individuals that we include in the Cognitive Performance Sample (all individuals in the cohorts ALSPAC, ERF, LBC1921, LBC1936, and MCTFR, and subsamples of the cohorts QIMR and STR) described in section "Cognitive Performance Sample" below. Thus, compared with the meta-analysis sample size of N = 126,559 in Rietveld et al., the sample size for our meta-analysis of years of schooling is N = 106,736. We obtained permission to use these data under the SSGAC data sharing policy (http://ssgac.org/documents/DatasharingpolicySSGAC.pdf). Our meta-analysis found 927 single-nucleotide polymorphisms (SNPs) meeting the inclusion threshold of p-value $< 10^{-5}$, which was chosen based on power calculations prior to conducting our study (see section 15.E of this SI Appendix). We pruned this set of SNPs for linkage disequilibrium using the clumping command in PLINK and the HapMap II CEU (r23) data. The physical threshold for clumping was 1000 kB, and the R^2 threshold for clumping was 0.01. This pruning procedure resulted in a set of 69 approximately independent SNPs, which is our set of "education-associated SNPs." These are listed in Supplementary Table S4.

We note that the education-associated SNPs (Table S4) are independent from *APOE*, a gene that has previously been associated with cognitive decline in older individuals (2–6). The *APOE* gene is located on chromosome 19, while none of our education-associated SNPs are located on that chromosome; thus, *APOE* status is inherited independently from all of our education-associated SNPs.

For the polygenic-score analyses in the Health and Retirement Study (HRS) described in section 14 below, we conducted the same meta-analysis, except that we additionally exclude the HRS cohort. The sample size of this meta-analysis is N = 98,110.

2. Cognitive Performance Sample

The Cognitive Performance Sample that we use in the second stage of our two-stage procedure consists of CHIC (the Childhood Intelligence Consortium (7)) and five additionally recruited GWA samples. CHIC consists of six studies: the Avon Longitudinal Study of Parents and Children (ALSPAC, N = 5,517), the Lothian Birth Cohorts of 1921 and 1936 (LBC1921, N = 464; LBC1936, N = 947), the Brisbane Adolescent Twin Study subsample of Queensland Institute of Medical Research (QIMR, N = 1,752), the Western Australian Pregnancy Cohort Study (Raine, N = 936), and the Twins Early Development Study (TEDS, N = 2,825). The five additional samples are the Erasmus Rucphen Family Study (ERF, N = 1,076), the Generation R Study (GenR, N = 3,701), the Harvard/Union Study (HU, N = 389), the Minnesota Center for Twin and Family Research Study (MCTFR, N = 3,367) and the Swedish Twin Registry Study (STR, N = 3,215). This brings the total sample size to 24,189 individuals from 11 studies.

In most of these cohorts, cognitive performance was elicited before participants completed schooling (for details, see section 3). Exceptions are ERF and HU, which constitute ≈6% of the Stage 2 sample. In STR, cognitive performance was measured among males during military conscription at the age of 18. Some of these individuals may have also already completed schooling. However, some of the individuals in ERF and HU may have still been in school when cognitive performance was measured.

Participating studies were recruited from January 2013 – March 2013, and summary results were uploaded before the end of April 2013. All participants provided written informed consent, and the studies were performed in accordance with the respective Local Research Ethics Committees or Institutional Review Boards. The descriptive statistics and study designs are provided in Table S1.

To provide additional data for examining the within-family explanatory power of the polygenic score (see section 13), an additional cohort was recruited: Generation Scotland (GS). The sample consists of 1,081 siblings.

3. Cognitive performance measures

Measures of cognitive performance for the studies that are part of CHIC, and the cognitive performance measures for the other five GWA studies, are as follows:

ALSPAC: Cognitive performance at the age of 8 years was measured with the Wechsler Intelligence Scale for Children (WISC-III). A short version of the test consisting of alternate items only (except the Coding task) was applied by trained psychologists. Verbal (information, similarities, arithmetic, vocabulary, comprehension) and performance (picture completion, coding, picture arrangement, block design, object assembly) subscales were administered. Each subtest was age-scaled according to population norms, and a summary score for total cognitive performance was derived. We calculated the first two principal components of the genome-wide data using Eigenstrat. As inputs to the analysis reported here, we generated sex- and principal-component-adjusted Z-standardized cognitive performance scores for unrelated ALSPAC children for whom total cognitive performance and genome-wide data were available. To do so, cognitive performance scores within a range of ±4 SD relative to the total ALSPAC sample were regressed on sex and the principal components. The residuals were Z-transformed. Using the resulting data, genome-wide association analysis was conducted.

ERF: Scores on the following cognitive tests were used to create the fluid-type general cognitive ability factor: Stroop 3 (time needed to complete Stroop color-word card), TMT-B (time needed to complete Trailmaking Test part B), phonemic fluency (with D, A, T, number of words mentioned beginning with each letter, one minute each, sum of the three trials), 15-word Auditory Verbal Learning Test (AVLT-sum) (sum of immediate (5 iterations) and delayed recall (once)), WAIS block design test (*n* of correct answers, Wechsler scoring). The tests, the method of application, and key references are described in (8). Principal components analysis was applied to these 5 tests. The first unrotated principal component, which accounted for 50.1% of the total test variance, is the measure of *g*. The mean age at reporting is 33.2 (SD = 7.1).

GenR: The phenotype has been constructed using assessments of the Snijders-Oomen Non-Verbal Intelligence Test (SON-R 2.5–7). The overall cognitive performance score was calculated based on two subtests: Mosaics (performance) and Categories (reasoning). The mean age at reporting is 6.17 (SD = 0.50).

GS: Scores on the following cognitive ability tests were used to create the general cognitive ability factor: Wechsler Digit Symbol Substitution Task, Wechsler Logical Memory Test, Verbal Fluency (sum of letters C, F, and L), and the Mill Hill Vocabulary Scale. The tests, the method of application and key references have been described in detail elsewhere (9). The number of siblings used in the analysis was 1081 (mean age 41.1 (SD 11.0), range 18-77). The Pearson correlations (*r*s) among the 4 tests ranged from 0.07 to 0.40 (mean 0.22). Principal components analysis was applied to these 4 tests. The first unrotated principal component (FUPC) accounted for 42% of the total test variance. Loadings on the FUPC were as follows:

Wechsler Digit Symbol Substitution Task = 0.56, Wechsler Logical Memory Test = 0.63, Verbal Fluency = 0.71, Mill Hill Vocabulary Scale = 0.68.

HU: A composite score of several cognitive performance subtests was generated in the following way. A shortened version of Raven's Advanced Progressive Matrices (RAPM) (10); a 10-item vocabulary test; the Vocabulary, Similarities, and Arithmetic subtests of the Multidimensional Aptitude Battery II; and the number correct in a speeded version of the Shepard-Metzler Mental Rotation (SMMR) task were administered. RAPM, Arithmetic, and SMMR were standardized to have mean zero and variance one in the sample. The Vocabulary, Similarities, and separate 10-item vocabulary test were factor analyzed, and Bartlett's method was used to calculate a verbal factor score on the basis of the three observed scores. This verbal score was then standardized. The standardized verbal, RAPM, Arithmetic, and SMMR scores were added to form a raw composite, which was itself standardized separately for each sex. The composite IQ formed in this way showed a correlation of ~0.70 with self-reported SAT scores, which is quite good considering the restriction of range in SAT scores (a standard deviation only two-thirds of that observed in the total population of European-descent SAT examinees). The mean age at reporting is 25.48 (SD = 6.63).

LBC1921 and LBC1936: The measure of cognitive performance was the Moray House Test (MHT) No. 12. This is one of a series of tests of cognitive performance devised by Godfrey Thomson at the Moray House College, University of Edinburgh, from the late 1920s onwards. The MHT is a group test of cognitive performance with a time limit of 45 minutes. The test has 71 items and a maximum possible score of 76. It was also known as the "Verbal Test" because the items have a predominance of verbal reasoning. The test has a variety of items, as follows: following directions (14 items), same–opposites (11), word classification (10), analogies (8), practical items (6), reasoning (5), proverbs (4), arithmetic (4), spatial items (4), mixed sentences (3), cypher decoding (2), and other items (4). Mean age at reporting is 10.9 years (SD = 0.28).

MCTFR: Measurement of general cognitive ability in the Minnesota sample was based on an abbreviated form of the Wechsler Intelligence Scale for Children-Revised (WISC-R) for those 16 years or younger or Wechsler Adult Intelligence Scale-Revised (WAIS-R) for those older than 16 years. The short forms consisted of two Performance subtests (Block Design and Picture Arrangement) and two Verbal subtests (Information and Vocabulary), the scaled scores on which were prorated to determine Full-Scale IQ (FSIQ). FSIQ estimates from this short form have been shown to correlate greater than 0.90 with FSIQ from the complete test. The mean age at reporting is 14.2 (SD = 2.7).

QIMR: Cognitive performance was measured using a shortened version of the computerized Multi-dimensional Aptitude Battery (MAB), a general intelligence test similar to Wechsler Adult Intelligence Scale-Revised. The shortened MAB includes three verbal subtests (information, arithmetic, vocabulary) and two performance subtests (spatial, object assembly). Scaled scores for cognitive performance were computed in accordance with the manual.

Raine: Cognitive performance was estimated based on four cognitive tests carried out at approximately 10 years of age (Peabody Picture Vocabulary Test, Raven's Colored Progressive Matrices, Symbol Digits Modalities Test (SDMT) written score and SDMT oral score. The first principal component from the four cognitive measures was used for analyses.

STR: Men in the sample were matched to conscription data provided by the Military Archives of Sweden. Data on cognitive ability are available for most men in the sample born in 1936 or later. These men were required by law to participate in military conscription around the age of 18. They enlisted at a point in time when exemptions from military duty were rare and typically

only granted to men who could document a serious handicap that would make it impossible to complete training. For the men born after 1950, the military data have been digitalized. For men born 1936-1950, we manually retrieved the information from the Military Archives. The first test of cognitive ability used by the Swedish Military was implemented in 1944, and it has subsequently been revised and improved on a few occasions. (11) discusses the history of psychometric testing in the Swedish military and provides evidence that the measure of cognitive ability is a good measure of *g*. For men in the sample who did the military conscription before 1959, the cognitive ability test consisted of 5 subtests: logical, verbal, mathematical, spatial, and technical. The first subtest about logical ability was called "Instructions" and measured the ability to understand complicated instructions. The second subtest about verbal ability was called "Selection," and in these questions the subjects had to pick out one out of five words that differed from the four other words. The third subtest was called "Multiplication" and consisted of multiplying a two-digit number by a one-digit number. The fourth subtest was called "Levers." With the guidance of a graph depicting a system of levers, the subjects answered questions about the effect of a force applied to a specific point in the system. The final test was called "Technical comprehension," in which the subjects answered questions about technical problems with the guidance of graphs. In 1959 the cognitive ability test was revised, and men in the sample who did the military conscription in 1959 or later took this revised test. The logical and verbal ability subtests were kept. The mathematical subtest ("Multiplication") was dropped from the test. The spatial ability test ("Levers") was replaced by a test of spatial ability called "Composition," in which the subjects had to indicate which pieces fit with a specific figure. The technical ability test ("Technical comprehension") was revised (it was modernized). For both men who did the military conscription before and after 1959, we use data for the 4 subtests of logical, verbal, spatial, and technical ability (since subtests of these abilities were included at the military conscription both before and after 1959). We do not include the mathematical ability test since it was only given to subjects who did the military conscription in 1959 and later. At the military conscription, each subtest was given a raw score and a standardized 1-9 stanine score. The norm tables for the stanine scores were updated each year to ensure that there was no trend in the stanine scores over time. We use the stanine scores of the four subtests of logical, verbal, spatial and technical ability. We use the first principal component of these four stanine scores as the measure of cognitive performance.

TEDS: Individuals were tested at 12 years using two verbal and two nonverbal measures: WISC-III-PI Multiple Choice Information (General Knowledge) and Vocabulary Multiple Choice subtests (12), the WISC-III-UK Picture Completion (12) and Raven's Standard Progressive Matrices (13). Test scores were adjusted for age within each testing period, and the first principal component was derived.

Within each cohort the cognitive performance measure was adjusted for sex and age and standardized to have mean 0 and standard deviation 1.

4. Genotyping and imputation

All cohorts were genotyped using commercially available genotyping arrays. The study-specific details on genotype platform, genotype calling algorithm, imputation software, and imputation reference dataset are provided in Table S2.

5. Quality control

In CHIC extensive quality control has been performed at the meta-analysis stage (for details, see (7)). We followed CHIC's protocol and cleaned each GWA summary file from the five additionally recruited replication studies. First, the SNPs with a Minor Allele Frequency

(MAF) < 1%, imputation quality score < 40%, Hardy-Weinberg p-value < 10^{-6} and call rate < 0.95 were excluded. Quantile-Quantile plots of the cleaned summary files were visually inspected, and the genomic control (GC) inflation factor λ (14) was calculated for each cleaned summary file. The Quantile-Quantile plots (Supplementary Figure 1) did not reveal stratification problems. This is confirmed by the values of λ's, which are all close to 1. Second, following (7), we calculated the average effective sample size per cohort (as a function of the allele frequency and the standard error of the effect size from the association) and compared it with the actual sample size. We found that the average effective sample sizes were consistent with the reported sample sizes in all cohorts.

6. Association analysis

Each cohort was asked to follow a prespecified analysis plan (preregistered on the Open Science Framework website prior to conducting our study; see https://osf.io/z7fe2/). This plan requested from each study summary results of the ordinary least squares regression of the standardized measure of cognitive performance on the imputed SNPs. At least four principal components of the Identity-by-State (IBS) matrix (to control for subtle population stratification) were either added as covariates, or used in the standardization of the phenotype. Only individuals from recent Caucasian descent were included. Association software used by the studies is reported in Table S2.

7. Meta-analysis

The meta-analysis was performed with inverse-variance weighting using METAL (15). The necessary inputs from the study-specific GWA summary results were: SNP ID, coded allele (allele to which regression coefficient refers), non-coded allele, strand, beta (regression coefficient), standard error, p-value, and allele frequency for the coded allele.

8. Correction of effect sizes for winner's curse

The "winner's curse" refers to the fact that the estimated effect size for a SNP (and therefore the R^2 associated with the SNP) newly discovered to be statistically significant tends to be much higher than the unbiased effect size estimated subsequently in replication samples. It occurs because, although OLS gives an unbiased *unconditional* estimate of the true parameter value, the expected value of the estimate is biased away from zero conditional on the parameter meeting a threshold for statistical significance. This bias is more highly pronounced the more stringent the significance threshold (and therefore especially pronounced in GWAS because the significance threshold for "genome-wide significant" is especially stringent). In Subsection A, we walk through the (well-known) derivation of the analytic form for the expected value of the winner's curse. In Subsection B, we discuss several known methods for correcting for it. Subsection C contains a comparison of these methods in a simulation study of the current analysis of cognitive performance. We conclude in Subsection D by applying the winner's curse corrections to both Rietveld et al.'s (1) findings—a context where we can compare the winner's-curse-corrected estimates to the unbiased, replication-sample estimates—and to the findings from the current analysis of cognitive performance.

A. Derivation of the winner's curse

We derive the winner's curse for the simple case where outcome Y is truly related to a SNP's genotype $g \in \{0,1,2\}$ in accordance with the simple linear regression model:

$$Y = cons + \beta g + \varepsilon$$

where $\varepsilon \sim N(0,\sigma^2)$, and σ^2 and the SNP's MAF m are known. If the sample size n is large and if the SNP is in Hardy-Weinberg equilibrium, then the OLS estimate is drawn from the normal distribution $\hat{\beta} \mid \beta \sim N(\beta, v^2)$, where $\upsilon^2 \equiv \frac{\sigma^2}{2nm(1-m)}$ (and υ^2 is known because σ^2, m, and n are all known). Given statistical significance threshold α, the null hypothesis $\beta = 0$ is rejected if the test statistic, $\frac{\hat{\beta}}{\upsilon}$, falls within the $\left(1-\frac{\alpha}{2}\right)$ percentile right or left tail of this distribution:

$$\frac{\hat{\beta}}{\upsilon} > \Phi^{-1}\left(1-\frac{\alpha}{2}\right),$$

where Φ is the cdf of a standard normal distribution (that has corresponding pdf ϕ). Therefore, conditional on the SNP having been identified as statistically significant at size α, its coefficient $\hat{\beta}$ is distributed as a truncated standard normal distribution with the mass removed in a neighborhood of zero, with pdf:

$$(1) \qquad f(\hat{\beta} \mid \beta, sig_\alpha) = \left\{ \begin{array}{ll} \dfrac{\frac{1}{\upsilon}\phi\left(\frac{\hat{\beta}-\beta}{\upsilon}\right)}{1-[\Phi(T^+(\beta)) - \Phi(T^-(\beta))]} & if \left|\hat{\beta}\right| > \upsilon\Phi^{-1}\left(1-\frac{\alpha}{2}\right) \\ 0 & if \left|\hat{\beta}\right| \le \upsilon\Phi^{-1}\left(1-\frac{\alpha}{2}\right) \end{array} \right\},$$

where $T^+(\beta) \equiv \Phi^{-1}\left(1-\frac{\alpha}{2}\right) - \frac{\beta}{\upsilon}$ and $T^-(\beta) \equiv -\Phi^{-1}\left(1-\frac{\alpha}{2}\right) - \frac{\beta}{\upsilon}$. The mean of the distribution described by equation (1) is

$$(2) \qquad E(\hat{\beta} \mid \beta, sig_\alpha) = \beta + \upsilon \frac{\Phi(T^+(\beta)) - \Phi T^-(\beta)}{1-[\Phi(T^+(\beta)) - \Phi(T^-(\beta))]}.$$

The bias due to the winner's curse is the second term in equation (2). The numerator of this term signs the bias: if $\beta > 0$, then the bias is positive, while if $\beta < 0$, then it is negative. The bias therefore always pushes the estimate away from zero. In order to obtain a more accurate estimate of the SNP's effect size, it is necessary to apply a correction procedure that "shrinks" the OLS estimate toward zero. If α is smaller (that is, the significance threshold is more stringent), then the denominator of the bias term is smaller and hence the bias is larger in magnitude.

B. Correcting for the winner's curse

There are several methods that one might consider to correct for this bias. Here we briefly describe four: inverting the conditional expectation of the OLS estimator, maximum likelihood

estimation (MLE), Bayesian estimation, and empirical-Bayes estimation.

B.1. Inverting the conditional expectation of the OLS estimator

One approach is motivated by the seemingly straightforward idea of inverting the above conditional expectation equation (2) that is a function of the true parameter value:

$$E(\hat{\beta} \mid \beta, sig_{\alpha}) \equiv g(\beta) = \beta + \upsilon \frac{\Phi(T^{+}(\beta)) - \Phi(T^{-}(\beta))}{1 - [\Phi(T^{+}(\beta)) - \Phi(T^{-}(\beta))]}.$$

While $g(\beta)$ is not analytically invertible, it can be inverted numerically. However, $E(\hat{\beta} \mid \beta, sig_{\alpha})$ is not observed and so cannot be plugged into $g^{-1}(\cdot)$. The feasible version of this estimator must instead use the observed value $\hat{\beta}$. Unfortunately, though, the estimator $g^{-1}(\hat{\beta})$ is biased: that is, generically $E[g^{-1}(\hat{\beta}) \mid \beta, sig_{\alpha}] \neq \beta$. To see this, note that $g^{-1}[E(\hat{\beta} \mid \beta, sig_{\alpha})] = \beta$, and Jensen's inequality implies that $E[g^{-1}(\hat{\beta}) \mid \beta, sig_{\alpha}]$ is generically *not* equal to $g^{-1}[E(\hat{\beta} \mid \beta, sig_{\alpha})]$ since $g(\beta)$ is non-linear. Furthermore, it is difficult to assess the direction and amount of bias.

B.2. Maximum Likelihood Estimation

Some researchers have used MLE to correct for the winner's curse (16, 17). To estimate a MLE, we use the pdf of $\hat{\beta} \mid (\beta, sig_{\alpha})$, which is equation (1) above. Since we only have one observation of $\hat{\beta}$, the likelihood function in this case is simply equation (1). Taking the first-order condition with respect to β and rearranging terms, the ML estimator β_{MLE} is implicitly defined by the equation:

$$\hat{\beta} = \beta_{MLE} + \upsilon \frac{\Phi(T^{+}(\beta_{MLE})) - \Phi(T^{-}(\beta_{MLE}))}{1 - [\Phi(T^{+}(\beta_{MLE})) - \Phi(T^{-}(\beta_{MLE}))]}.$$

The right-hand side of this equation is identical to the right-hand side of equation (2) above. Therefore, the MLE is the same as the estimate obtained from inverting the conditional expectation of the OLS estimator, and thus the MLE will be biased in an identical manner. Via simulation, (16) shows that these methods will over-correct when β is large and under-correct when β is small.

We note a few observations about the bias correction implied by this estimator; similar points will hold for the Bayesian estimators that follow, but we make these observations here because they are particularly straightforward to see for the MLE estimator. First, when the estimated coefficient is large in magnitude, the bias correction is small; that is, the MLE-corrected estimate will be approximately equal to the uncorrected estimate. This can be seen in the above

formula: since $\lim_{|\beta|\to\infty} \phi(T^+(\beta)) - \phi(T^-(\beta)) = 0$ and $\lim_{|\beta|\to\infty} \Phi(T^+(\beta)) - \Phi(T^-(\beta)) = 0$, it follows that $\lim_{|\hat{\beta}|\to\infty} \beta_{MLE}(\hat{\beta}) = \hat{\beta}$. Intuitively, when the uncorrected estimate is large in magnitude, it is very likely to have been resulted from a true β that is large in magnitude and hence very likely that we would have observed a statistically significant estimate regardless of our sample realization; therefore, the fact that the observed estimate was statistically significant provides little additional information about the value of β.

Second and on the flipside, when the estimated coefficient is close to the significance threshold, the bias correction may be quite large. Intuitively, it is actually fairly likely that a barely statistically significant estimate resulted from a true β that is below the threshold.

B.3. Bayesian and Empirical-Bayes Estimation

Two alternative approaches are Bayesian and are closely related. We follow a derivation similar to (18), who adjust the winner's curse of the odds ratio in a binary setting. However, we consider a more general setting, correcting the underlying β parameters, which are defined over the real line and therefore require a different class of priors and posteriors (for a closely related approach, see (19)). For a normally-distributed prior $\beta \sim N(\mu, \tau^2)$, the posterior is given by the pdf

$$f(\beta \mid \hat{\beta}, sig_\alpha) = \frac{\dfrac{\phi\left(\left(\beta - \dfrac{\tau^2\hat{\beta} + \upsilon^2\mu}{\tau^2 + \upsilon^2}\right) / \sqrt{\dfrac{\tau^2\upsilon^2}{\tau^2 + \upsilon^2}}\right)}{1 - [\Phi(T^+(\beta)) - \Phi(T^-(\beta))]}}{\displaystyle\int_b \dfrac{\phi\left(\left(b - \dfrac{\tau^2\hat{\beta} + \upsilon^2\mu}{\tau^2 + \upsilon^2}\right) / \sqrt{\dfrac{\tau^2\upsilon^2}{\tau^2 + \upsilon^2}}\right)}{1 - [\Phi(T^+(b)) - \Phi(T^-(b))]} db}$$

The mean of this distribution is

$$E(\beta \mid \hat{\beta}, sig_\alpha) = \frac{E[g_1(X)]}{E[g_2(X)]}, \tag{3}$$

where $X \sim N\left(\dfrac{\tau^2\hat{\beta} + \upsilon^2\mu}{\tau^2 + \upsilon^2}, \dfrac{\tau^2\upsilon^2}{\tau^2 + \upsilon^2}\right)$, $g_1(x) = \dfrac{x}{1 - [\Phi(T^+(x)) - \Phi(T^-(x))]}$, and $g_2(x) = \dfrac{1}{1 - [\Phi(T^+(x)) - \Phi(T^-(x))]}$.

The right-hand side of equation (3) can be evaluated numerically by taking a set of *M* draws of the random variable *X*, $\{x_m\}$, and taking the ratio of the sample means of $\{g_1(x_m)\}$ and $\{g_2(x_m)\}$. In the implementations below, we use *M* = 10 million.

The Bayesian and empirical Bayes approaches are distinguished by the way that the parameters of the prior distributions, μ and τ^2, are chosen. The Bayesian method we consider is to assume an uninformative prior: $\tau \to \infty$ (and in this case, the choice of μ does not matter). Using this

method, equation (3) is evaluated using $X \sim N(\hat{\beta}, \upsilon^2)$. Similar to with the MLE correction, the Bayesian (and empirical Bayes) correction will be small when the uncorrected estimate is far from the significance threshold and large when it is close. Intuitively, when the observed estimate is large in magnitude, the probability that the true β that is below the threshold is negligible, so the bias correction has very little impact on the posterior mean.

In the empirical Bayes approach, the data are used to estimate appropriate values for μ and τ^2. To develop intuition, we first consider a method (simpler than the method we use) that would be appropriate if one had access to OLS estimates for a large random sample of SNPs (for example, from complete GWAS meta-analysis results), $s = 1,...,S$. Since for each SNP the choice of reference allele is arbitrary, the mean of the true effects across the *S* SNPs is zero: $\mu = 0$. Now, note that since $\hat{\beta}_s \mid \beta_s \sim N(\beta_s, \upsilon_s^2)$ and $\beta_s \sim N(0, \tau^2)$, it follows that $\hat{\beta}_s \sim N(0, \tau^2 + \upsilon_s^2)$. Therefore, τ^2 can be estimated as the variance of all of the $\hat{\beta}_s$ estimates minus the mean of the square of their estimated standard errors:

$$\hat{\tau}^2 = \frac{1}{S-1}\sum_{s=1}^{S}\hat{\beta}_s^2 - \overline{\hat{\upsilon}_s^2}.$$

We do not use this approach because assuming $\mu = 0$ would be extremely conservative in our context, where the SNPs we study are not a random sample—rather, they were selected as candidates for cognitive performance because they had strong impacts in a previous GWAS on educational attainment.

The empirical-Bayes approach that we employ exploits information available from the GWAS results on educational attainment to inform our choice of μ. Specifically, we set μ equal to the magnitude of a SNP's effect that would be needed in order for the SNP to explain the same fraction of variance in cognitive performance as it explains in educational attainment. To be more precise, let $\hat{\beta}_{educ,s}$ be the estimated effect of SNP *s* on years of schooling taken from Rietveld et al. (2013). The fraction of variance in years of schooling explained by the SNP can be calculated as $R^2_{educ,s} = \frac{2m_s(1-m_s)\hat{\beta}_{educ,s}}{\sigma^2_{educ}}$, where m_s is the MAF of SNP *s* and σ^2_{educ} is the variance of years of schooling. We can calculate that SNP *s* would have the same R^2 for cognitive performance if $\beta_{cog,s} = \frac{\sigma_{cog}}{\sigma_{educ}}\hat{\beta}_{educ,s}$, where $\beta_{cog,s}$ is the putative effect of SNP *s* on cognitive performance, and σ^2_{cog} is the variance of cognitive performance. Thus, we set the mean of our prior for the effect of the SNP on cognitive performance as $\mu = \frac{\sigma_{cog}}{\sigma_{educ}}\hat{\beta}_{educ,s}$.

While not as conservative as setting a prior of zero, this prior mean is still likely to be conservative (i.e., too close to zero) to the extent that a SNP's effect on educational attainment works through a more direct effect on the mediating phenotype of cognitive performance; in that case, the SNP would be expected to explain a *larger* fraction of variance in cognitive performance than in years of schooling. We calculate the prior parameter τ^2 similarly as in the mean-zero empirical-Bayes procedure above (but rather than estimating the variance about zero, we estimate the variance about the mean of the prior):

$$\hat{\tau}^2 = \frac{1}{S-1}\sum_{s=1}^{S}(\hat{\beta}_s - \mu)^2 - \overline{\hat{\upsilon}_s^2}.$$

(18) prove that there is no winner's curse correction that is unbiased for all values of β, but an advantage of a Bayesian approach is that the estimates will be on average unbiased. As an intuitive rationale for a choice for a prior, note that the Bayesian method with a diffuse prior will be unbiased on average across all real-valued effect sizes, while the empirical Bayes method is unbiased across a weighted average of effect sizes with the weights given by the prior. Thus, the empirical-Bayes-corrected estimate should be less biased if the true effect size is local to the mean of the selected prior but more biased if the true value is distant from the mean.

As a final note on implementation: all of the above approaches require a value for $\upsilon^2 \equiv \frac{\sigma^2}{2nm(1-m)}$, which we have assumed is known, but it is in fact not known because *m* and σ^2 are not known. For *m*, we just use the empirical frequency of the minor allele in our data. We estimate σ^2 iteratively, starting with the naive estimate of β, $b_0 = \hat{\beta}$. Then we calculate $\sigma_0^2 = \mathrm{var}(Y) - 2b_0^2 m(1-m)$. Using σ_0^2, we estimate $b_1(\sigma_0)$. We iterate this procedure until it converges, giving us estimates of both σ^2 and $\hat{\beta}$. (In the implementations below, we ran the algorithm for ten iterations, but convergence was virtually always apparent after only two.)

C. Simulation Study

We now examine and compare the MLE and Bayesian methods via simulation. To roughly match the analysis of the top three SNP associations with cognitive performance from the main text, we set the sample size n = 25,000, MAF m = 0.4734, dependent-variable variance $\sigma^2 = 1$ (that is, the dependent variable is standardized), and significance threshold α = 0.05/69 (the conventional significance threshold after Bonferroni correction for analysis of 69 SNPs). For each fixed true value of β, in each iteration *i* of the simulation, we draw an *n*-length genotype vector g_i, and we draw an *n*-length error $\varepsilon_i \sim N(0, \sigma^2 I_n)$. In each iteration, we estimate the naïve $\hat{\beta}_i$, which we keep if it passes the significance threshold and ignore otherwise. If we keep $\hat{\beta}_i$, we then estimate $\tilde{\beta}_{MLE,i}$ using maximum likelihood and $\tilde{\beta}_{Bayes,i}$ using the diffuse-prior Bayesian method described above. (We do not perform simulations for an empirical Bayes approach since it is not clear what the right choice should be for an empirical prior for the simulation.) We perform 1,000,000 replications of this simulation.

Supplementary Figure 3 below shows the winner's-curse corrected estimate as a function of the true β, grouped in bins of the true β that are 0.002 units wide. For each estimate, the light dotted lines in the corresponding color show the interval that contains 95% of the estimates. The figure suggests that there can be significant bias from the winner's curse in this parameterization when the true β is less than 0.04, but this bias becomes negligible for higher values. It is also evident that neither correction procedure gives an unbiased estimate of the true β for every particular value of β. In this example, it seems that MLE performs slightly better when the true β is very small, while the Bayesian method performs better for medium values of β. If an empirical-Bayes approach were used, it would perform better than the Bayesian approach for the more common values of β and worse elsewhere.

D. Applications

We now apply these winner's-curse-correction methods to actual data. We begin with the findings of (1) for educational attainment, where we can compare the unbiased replication-stage estimates to the results from applying the winner's-curse-correction methods to the inflated discovery-stage estimates. The first and fourth columns of Supplementary Table S5, respectively, report the discovery-stage estimates and the replication-stage estimates for the three SNPs that (1) report passed a significance threshold of $p < 5 \times 10^{-8}$ (the linear regression coefficients for the SNP associated with years of education are from (1)'s Table 1, and the logistic regression coefficients for the SNPs associated with college completion have been provided by the SSGAC). The second and third columns, respectively, show the discovery-stage estimates corrected by MLE and by the Bayesian method with a diffuse prior. Supplementary Table S6 is the same, except that it shows the 10 SNPs that passed a suggestive significance threshold of $p < 10^{-6}$ (including the three that are genome-wide significant). The results in the tables indicate that in these data, both correction methods do a reasonable job of predicting the effect size that is estimated in the replication.

Finally, we apply the winner's-curse-correction methods to the cognitive performance findings reported in the main text. The first column of Supplementary Table S7 shows the effect size estimates for the three education-based SNPs that passed the (Bonferroni-corrected) significance threshold of $p < 0.05/69$. The second, third, and fourth columns, respectively, show the estimates corrected by MLE, by the Bayesian method with a diffuse prior, and by empirical Bayes.

There are two reasons why the corrections as applied to the cognitive performance findings are large relative to the corrections as applied to Rietveld et al.'s (1) findings (despite the fact that the more stringent significance threshold of genome-wide significance used in (1) would tend to generate a larger correction, all else equal). First, the sample size on which the uncorrected estimates are based is much larger in (1) than for the cognitive performance estimates (approximately 100,000 versus 25,000, respectively). Second and more subtly, simulations (not reported here) show that the uncorrected estimates for the cognitive performance results fall within the region around the significance threshold where the corrections are relatively large.

To provide another way of assessing the magnitude of the SNP associations with cognitive performance, the fifth and sixth columns of Supplementary Table S7 show the R^2 associated with the uncorrected estimates and with the empirical-Bayes-corrected estimates. The R^2, which is defined as the ratio of the variance explained by the SNP to the total phenotypic variance, is here simply equal to the variance explained by the SNP, because the phenotypic variance has been normalized to 1:

$$R^2 = 2m(1-m)\hat{\beta}^2 ,$$

where $\hat{\beta}$ is either the uncorrected (naïve) effect size estimate or the empirical-Bayes-corrected estimate. The results reported in the table suggest that the winner's curse adjustment reduces the SNPs' R^2 from ≈0.0006 to ≈0.0002.

9. Bayesian analysis of the credibility of the SNP associations

Here, we report a heuristic Bayesian calculation along the lines of (20) and (21) to assess the likelihood that the three individual SNP associations we find with cognitive performance are false positives attributable to sampling variation. Several simplifying assumptions make the calculations especially straightforward. First, we assume that each SNP has only two (rather

than three) possible genotypes. Second, we assume for each of the three SNPs, there are only two possibilities: either there is no true association (the null hypothesis H_0), or there is a true association that explains a known fraction of phenotypic variance, R^2 (the alternative hypothesis H_1). Let the prior probability of H_1 be denoted by π; hence the prior probability of H_0 is $1-\pi$. Third, we assume the information available to us is that for each SNP, using a two-sided t-test, we rejected the null hypothesis of no association at the standard significance threshold after Bonferroni correction for testing 69 SNPs, i.e., we rejected H_0 at the significance threshold $\alpha = 0.05/69 \approx 0.00072$.

By Bayes' Rule, the probability that there is a true association given that we observed a significant association is:

$$P(H_1 \| t| > t_{\alpha/2}) = \frac{P(|t| > t_{\alpha/2} \mid H_1)P(H_1)}{P(|t| > t_{\alpha/2} \mid H_1)P(H_1) + P(|t| > t_{\alpha/2} \mid H_0)P(H_0)} = \frac{(power)(\pi)}{(power)(\pi) + (\alpha)(1-\pi)},$$

where "power" (as well as the significance test) is two-sided. Using (22) (http://pngu.mgh.harvard.edu/~purcell/gpc/qtlassoc.html), we calculate statistical power for several different values of R^2 and for the sample size of $N = 24{,}189$ (the actual sample size of the Cognitive Performance Sample).

Supplementary Table S8 shows posterior probabilities that there is a true association, given specific values for R^2 and π. The larger value for R^2 is 0.0006, which roughly corresponds to the estimated magnitude of the association in the Cognitive Performance Sample for each of the three SNPs that are statistically significant after Bonferroni correction (their R^2's are 0.00064, 0.00058, and 0.00056; see Supplementary Table S4). Because this estimate is likely to be inflated by the winner's curse, we also examine the smaller value of $R^2 = 0.0002$. This value roughly corresponds to the estimated magnitude of the association for each of the three SNPs after adjustment for the winner's curse, as discussed in Supplementary Information section 8 (these winner's-curse-adjusted R^2's are 0.00027, 0.00019, and 0.0017; see Supplementary Table S7).

In the simple set-up here, we view a prior probability π in the range of 0.2% to 2% as the right order of magnitude for an *arbitrarily* selected SNP to be associated with cognitive performance with effect sizes of order of magnitude $R^2 = 0.0002$. To see why, begin by taking one extreme: suppose all independent associated SNPs had effect sizes $R^2 = 0.0002$. Since the proportion of variance in cognitive performance explained by the linear, additive effect of all SNPs jointly is roughly 0.40 (23, 24), there would be 0.40 / 0.0002 = 2,000 independent associated SNPs. Given that there are approximately 1 million independent loci in the human genome (25), each of the loci would have prior probability 2,000 / 1 million = 0.2%. However, in reality, most SNPs associated with cognitive performance surely have smaller effect sizes than $R^2 = 0.0002$. In this simple set-up with only two hypotheses, if we consider any SNP whose association is more than an order of magnitude smaller than $R^2 = 0.0002$ as consistent with the "null hypothesis," then the largest number of independent SNPs that are non-null is 20,000 (because 0.40 / 0.00002 = 20,000). In that case, each locus has prior probability 20,000 / 1 million = 2%.

Since the 69 SNPs we study are not arbitrary but are instead selected from those most strongly associated with educational attainment, the prior probability for each of those SNPs should be much higher than for a randomly selected locus in the genome—indeed, this observation is what motivates the proxy-phenotype method in the first place. Therefore, we view $\pi = 0.1\%$ as an extremely conservative lower bound for the prior probability on the three SNPs being true positives. Since we suspect that a number of the 69 SNPs we study are probably truly associated with cognitive performance, we believe that priors of $\pi = 5\%$ and $\pi = 10\%$ are more reasonable.

Given priors of $\pi = 5\%$ or $\pi = 10\%$, together with a reasonable assumption about the true effect size (the winner's-curse-adjusted R^2 of 0.0002), Supplementary Table S8 indicates that the evidence very strongly evidence favors H_1 over H_0: the posterior probability of each SNP association being a true positive is 90% or 95%, respectively. According to the table, a proper Bayesian thinker should be skeptical only when the prior probability becomes so conservative that the first stage of selecting SNPs on the basis of their being associated with years of schooling is treated as uninformative (π less than 1%).

10. Selection of theory-based candidate SNPs

To select a set of SNPs that would fairly represent those that would be nominated as candidates on theoretical grounds, we required a method of constraining the search. One challenge for candidate-gene approaches is that any of the thousands of genes that are expressed in the central nervous system could be selected as a theoretical candidate for association with cognitive performance. Therefore, we chose to use only SNPs that had at least one published positive association with IQ, *g*, or a measure of general cognitive ability, including higher-order facets of IQ such as verbal or spatial IQ (but *not* episodic memory, working memory, dementia, MMSE, autism, schizophrenia, etc.) in a healthy sample, regardless of whether there are any published negative associations (non-replications), as of May 2013. PubMed was used for the searches, and the results were required to be publications in peer-reviewed journals (not conference abstracts, etc.). This selection method should be biased in favor of "good candidates" in the sense that they are more likely to be true associations than would be a randomly chosen set of common SNPs in central-nervous-system-expressed genes. We excluded SNPs that originated as discoveries in GWAS studies, SNPs that were only significant in association with IQ as large haplotypes, and polymorphisms that are not SNPs. The first exclusion was applied because GWAS-discovered SNPs are not traditional candidates, since they were by definition derived in an atheoretical manner. The latter two were applied so as to restrict our set of theory-based candidates to individual SNPs that could be compared directly to the set of SNPs nominated from the results of the years-of-schooling (proxy phenotype) GWAS. Finally, we confirmed that none of the positive associations reported in the literature for the theory-based SNPs used a cohort included in the Cognitive Performance Sample. Our set of theory-based SNPs is listed in Supplementary Table S3.

(While the SNPs comprising the two-SNP haplotype for *APOE*, rs429358 + rs7412, were retained on our initial list, these SNPs were not available in the cohort GWAS results.)

11. Testing the Q–Q plots for the education-associated and the theory-based candidates

To test whether the Q–Q plot for the education-associated SNPs (Figure 2 in the main text) differs from the null of a uniform distribution, we use as our test statistic

$$Z = \frac{\frac{1}{S}\sum_{s=1}^{S} z_s^2 - 1}{\sqrt{2/S}},$$

where s indexes the $S = 69$ education-associated SNPs, and z_s^2 is the squared z-statistic from the regression of cognitive performance on SNP s. This squared z-statistic captures the strength of the association between cognitive performance and SNP s (while ignoring the sign of the association, which depends on the arbitrary choice of reference allele). Under the null hypothesis, each $z_s \sim N(0,1)$, and thus $z_s^2 \sim \chi^2(1)$, which has mean 1 and variance 2. Therefore, under the null:

$$E(Z) = 0, \mathrm{var}(Z) = \frac{(1/S)^2 S \,\mathrm{var}(z_s^2)}{2/S} = 1.$$

We calculate a p-value for the test of whether the realized value of the test statistic, $Z = z$, differs from zero using the inverse cdf of the standard normal distribution. As reported in the main text, for the education-associated SNPs, we calculate $z = 5.98$, corresponding to p-value $= 1.12\times10^{-9}$.

We test the theory-based SNPs analogously, but with $S = 24$. As reported in the main text, we calculate $z = 1.19$, corresponding to p-value $= 0.12$.

To calculate the 95% confidence bounds around the null hypothesis shown in Figure 2, we use the fact that the sth order statistic out of S from a Uniform(0,1) random variable has a Beta(s, $S–s+1$) distribution (*33*, p. 230). These confidence bounds differ for the two sets of SNPs because S differs.

12. Biological annotation

In this section, we describe the methods used in our biological annotation analyses. In order to focus on the SNPs most strongly implicated in cognitive performance, we study a subset of the 69 education-associated SNPs described in Supplementary Information section 1. Specifically, we analyze the 14 SNPs that reach a nominal significance level of 5% in the meta-analysis of cognitive performance in the Cognitive Performance Sample. (A more stringent significance threshold would retain too few SNPs for substantial analysis.) Throughout, we refer to these SNPs as the *Nominally-Significant Education-Associated SNPs* (the *NSEA* SNPs).

We conduct five types of analyses. In Subsection A, we examine which non-synonymous coding variants are known to be in strong linkage disequilibrium with the *NSEA* SNPs. In Subsections B and C, we investigate if the *NSEA* SNPs are associated with gene expression levels in, respectively, blood and three distinct brain regions. In Subsection D, to shed light on the biological function of the genes implicated in our analyses, we conduct a gene function prediction analysis. Subsection E, which builds on the analysis from Subsection D, tests whether the loci implicated in our analyses are more enriched for nervous system functioning than SNPs that are similar to our 14 SNPs in terms of minor allele frequency, gene proximity, and gene density, but that are otherwise randomly selected from the GWAS data.

Our analyses here differ in a number of ways from those reported in (1), in which similar biological annotation analyses were conducted in an expanded version of our Education Sample on SNPs reaching $p < 5\times10^{-8}$ (genome-wide significance) or $p < 10^{-5}$ (suggestive significance) for association with educational attainment (with the p-value threshold depending on the biological analysis). First and most importantly, by restricting attention to the *NSEA* SNPs, all of our analyses are based on a set of SNPs for which there is especially strong reason to believe that at least some are related to cognitive performance (as opposed to other endophenotypes that matter for educational attainment). Second, our eQTL look-ups (in Subsections B and C) have substantially more statistical power because our gene-expression databases have larger sample sizes. In particular, the brain sample we work with is four times larger than the one analyzed in (1). Third, the gene-prediction analyses we conduct (in Subsection D) are more expansive. Specifically, our analyses include predictions from mouse models about the phenotypic effects of a gene and inferences about the types of tissue in which the gene is expressed. Finally, we report (in Subsection E) formal tests of the hypothesis that the loci implicated in our analyses are more likely than would be expected by chance for otherwise-similar SNPs to be in the vicinity of genes with neuronal functionality. Such formal

tests are novel, as far as we are aware. Subsection F provides a summary of the evidence for biological candidates.

A. Non-Synonymous Variants in Strong LD with Candidate SNPs

We used the software tool HaploReg to identify missense variants in close linkage disequilibrium ($r^2 \geq 0.5$) with at least one of the 14 *NSEA* SNP*s*. In total we identified 8 such non-synonymous variants in the 1000 Genomes database tagged by 6 *NSEA* SNPs. These 8 variants are within 8 genes: *JMJD1C*, *RECQL4*, *LRRC14*, *SH2B1*, *SDCCAG8*, *DNAJC28*, *GART*, and *SBNO1*. See Supplementary Table S9 for more information about these variants.

B. Blood *cis*-eQTL Lookup

We conducted gene expression analyses from blood using publicly available data (downloadable from http://genenetwork.nl/bloodeqtlbrowser/) from a recently published paper by (27). (27) conducted *cis*-eQTL mapping by testing, for a large set of genes, all SNPs within 250 kb of the transcription start site of the gene for association with total RNA expression level of the gene. The publicly available data contain, for each gene, a list of all SNPs that were found to be significantly associated with gene expression using a False Discovery Rate (FDR) of 5%. For a detailed description of the quality control measures applied to the original data and an overview of the statistical framework, see (27). Their meta-analysis is based on a pooled sample of 5,311 individuals with gene expression levels measured from full blood. We looked up the 14 *NSEA* SNPs in this publicly available data and found 8 that were significantly associated with gene expression levels in a total of 19 different genes and transcripts: *LRRC24*, *GPT/PPP1R16A*, *VPS28*, *MFSD3*, *TUFM*, *SPNS1*, *CCDC101*, *SULT1A2/SULT1A1*, *LAT*, *SDCCAG8*, *GART*, *ITSN1*, *RILPL2*, *SETD8*, *STK24*, *TANK*, and *PSMD14*. The effect sizes and statistical significance for the *NSEA* SNPs and strongest eQTL signal for each gene are presented in Supplementary Table S10.

C. Brain *cis*-eQTL Lookup

To investigate if any of the *NSEA* SNPs are associated with gene expression levels in human neural tissue, we utilized data from the Harvard Brain Tissue Research Center. The total sample of 742 individuals is comprised of 376 Alzheimer patients, 193 Huntington patients, and 173 individuals without a known neurological disorder. The dataset contains data on expression probes obtained from postmortem brains and measured in three distinct neural regions: prefrontal cortex, visual cortex, and cerebellum (28). The probe data on the Huntington patients have not previously been reported.

The quality control and probe-data normalization steps are each extensive and are described in detail in Zhang et al. After these steps, 39,579 probes were taken forward as dependent variables for subsequent eQTL analysis.

As is standard, we tested the probes for association with all of the SNPs in the GWAS data; below, we report the results from "looking up" our prioritized SNPs in the results. We eliminated SNPs with a minor allele frequency below 0.01, SNPs that failed a test of Hardy-Weinberg equilibrium at a nominal p-value $< 10^{-6}$, and SNPs with a call rate below 95%. After quality control, 838,958 SNPs remained. We used a Kruskal-Wallis test to test all SNPs within one Mb of the transcription start site of each gene for association with gene expression level of a given probe. We adjusted the resulting p-values to control for testing of many SNPs and probes. To take into account the correlation structures among the probes and among the SNP genotypes, we estimated an empirical FDR: the ratio of the average number of eQTLs found in datasets with randomly permuted sample labels to the number of eQTLs identified in the original data set. Since the number of tests was large, we found that the empirical null distribution converges after a relatively small number of permutation runs; thus, we used ten permutation runs to estimate the empirical FDR. We focus on the associations that survive after constraining the empirical FDR to be less than 10% (which corresponds to a nominal p-value cutoff of approximately 5×10^{-5}).

In the meta-analytic results for the three different brain regions, we looked up a total of 580 SNPs: the original 14 SNPs together with all SNPs in high linkage disequilibrium ($r^2 > 0.5$) with one of these 14 SNPs. We observed 40 significant *cis*-effects for 27 of these 580 SNPs (significant at FDR 10%, as described in the previous paragraph): 13 for prefrontal cortex, 10 for visual cortex, and 15 for cerebellum. These 27 SNPs, which proxy for 6 of the 14 *NSEA* SNPs, regulate gene expression for 18 distinct transcripts (some of which are genes and some of which are non-coding, regulatory RNAs): *LRRC14*, *LRRC24*, *KIFC2*, *AF075035*, *EIF3C*, *LAT*, *NUPR1*, *NFATC2IP*, *TUFM*, *SDCCAG8*, *SBNO1*, *C12ORF65*, *MPHOSPH9*, *TMEM50B*, *GART*, *IFNGR2*, *AK026896*, and *AF33979*. Supplementary Table S11 lists the effect-sizes, p-values, LD metrics, and brain regions.

D. Co-expression-driven Gene Functional Prediction

We used a recently developed method (extensively described and implemented by (29)) to gain insight into the putative functions of the genes in the vicinity of the *NSEA* SNPs. Gene function prediction is based on the idea that genes with shared expression profiles are likely to have related biological functions. For example, if there are 50 genes known to play a role in apoptosis, then a gene with unknown function that is strongly co-expressed with these 50 genes is likely to be part of apoptotic pathways as well. The method described in (29) uses data on co-expression profiles to predict the likely functions of as-of-yet uncharacterized genes and refine our understanding of the function of other genes (achieving this by reconstituting the

existing gene sets – described below). In addition to proposing the method, (29) also report evidence that a prediction coming out of the framework was validated by subsequent wet-lab experiments.

To apply the method, we queried the co-expression database described by (29) with our list of genes (our list is explained below). The query for each gene returned the probable function of the gene or the reconstituted pathway in which it operates (more specific details are given below). In the remainder of this paragraph, we briefly summarize the information from which the co-expression database was generated. The database was generated by linking information about gene expression obtained from published data on approximately 80,000 gene expression profiles (from the database Gene Expression Omnibus (GEO) (30), which itself was generated using data from humans, animals, and/or cell lines) with three other distinct types of information:

1. A list of pathways and gene sets that a given gene is believed to be involved in, obtained from the databases: REACTOME pathways (31), Gene Ontology terms (32), and KEGG pathways (33).
2. The phenotypic effects of perturbing the normal functioning of a given gene in mice (e.g., knock-out models, overexpression), obtained from the Mouse Genetics Initiative database (http://www.informatics.jax.org).
3. More than 200 specific tissues, organs, or cell types within which a given gene is highly expressed in the co-expression dataset, for which annotation was obtained from searching the U.S. National Library of Medicine's Medical Subject Headings (MeSH) database (http://www.nlm.nih.gov/mesh/).

(In contrast to the functional prediction analysis that we describe here, the analogous analysis in (1) was conducted at a time when the co-expression database included only information from #1 in the above list.)

In our analyses, we queried a list of 83 genes that were derived from the list of 14 *NSEA* SNPs: we included every gene that is located within 250 kb of the 14 SNPs; and if the SNP is located within a gene desert (defined by having no gene located within 250 kb base pairs of the SNP), we included the nearest gene. Two of the 14 SNPs were located within a gene desert: rs1487441 (nearest annotated gene *POU3F2* is located ~700kb away) and rs1606974 (nearest annotated gene *NRXN1* is located ~600kb away).

Among the 83 genes we queried, we found that 15 genes are in relevant gene sets related to reconstituted pathways and biological functions (for specific predictions, see Supplementary Table S12), 23 genes are predicted to cause relevant neuronal phenotypes in mouse models (for specific predictions, see Supplementary Table S13), and 29 genes are highly expressed in nervous-system-related tissues and cell types (for specific tissues and cell types, see Supplementary Table S14). Given that there is overlap between the genes in these three sets, our co-expression analyses identified 36 genes in total as potential biological candidates for cognitive performance (see Supplementary Table S15 for a list of these genes). (Note that *APOE*, which may be associated with cognitive decline in older individuals (*6*) is *not* among our list of genes. This is perhaps as expected given our results from section 'Polygenic score analyses in the Health and Retirement Study', in which we find that a polygenic score comprised of our educated-associated SNPs is associated with the *level* of cognitive function in older individuals but not with cognitive decline.)

While the full list of all implicated reconstituted pathways is available online at http://www.ssgac.org[1], we conclude our discussion of this analysis by listing the top 5 most frequently occurring search terms from the analysis for each category (with the count given in square brackets) listed in the Supplementary Tables S12, S13 and S14:

1. **Gene Ontology: Biological Processes** – neuron-neuron synaptic transmission [3]; neurotransmitter secretion [3]; regulation of neurotransmitter levels [3]; synaptic transmission, glutamatergic [3]; axonogenesis [2].

2. **Gene Ontology: Cellular Compound** – synapse [6]; dendrite [5]; synapse part [5]; cation channel complex [4]; synaptic membrane [4].

3. **Gene Ontology: Molecular Function** – cation channel activity [5], gated channel activity [5]; voltage-gated cation channel activity [5]; voltage-gated channel activity [5]; voltage-gated ion channel activity [5].

4. **KEGG** – Calcium signaling pathway [4], Neuroactive ligand-receptor interaction [3], axon guidance [2], Long-term potentiation [2].

5. **REACTOME** – Neuronal System [6] Potassium Channels [5]; Transmission across Chemical Synapses [5]; Voltage gated Potassium channels [5]; Ras activation uopn Ca2+ infux through NMDA receptor [4]; Unblocking of NMDA receptor, glutamate binding and activation [4].

6. **Mouse Genome Informatics** – abnormal brain wave pattern [5]; abnormal excitatory postsynaptic currents [5]; abnormal excitatory postsynaptic potential [5]; abnormal inhibitory postsynaptic currents [5]; abnormal CNS synaptic transmission [4].

7. **Site-specific expression** – Prefrontal Cortex [12]; Visual Cortex [12]; Occipital Lobe [12]; Cerebral Cortex [11]; Entorhinal Cortex [11].

E. Evaluating for Enrichment of Genes Related to Neuronal Function

Our prediction analyses showed that all 12 *NSEA* SNPs not located in a gene desert were within 250 kb of at least one gene predicted to be related to neuronal function. While this finding seems impressive, it is well understood that many genes can been linked to neuronal function. It is therefore important to evaluate whether the 12 non-desert *NSEA* SNPs in our analysis are more associated with neuronal function than would be expected by chance. To do so, we calculated an empirical *p*-value using a matching procedure that we describe in this section.

As a first step, for each of the 12 non-desert *NSEA* SNPs, we randomly sampled a vector of 1,000 "matched SNPs" that resembled the *NSEA* SNPs in terms of minor allele frequency, gene density, and distance to nearest gene. For each *NSEA* SNP, we generated the 1,000 matched SNPs using the following algorithm:

1. We identified the set of all SNPs covered by our GWAS data that have a minor allele frequency within 5 percentage points of the given *NSEA* SNP's minor allele frequency.

[1] The link will be activated on the day of publication of this article. The materials that will be posted online are included as a separate appendix to the submitted manuscript.

2. We discarded SNPs from this set whose gene density differed from the given *NSEA* SNP's gene density by more than 10%, where "gene density" is defined as the total number of genes containing a SNP that is in LD $r^2 > 0.5$ with the focal SNP.

3. We then further discarded SNPs from the set whose distance to the nearest gene exceeds the given *NSEA* SNP's distance to nearest gene by more than 20 kb.

4. Finally, from the remaining SNPs in the set, we randomly sampled 1,000 of them. (Up to this point in the algorithm, there were always more than 1,000 SNPs remaining in the set.)

As a second step, for each of the 12 *NSEA* SNPs and each of their respective 1,000 matched SNPs, we coded a SNP as either "enriched for neuronal functioning" or "not enriched for neuronal functioning." We did so using a version of the gene function prediction procedure outlined in section 4, but we modified the procedure in two ways. First, to make our definition of "enriched for neuronal functioning" in this analysis more stringent and specific to reconstituted *pathways*, we only used the type of information listed in bullet point #1 from section 4: the pathways and gene sets that a given gene is believed to be involved in. Specifically, we manually annotated *all* of the 6,004 functionality terms from the relevant databases (737 REACTOME pathways, 5,083 Gene Ontology terms, and 184 KEGG pathways), categorizing each as either "related to neuronal function" or "not related to neuronal function" depending on the direct or indirect involvement in the central nervous system via anatomy, cellular structure, or physiological processes (information drawn from published literature). We have posted this annotated list on the following website: http://www.ssgac.org[2]. Second, rather than identifying genes in the vicinity of a SNP as those genes containing a SNP within a window of 250 kb around the focal SNP (as we did in section 4), here we identify genes in the vicinity of a SNP as those genes containing a SNP that is in LD $r^2 > 0.5$ with the focal SNP; this latter definition is generally more stringent and therefore may be considered more appropriate for the kind of enrichment analysis we conduct here. For each gene in the vicinity of one of the *NSEA* SNPs or in the vicinity of one of the matched SNPs, we code the gene as "related to neuronal function" if and only if at least one of its predicted functionality terms is categorized as "related to neuronal function." We then code each *NSEA* SNP as "enriched for neuronal functioning" if and only if at least one of the genes in its vicinity is "related to neuronal function," and we code each of its respective matched SNPs analogously.

In the final step, we tested the null hypothesis that the 12 *NSEA* SNPs are no more "enriched for neuronal functioning" than would be expected by chance. Using the definition of "enriched for neuronal functioning" from the previous paragraph, 10 out of the 12 *NSEA* SNPs are "enriched for neuronal functioning." For comparison, among the 1,000 random matched sets, we observed 88 sets with at least 10 out of 12 SNPs "enriched for neuronal functioning." Hence, the empirical p-value is 0.088. While this p-value does not reach the standard statistical significance threshold of 0.05, we nonetheless view it as fairly strong evidence in favor of the biological significance of the *NSEA* SNPs: our procedure of matching the SNPs on minor allele frequency, gene density, and distance to nearest gene leads to a very conservative test because if the properties of the *NSEA* SNPs—say, their distance to nearest gene—is typical of functional SNPs, then the SNPs matched to them are also reasonably likely to be functional. Thus, our test does not just require that the *NSEA* SNPs are more likely to be "enriched for neuronal functioning" than any randomly chosen SNPs, but more likely than SNPs that are already chosen to be reasonably likely to be functional.

[2] The link will be activated on the day of publication of this article. The materials that will be posted online are included as a separate appendix to the submitted manuscript.

(We note that our approach is an improvement compared to current standard practice in enrichment analysis. Instead of investigating only established functions and links to pathways, we apply functional prediction, which extends over known biology and is likely more accurate and stringent. It is not common practice yet to conduct the kind of statistical test that we introduce here, and we suspect that our results are statistically stronger than those that would be obtained from many published findings using related bioinformatics procedures.)

F. Summary of the Evidence for Biological Candidates

In this section we briefly summarize the cumulative evidence arising from our extensive bioinformatics annotation analyses regarding which genes are associated with cognitive performance. In Supplementary Table S15 we outline the positive findings from our 4 different computational approaches (described above), in total 8 distinct categories: (1) non-synonomous variants; (2) blood eQTL; (3) brain eQTL–prefrontal; (4) brain eQTL–visual; (5) brain eQTL–cerebellum; (6) functional prediction–GO, KEGG, REACTOME; (7) functional prediction–mouse phenotypes; and (8) functional prediction–tissue expression. In the last two columns of Supplementary Table S15, we additionally report the results from looking for overlap between our list of 83 genes and the genes implicated in two recent analyses of neural function:

1. (28) report functional modules constructed using brain-derived gene expression profiles from three regions (prefrontal cortex, visual cortex and cerebellum). We looked up which if any of our 83 genes were reported as clustered into any of the 62 network modules containing at least 50 genetic nodes as defined in (28). Here, we find that six of the genes (*POU3F2*, *CPSF1*, *AKT3*, *NMS*, *TMED2* and *TMEM50B)* map to the neuropeptide hormone specific module (Fisher's exact test (FET) enrichment p-value = 0.004, analytical framework explained extensively at (28). Furthermore, we combined all neuronal specific modules (synaptic transmission; neurogenesis; neuropeptide hormone and/or nerve myelination) from (28): this approach implicates 12 of the following genes – *POU3F2*, *CPSF1*, *KCNMA1*, *AKT3*, *KIFC2*, *FARP1*, *NMS*, *NRXN1*, *SCRT1*, *TBR1*, *TMED2* and *TMEM50B*, in neuronal-related module functions (FET enrichment p-value = 0.015).

2. (34) identifies genes that code for proteins isolated from the postsynaptic density from human neocortex [hPSD]. We looked up which if any of our 83 genes were reported as part of this protein complex. This exercise implicates the following genes: *FARP1*, *ITSN1*, NRXN1, and *TUFM*.

In total we found some supportive evidence for 56 out of the 83 genes. Furthermore, 21 genes were prioritized by at least 3 of the methods, 12 genes by at least 4 methods, and 6 genes by up to 5 methods. These 6 genes that have highly convergent evidence of biological functionality are: *LRRC14*, *KIFC2*, *NRXN1, C12ORF65*, *ITSN1* and *TMEM50B*. Furthermore, the results from the above two analyses of blood and brain *cis*-eQTLs indicate that the *NSEA* SNPs or respective proxies affect the gene expression levels of almost half of the 21 top-ranking implicated genes, and hence these analyses may reveal potential regulatory mechanisms. As noted in the main text, in total 4 of the highly prioritised genes (*KCNMA1*, *NRXN1*, *POU3F2*, and *SCRT*) are predicted (in the analysis in the section "Co-expression-driven Gene Functional Prediction" above) to be involved in a particular reconstituted neurotransmitter pathway, labeled in REACTOME as "unblocking of NMDA receptor, glutamate binding and activation."

13. Polygenic score analyses in family samples

A. Results from analyses in family samples

We used a polygenic score to explain cognitive performance in MCTFR, QIMR, STR, and in the additionally recruited cohort Generation Scotland (GS). To construct the weights for the polygenic score used for each of these cohorts, we performed a meta-analysis on cognitive performance, excluding respectively MCTFR, QIMR, STR, and no cohorts (for GS, we use the complete cognitive performance meta-analysis since GS was not included in the meta-analysis). This resulted in a meta-analysis of N = 20,822 for MCTFR, N = 22,437 for QIMR, N = 20,974 for STR, and N = 24,189 for GS. We constructed a linear polygenic score by weighting the 69 education-associated SNPs by the coefficient estimates obtained from these meta-analyses (in QIMR, the SNP rs2970992 was excluded because it exhibited a very high number of Mendelian errors and extreme Hardy-Weinberg irregularity: HWE test $p = 1.98\times10^{-17}$). In MCTFR the sample is restricted to 1,346 siblings from 673 families. In QIMR the sample is restricted to 5 siblings from 1 family, 4 siblings from 19 families, 3 siblings from 129 families, and 2 siblings from 479 families, yielding a total of 1469 pseudo-independent siblings. In STR the sample is restricted to 810 DZ twins from 405 distinct families. In GS there are 1,081 siblings from 476 independent families. In each regression the standard errors are clustered (35) at the family level to take into account the non-independence of individuals within a family. The results are reported in Supplementary Table S16. Using both within-family and between-family variation (the top panel: "Without family dummies"), pooling the coefficients across GS, MCTFR, QIMR, and STR with inverse-variance weighting (the right-most column), we find that the score is significantly protectively associated with cognitive performance (p-value = 8.17×10^{-4}). Using only within-family variation (the bottom panel: "With family dummies"), the pooled coefficient has the same sign but is smaller with a larger standard error, and is thus not statistically significant (p-value = 0.36).

B. Power calculations for within-family analysis

In the main text, we claim that "even without stratification, the non-significance of the within-family coefficient is not surprising given the low power of this test." Here we substantiate that claim.

We estimate the power of this analysis by simulation. We assume that cognitive performance Y of sibling i from family j is determined according to the following simple model:

$$Y_{ij} = \beta s_{ij} + z_j + \varepsilon_{ij},$$

where s_{ij} is the polygenic score, z_j is a family effect, and ε_{ij} is the residual from a projection of Y_{ij} on s_{ij} and z_j in the population and is therefore uncorrelated with both by construction. The variables Y_{ij} and s_{ij} are standardized to have mean 0 and variance 1. We assume that $\varepsilon_{ij} \sim N(0,\sigma_\varepsilon^2)$ and that the family effects are distributed normally in the population: $z_j \sim N(0,\sigma_z^2)$. Since we are interested in testing our power to detect a polygenic score effect within families under the assumption that the size of the effect is the same as it is without family effects, we assume that s_{ij} is uncorrelated with z_j.

To match the empirical fact that the correlation of cognitive performance between siblings is about 0.5, we assume that $\sigma_z^2 = \sigma_\varepsilon^2 \equiv \sigma^2$. Now, note that the explanatory power of the polygenic score is given by:

$$R^2 = \frac{\beta^2 \operatorname{var}(s_{ij})}{\beta^2 \operatorname{var}(s_{ij}) + \operatorname{var}(z_j) + \operatorname{var}(\varepsilon_{ij})} = \frac{\beta^2}{\beta^2 + 2\sigma^2}.$$

In the simulations below, we examine two different values for β, 0.045 and 0.065. For each β, the value of σ^2 is set to satisfy $\beta^2 + 2\sigma^2 = 1$ (which ensures that Y_{ij} has variance 1 and that $R^2 = \beta^2$). Given this, the two values of β correspond to R^2 equal to 0.20% and 0.42%, respectively, which roughly correspond to the lower and upper end of the range of R^2's we estimate for the score across samples (in Table S16).

For each assumed true value of β, we conduct 500 simulation runs. In each run, we generate data as follows for a sample of 2,182 families that matches the data used in our estimation: 1,950 two-sibling families, 181 three-sibling families, 42 four-sibling families, 4 five-sibling families, 3 six-sibling families, and 2 seven-sibling families. We generate SNP-level data for the parents by assuming that the allele frequency for 69 SNPs matches the empirical frequency measured in our data, that parental genotypes are drawn independently, and that all SNPs are in Hardy-Weinberg equilibrium. Children are then simulated by drawing one allele from each parent with equal probability. The weights to calculate the score are drawn from a normal distribution (with mean 0 and variance scaled such that s_{ij} has variance 1). This data-generating process produces scores that have a within-family correlation of 0.5.

Given the data in each run, we estimate β in two regressions. In the first, we regress Y_{ij} on s_{ij} (i.e., we not include family dummies as covariates); this is the "Without family dummies" model in table S17 discussed below. In the second, we regress Y_{ij} on s_{ij} and z_j; this is the "With family dummies" model in table S17 discussed below. Note that in the second model, we are estimating the family effect as a fixed effect (even though we model it as a random effect, which is normally distributed, for the purpose of doing the power calculation) because in the analysis of the actual data we estimate the family effect as a fixed effect. In both regressions, we take into account the non-independence of individuals within a family by clustering standard errors within family (35), just as we do in the analysis of the actual data.

We estimate power as the fraction of the 500 runs in which we reject the null hypothesis $\beta = 0$ with a p-value less than 0.05. Table S17 shows the average regression output over the 500 simulations for the two different values of β, 0.045 and 0.065.

As can be seen in table S17, power is much higher in the model estimated without family dummies; it is very nearly 80% even at the lower end of the range of R^2's. With family dummies, however, the range of R^2's corresponds to power between 31.2% and 64.2%. Thus, our power to detect a significant effect in the within-family analysis is relatively low even if the true effect size is at the upper end of our range of estimates.

14. Polygenic score analyses in the Health and Retirement Study

A. HRS data description

The Health and Retirement Study (HRS; (36)) is a representative sample of Americans over the age of 50 who have been surveyed every two years since 1992. The survey data from all 10 waves of the study are publicly available. The total sample size of the HRS is 30,671, including respondents who entered the sample in wave 1, replenishment samples who entered in subsequent waves, and spouses of respondents. However, for all analyses using the HRS described in this section and elsewhere in this paper, the sample is restricted to genotyped individuals from European ancestry (N = 8,652). Because testing individual SNPs in a sample of this size would have low power, we instead analyze a polygenic score.

To combine the education-associated SNPs into a linear polygenic score that exploits their joint explanatory power, we generated a linear combination of the SNPs' number of reference alleles, weighted by their coefficient estimates from the GWAS meta-analysis of years-of-schooling (as in (37)). In particular, we use the results from the meta-analysis that excludes the HRS; this meta-analysis is described in section 1 above. We construct the score in the HRS using the 60 out of 69 education-associated candidate SNPs available in the imputed genotype data.

We obtained the cognitive measures from the HRS datafile as prepared by RAND (RAND v.L, available at http://hrsonline.isr.umich.edu). This datafile contains cognitive scores harmonized across all waves of the study in which the data were collected. We use the two summary cognitive-health measures that are available in more than one wave: Total Word Recall (TWR) and Total Mental Status (TMS). TWR is the sum of scores on immediate and delayed word-recall tasks. In each task, the recall list contains 10 words, and scores ranged from 0-20. TMS is a dementia battery. It is the sum of scores for the following tasks: serial 7's (repeatedly subtracting the number 7), backwards counting from 20, and naming objects, the current date, and the current President and Vice-President. The resulting range is 0-15. Because these batteries focus on identifying cognitive problems and early signs of dementia (rather than measuring cognitive ability among healthy individuals), the resulting variables are viewed as measures of cognitive health (for discussion, see (38) p.10, which is posted online as part of the HRS data documentation: http://hrsonline.isr.umich.edu/sitedocs/dmc/Lachman_hrscognitive.pdf). Below, we also report results for Total Cognition (TC), which is the sum of TWR and TMS, resulting in a range of 0-35. Consistent measures for TWR, TMS, and TC are available in wave 3-9.

Prior to wave 4, all cognitive tests were administered to all respondents. Starting in wave 4, all cognitive tests were administered to new respondents, but for those who had participated in a prior wave, the respondent's age determined which cognitive measures were administered. Respondents 65 years or older received the full set of cognitive tests. Respondents under 65 received the full TWR battery but only two of the tasks comprising TMS (serial 7's and backwards counting from 20). For this reason, we have more observations for the TWR measure than for the TMS and TC measures.

B. HRS regression results

For each of the cognitive measures—TWR, TMS, and TC—we run two sets of regressions: one in which the dependent variable is the cognitive measure itself (the "levels" regressions), and one in which the dependent variable is the difference between the cognitive measure in the current wave and the previous wave (the "changes" regressions). All dependent variables are

standardized to have mean 0 and standard deviation 1. In all analyses we control for gender and an age spline. Knots of the age spline are at 60, 70, and 80, except for the changes regressions for TMS and TC, in which the knots are at 70 and 80 because there are only 9 respondent-wave observations with age < 60. We exclude these nine observations from the analysis. For each dependent variable we run two regression specifications. The first includes as a regressor (in addition to gender and the age spline) the polygenic score, and the second additionally includes as regressors the interactions of the polygenic score with the age spline. Because the data include observations from the same respondent in multiple waves, we cluster the standard errors (35) at the respondent level.

Supplementary Table S18 displays the regression results, with each column representing a different regression specification. The odd-numbered columns include only controls for sex and an age spline, while the even-numbered columns additionally control for interactions between the score and the age spline. For each column, the "ΔR^2" row shows the increase from including the score variables (either just the score, or the score and its interactions, depending on the specification) in the regression.

In the levels regressions (columns 1-6), the increasingly negative coefficients on the age spline indicate that cognitive performance is decreasing with age, as expected. The coefficients on the indicator for being female show that females on average have higher scores in TWR and lower scores on TMS, with the net effect on TC being higher scores. Turning to the main coefficient of interest, in all of the levels regressions a higher value for the score is associated with a higher level of cognitive performance. In terms of magnitude, a one standard-deviation increase in the score is associated with approximately a 0.04 increase in TWR, a 0.06 increase in TMS, and a 0.06 increase in TC.

In the levels regressions that include an interaction between the score and the age spline (columns 2, 4, and 6), we find that the effect of the score is approximately unaffected by age, except possibly for the age category ≥80, where there appears to be some reduction in the magnitude of the protective effect of the score (but statistically significantly only for TWR). This pattern is consistent with the results shown in Figure 3 in the main text.

In the changes regressions (columns 7-12), the negative coefficients on the age spline again reflect that cognitive performance is decreasing with age, and indeed at an increasing rate. The negative coefficient on the indicator for being female in the ΔTMS regressions suggests that the decline is slower for females for this measure, but the coefficients are not statistically distinguishable from zero for the other measures. The coefficient on the score is not significantly distinguishable from zero for any of the measures in the changes regressions. Thus, even though the score is associated with a higher *level* of cognitive performance, it does not appear to be protective against *declines* in cognitive performance.

In the changes regressions that include an interaction between the score and the age spline (columns 8, 10, and 12), we again find a negative coefficient for the age category ≥80 (statistically significant for ΔTWR and ΔTC). This negative coefficient means that cognitive performance declines more quickly for those respondents over the age of 80 who have higher values of the score—and hence had higher cognitive performance on average at younger ages. This negative coefficient in the changes regressions is thus consistent with the negative coefficient on the analogous interaction term in the levels regressions.

To probe the robustness of the results to population stratification, we repeated the levels regressions for TWR, TMS, and TC, omitting the interaction between the polygenic score and the age spline as a regressor, and instead including different numbers of principal components of the genome-wide data. For each dependent variable, 20 additional regressions are performed,

in which principal components are iteratively added. Supplementary Figure S4 shows how the coefficients for the polygenic score change as principal components are added. The coefficients for the polygenic score may decline slightly as principal components are added, but the decline is very small, and the coefficients with 20 principal components and essentially the same as those without any principal components. Thus, we find no evidence that population stratification is driving the HRS results.

Table S19 presents the same analyses as those in Table S18, however, in these analyses years of education (0-17+) is added as control variable to the model. There is a slight decrease in sample size, because years of education is missing for a few individuals. In the levels regressions (columns 1-6), the coefficient for the polygenic score remains statistically significant, but the magnitude of the coefficient is about half as large as when educational attainment is not included as a control, and ΔR^2 is much smaller. In the changes regressions (columns 7-12), the polygenic score is not statistically significant.

C. HRS sign tests on the education-associated SNPs

We also tested whether the direction of the SNPs' effects on educational attainment generally coincide with the direction of their effects on cognitive performance. For each of the three dependent variables, we ran 60 regressions, using the 60 out of 69 SNPs available in the HRS data as regressors instead of the polygenic score in regression specifications (2), (4), and (6) from Table S18. For each SNP, we compared the sign of the SNP's coefficient with the sign of the same SNP's coefficient from the meta-analysis of educational attainment that excludes the HRS. We computed the *p*-value using a binomial distribution with probability 50% of matching the sign. The resulting *p*-values are: 0.0067 for TWR (39 out of 60 SNPs with identical sign), 0.0775 for TMS (35 out of 60 SNPs with identical sign), and 0.0775 for TC (35 out of 60 SNPs with identical sign).

15. Statistical Framework for the Proxy-Phenotype Method as Applied to Cognitive Performance

A. Statistical power of GWAS vs. candidate-SNP (including proxy-phenotype) method for gene discovery

Consider the problem of estimating the association between a phenotype of interest Y, say cognitive performance, and the genotype g_k of each of k = 1, 2, …, K SNPs. The standard approach is to estimate K separate linear regressions of Y on each g_k. After standardizing Y and g_k so that each has mean 0 and variance 1, the regression equations to be estimated can be written as

(1) $Y = \beta_k g_k + \varepsilon_k$,

for k = 1, 2, …, K. (For simplicity, we omit the covariates, which would typically include age, sex, and possibly principal components of genetic data, and to avoid cluttering notation, we suppress indexing variables by individual.) Because Y and g_k are standardized, in a large sample the estimated regression coefficient β_k is equal to the correlation between Y and g_k, and the coefficient of determination is $R^2{}_{Y,g_k} = \beta_k^2$.

In terms of statistical power, the key difference between a GWAS approach to gene discovery and a candidate-SNP approach is the size and composition of the set of K SNPs. In GWAS, the set includes all SNPs measured by the dense SNP genotyping platform (typically 0.5-2.5 million). The statistical significance threshold is set at the "genome-wide significance" level of $\alpha = 5\times10^{-8}$, which can be interpreted as a Bonferroni correction for the effective number of independent loci in European populations (25, 39). In contrast, in a candidate-SNP approach—either theory-based or proxy-phenotype-based—K is a much smaller number of SNPs that the researcher considers to be reasonable candidates for association with the phenotype. In a theory-based method, the candidates are chosen on the basis of what is known or believed about their biological function, while in a proxy-phenotype method, the candidates are chosen on the basis of their association with a proxy phenotype. Either way, in terms of statistical power, the advantage of a candidate-SNP approach is that the Bonferroni-corrected significance threshold can be set at the much less stringent level of $\alpha = 0.05 / K$. The potential disadvantage is that the effect sizes of the most strongly associated SNPs in a candidate-SNP approach may be smaller than in a GWAS, since the method of choosing the candidates may not succeed in selecting those that are most strongly associated with the phenotype of interest.

Table S20 calculates power for GWAS vs. candidate-SNP methods of gene discovery that could be pursued in our Cognitive Performance Sample of size $N = 24{,}189$. The columns show different effect sizes for a SNP: $R^2 \in \{0.02\%, 0.04\%, 0.06\%, 0.08\%\}$, a range from the size of our estimated winner's-curse-adjusted effect size for cognitive performance of $R^2 \approx 0.02\%$ up to four times that size. The top row shows statistical power to detect each of these effect sizes at the genome-wide significance threshold, $\alpha = 5\times10^{-8}$. The bottom row shows statistical power to detect each of these effect sizes at the experiment-wide significance threshold for 69 SNPs, $\alpha = 0.05 / 69 \approx 0.00072$.

As explained in the next subsection below, our calculations prior to the study (based on the results of Rietveld et al., (1)) led us to expect an effect size of $R^2 \approx 0.08\%$ for the strongest associations in our set of proxy-based candidate SNPs. In that case, our power to detect such associations would have been 85%. In contrast, a direct GWAS on cognitive performance in our Cognitive Performance Sample would have had power of 15% to detect these SNPs. Given our estimated winner's-curse-adjusted effect size for cognitive performance of $R^2 \approx 0.02\%$, our actual power to detect the largest associations we found was 12%–which in turn suggests that there are roughly 8 times as many SNPs with the same effect sizes as the 3 significant SNPs we identified (since 1/0.12 = 8.33). A direct GWAS on cognitive performance in our sample would have had power of only 0.06% to detect these SNPs. Therefore, even if there are 25 SNPs with associations of magnitude $R^2 \approx 0.02\%$ with cognitive performance, a GWAS with the available sample size would very likely not have detected any of them.

B. Statistical power of proxy-phenotype method under plausible effect sizes for cognitive performance

Prior to conducting this study, we calculated expected effect sizes using the formal framework introduced by Rietveld et al. (1) (SOM pp. 22-27) and the results reported in that paper. Here we sketch a slightly simplified version of that framework (also note that our notation here differs somewhat). Let $s = 1, \ldots, S$ index the SNPs that are causally related to cognitive performance or any other genetically-influenced factor that matters for educational attainment.

We assume that cognitive performance is a simple linear function of the individual's genotype and determined by:

$$(2)\, Y = \sum_{s=1}^{S} \beta_{Y,s} g_s + \varepsilon_Y \ ,$$

where g_s is the individual's genotype at SNP *s* (as above, normalized to have mean zero and variance one), $\beta_{Y,s}$ is the effect of g_s on *Y*, and ε_Y is a random variable with mean zero that we assume is independent of the g_s's. The error term ε_Y captures all other factors besides the SNPs, including exogenous environmental factors, that affect cognitive performance.

We assume that the proxy phenotype *P*, in this context educational attainment, is determined by a simple linear function of cognitive performance and other factors:

$$(3)\, P = \gamma_Y Y + \gamma_X X + \varepsilon_P \, .$$

X captures genetically-influenced factors that affect educational attainment, including personality traits (such as perseverance) and early-life health conditions. The error term ε_P captures all other factors, including exogenous environmental factors that affect *P*. We assume that ε_P is a random variable with mean zero and is independent of *Y* and *X*. We normalize *P*, *Y*, and *X* so that they have mean zero and variance one (hence regression coefficients are equal to partial correlation coefficients). Without loss of generality, we assume that both *Y* and *X* are oriented in the direction that increases educational attainment: $\gamma_Y > 0$ and $\gamma_X > 0$.

To complete the model, we write *X* as an analogous linear function of the individual's genotype:

$$(4)\, X = \sum_{s=1}^{S} \beta_{X,s} g_s + \varepsilon_X \, ,$$

where $\beta_{X,s}$ is the partial correlation coefficient of g_s with *X*, and ε_X is a random variable with mean zero that we assume is independent of the g_s's. Now, educational attainment *P* can be expressed as a function of the SNP genotypes by substituting equations (2) and (4) into equation (3):

$$(5) P = \sum_{s=1}^{S} (\gamma_Y \beta_{Y,s} + \gamma_X \beta_{X,s}) g_s + (\gamma_Y \varepsilon_Y + \gamma_X \varepsilon_X + \varepsilon_P) = \sum_{s=1}^{S} \delta_s g_s + u_Y \, ,$$

where $\delta_s \equiv (\gamma_Y \beta_{Y,s} + \gamma_X \beta_{X,s})$ is the effect of SNP *s* on educational attainment, and $u_Y \equiv \gamma_Y \varepsilon_Y + \gamma_X \varepsilon_X + \varepsilon_P$ is a mean-zero composite error term that is independent of the g_s's. Note that a GWAS of educational attainment *P* estimates the δ_s's in equation (5). Note that if $\delta_s \neq 0$, then either $\beta_{Y,s} \neq 0$ or $\beta_{X.s} \neq 0$ or both. Therefore, if the GWAS of *P* credibly identifies a SNP, then that SNP can serve as a plausible "candidate SNP" for genetically influenced factors that matter for *P*.

To generate a first-pass estimate of the effect size of SNPs associated with cognitive performance, we begin with the special case in which genetic factors matter for educational attainment exclusively through cognitive performance: $\gamma_X = 0$. In that case, $\delta_s = \gamma_Y \beta_{Y,s}$. Rearranging, the R^2 from a regression of cognitive performance on SNP *s* is equal to the R^2 from a regression of educational attainment on SNP *s* is divided by the squared phenotypic correlation: $\beta_{Y,s}^2 = \delta_s^2 / \gamma_Y^2$. The largest SNP effects on educational attainment are likely to have

a coefficient of determination of roughly 0.0003 (see Table S20), and since $\gamma_X = 0$, these same SNPs will be the ones with the largest effects on cognitive performance. Using $\delta_s^2 \approx$ 0.0003 and an estimated phenotypic correlation of γ_Y = 0.6 (40, 41) gives $\beta_{Y,s}^2 \approx 0.0008$ (our reading of the evidence is that estimates of the phenotypic correlation have generally been in the range 0.4-0.6; our high-end estimate of the correlation yields a lower, and hence more conservative, estimate of the SNP effect size). As mentioned in the previous subsection, this was our best guess of the effect size before we conducted our study and was the basis of our ex ante power calculations. Although we anticipated that the largest SNP effects on cognitive performance would have $\beta_{Y,s}^2 \approx 0.0008$, what we found was $\beta_{Y,s}^2$ = 0.0006, which became $\beta_{Y,s}^2$ = 0.0002 after correction for the winner's curse (Table S7).

The more realistic case where $\gamma_X > 0$ opens up the possibility that the SNPs most strongly associated with cognitive performance are not the same SNPs as those most strongly associated with educational attainment. To see this, note that since $\delta_s = \gamma_Y \beta_{Y,s} + \gamma_X \beta_{X,s}$, the SNPs with the largest effect on educational attainment—those most likely to be picked out from a GWAS of educational attainment as candidate SNPs—will tend to be those for which *both* $\beta_{Y,s}$ and $\beta_{X,s}$ are positive and large in magnitude. Rietveld et al. use the term "mono-directional" to refer to such a SNP: a SNP that has pleiotropic effects on *Y* and *X* such that it affects *P* in the same direction through both pathways. A SNP has a stronger association with educational attainment than it does with cognitive performance if $\delta_s > \beta_{Y,s}$.

C. Explaining the negative correlation between coefficients for educational attainment and cognitive performance

As noted in the main text, Figure 1 shows a negative correlation between the coefficients on educational attainment and the coefficients on cognitive performance. Also as mentioned in the text, this negative correlation seems somewhat robust to dropping the most conspicuous possible outlier, although we view the evidence for negative correlation as relatively weak. Here we note that according to the framework developed in this section, a negative correlation between δ_s and $\beta_{Y,s}$ implies that $\beta_{Y,s}$ and $\beta_{X,s}$ are negatively correlated. In words, SNPs that affect cognitive performance more strongly tend to affect other factors that matter for educational attainment (such as personality traits) less strongly, and vice-versa.

D. Relating the genetic correlation between educational attainment and cognitive performance to the above framework

According to the framework above, a GWAS of educational attainment (EA) generates good candidate SNPs for cognitive performance (CP) because CP is an important causal factor in determining EA. Moreover, if CP is the primary genetically-influenced factor that matters for EA ($\gamma_X \approx 0$), then the effect size of the SNPs on CP is expected to be larger when the phenotypic correlation between EA and CP (γ_Y) is *smaller*, because the smaller phenotypic

correlation means that the effect of the SNP on EA is more attenuated relative to its more direct and larger effect on CP.

Intuitively, it might seem that the *genetic* correlation between EA and CP would be at least as relevant as the phenotypic correlation. In this subsection, we address the relevance of the genetic correlation within the context of our formal framework; we conclude that the high genetic correlation can be viewed as providing a justification for using EA as a proxy phenotype for EA, but the argument is somewhat loose.

What *can* be shown formally and straighforwardly is that the statistical power of the proxy-phenotype approach is increasing in $\text{corr}(\delta_s, \beta_{Y,s})$. The assumption that CP is the only genetically-influenced factor that matters for EA ($\gamma_X = 0$) implies that $\text{corr}(\delta_s, \beta_{Y,s}) = 1$. If other genetically-influenced factors also matter for EA ($\gamma_X > 0$), then $\text{corr}(\delta_s, \beta_{Y,s})$ can be smaller than 1, and the SNPs with the largest effects on EA may not be those with the largest effects on CP.

The genetic correlation is a different object: $\text{corr}\left(\sum_{s=1}^{S} \delta_s g_s, \sum_{s=1}^{S} \beta_{Y,s} g_s\right)$. In words, the genetic correlation is the correlation between the population polygenic score for EA and the population polygenic score for CP. It follows from this definition that if the genetic correlation is high, a polygenic score estimated from EA is likely to explain more of the variance in CP. However, the genetic correlation does not have direct implications about the statistical power for identifying individual SNPs unless the (unconditional) genetic correlation is equal to the genetic correlation *conditional* on including only the SNPs with largest effect sizes in the polygenic score. The evidence discussed in subsection C above casts some doubt on this assumption. Therefore, while in general we view the high genetic correlation between EA and CP as supportive of our use of EA as a proxy phenotype, we view our overall framework as providing a more solid justification.

E. Setting the *p*-value threshold for the proxy-based SNPs

The power calculations in Table S21 take as given the fact that we included 69 SNPs in the set of proxy-based candidates. We used 69 SNPs because this is the number that passed our inclusion threshold of $p < 10^{-5}$ from the first-stage GWAS on educational attainment. In this subsection, we explain why we chose this particular inclusion threshold.

We chose our inclusion threshold of $p < 10^{-5}$ prior to conducting any analyses on cognitive performance, on the basis of power calculations using the results from the first-stage GWAS on educational attainment. Our goal was to design the study in a way that would maximize the expected number of true positive results in the second stage analyses on cognitive performance. The optimal threshold trades off between two opposing effects. On the one hand, a less stringent threshold yields a larger number of candidates that are forwarded to the second stage. A larger set of candidates is more likely to contain true positives. On the other hand, a larger number of candidates requires that a more stringent experiment-wide significance level needs to be applied in the second stage to adjust for multiple testing, which decreases power to pick out the true positives from among the set of candidates.

Our calculations are reported in Table S21. Row (1) reports the number of LD-pruned SNPs in the first stage GWAS on EA that passed the *p*-value threshold of the respective column. Row (2) is the observed average R^2 of these SNPs on EA. The R^2 estimates deviate slightly from those reported in (1) due to the slightly different set of subjects that were included in the two

analyses. The ex-post power (i.e., assuming that the observed average R^2 is the true effect size) to find such an effect size in our EA sample is reported in row (3), again always for the *p*-value threshold of the respective column. Row (4) reports the posterior belief that a randomly chosen SNP from the set included in the column is truly associated with EA. To calculate this value, we used Bayes' formula, with a conservative prior belief equal to 0.01%, power equal to row (3), and α equal to the respective *p*-value threshold of the column (see Section 9 for the formula we use, as well as a discussion of why we consider the larger prior belief of 0.02% to be quite conservative).

Row (5) reports the Bonferroni-adjusted *p*-value threshold for stage 2, given a family-wide significance level of 0.05 and the number of independent hypotheses that will be tested, given by row (1). Row (6) uses the statistical proxy-phenotype framework reported above to calculate the expected average R^2 of SNPs in the second stage on CP. We assumed a phenotypic correlation of 0.6 between EA and CP, and we assumed that the selected SNPs influence EA only through their influence on CP. Row (7) calculates the expected power for a two-sided test given the available sample size in the second stage on CP, as well as the *p*-value threshold given by row (5) and the expected effect size given by row (6).

Row (8) reports the expected number of true positive SNPs that would be discovered in the study overall, given by multiplying the number of candidate SNPs given by row (1), the posterior belief that these candidates are truly associated with EA (row 4), and the expected power of stage 2 (row 7). The choice of the *p*-value threshold we have chosen for our study ($p < 10^{-5}$) was given by the column that maximized the value of row (8). The optimal *p*-value threshold turns out to depend only on the results of the first-stage GWAS on EA, and not on our assumptions about prior beliefs, phenotypic correlation, or available sample size in stage 2. These assumptions influence the absolute magnitudes in row (8) but not their relative magnitudes.

Finally, row (9) reports the expected posterior belief that a SNP associated with CP at the Bonferroni-adjusted *p*-value is truly associated with CP, using Bayes' formula, prior beliefs equal to row (4) and power equal to row (7). These calculations were included with the analysis plan that was forwarded to cohorts participating in early 2013. The analysis plan was also posted on Open Science Framework on 14 Apr 2013 (see https://osf.io/z7fe2/).

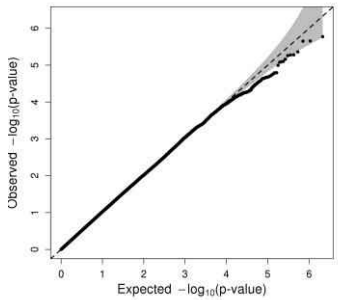

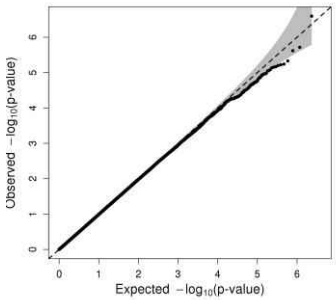

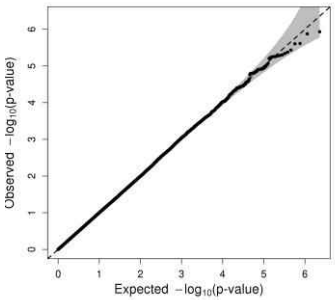

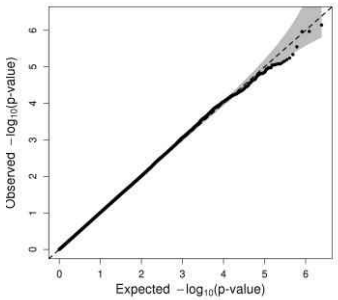

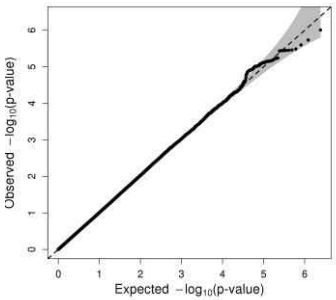

Supplementary Figures

Figure S1. Quantile-Quantile plots and Genomic Control λ for the summary results of the five GWA studies after quality control.

ERF, λ = 1.039	GenR, λ = 0.975	HU, λ = 1.001	MCTFR, λ = 1.006	STR, λ = 1.015

Figure S2. Quantile-Quantile plots of the cognitive performance meta-analysis results for the theory-based and education-associated candidate SNPs. The joint plots show in black the QQ-plot for the education-associated candidate SNPs, and in red the theory-based candidate SNPs.

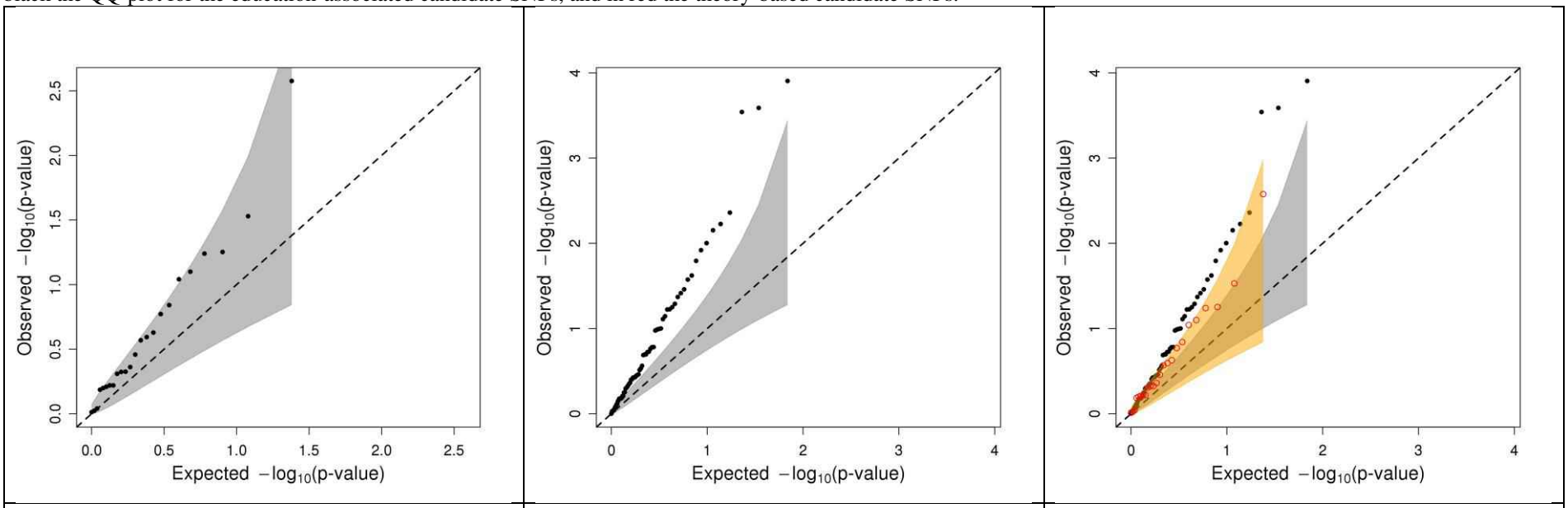

Theory-based candidate SNPs	Education-associated candidate SNPs	Joint plot

Figure S3. Simulation study of winner's curse corrections: MLE versus diffuse-prior Bayesian. The *x*-axis is the true effect size β, grouped in bins that are 0.002 standard-deviation units wide. The *y*-axis is the estimated effect size. The dots show the naïve OLS estimate (red), the MLE-corrected effect size estimate (green), and the Bayesian-corrected effect size estimate (blue). The light dotted lines are 95% confidence intervals around the estimates. For the simulation parameters, see section 8.

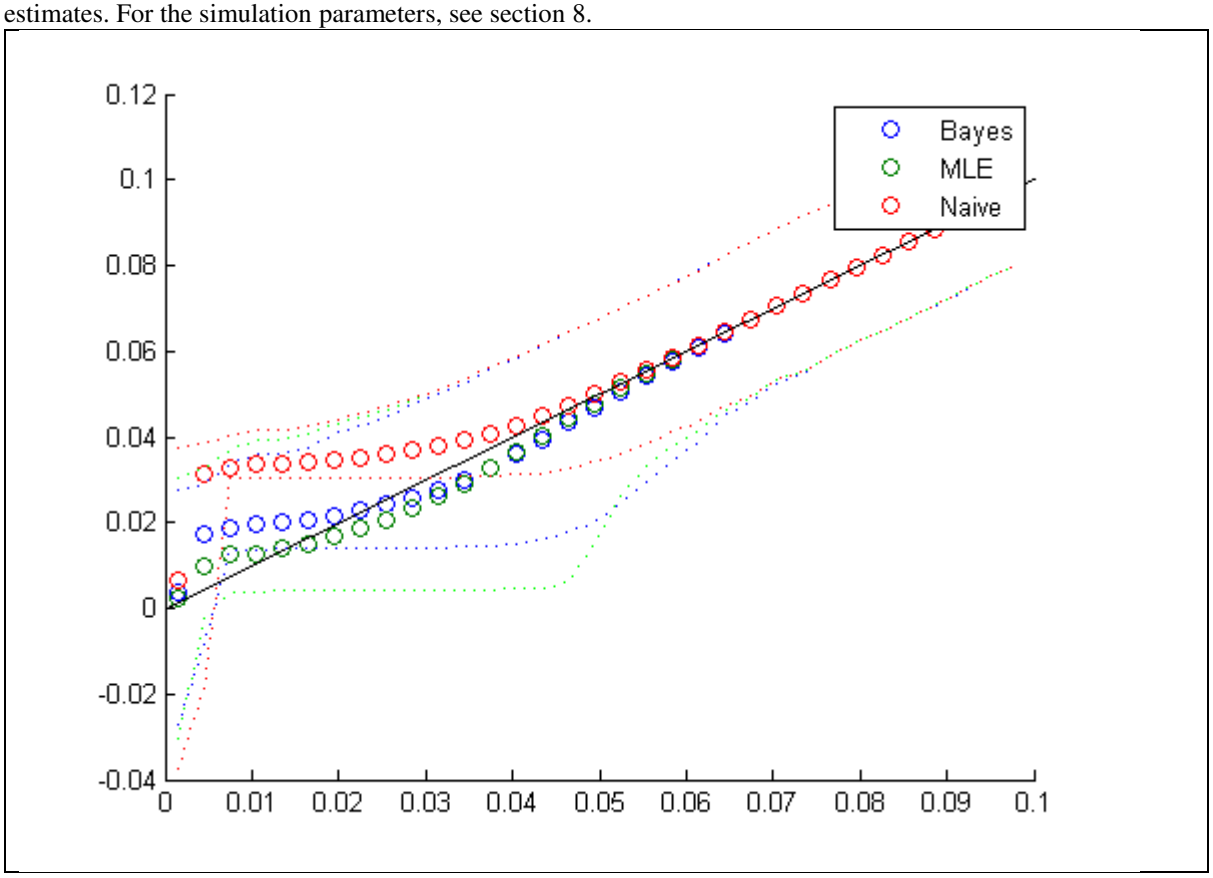

Figure S4. Coefficient on the polygenic score in the regressions explaining the level of TWR, TMS, and TC and controlling for an increasing number of principal components. TWR = Total Word Recall, TMS = Total Mental Score.

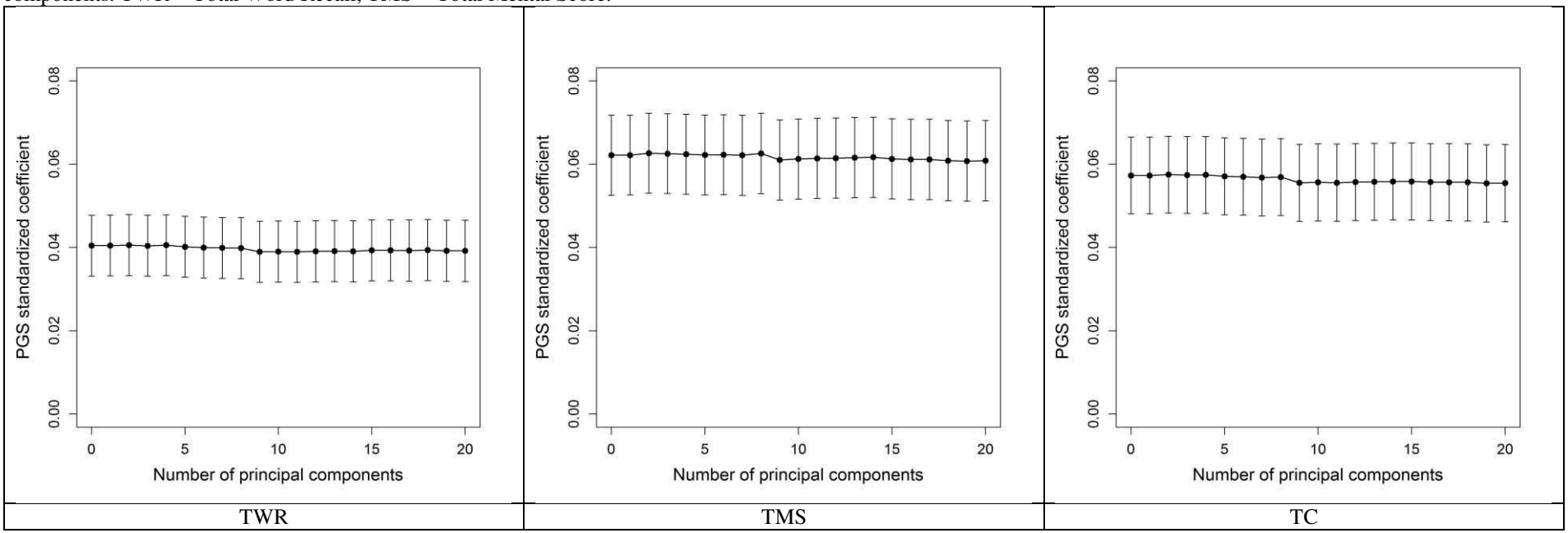

Supplementary Tables

Table S1. Study design, numbers of individuals, and quality control for GWAS cohorts. "Call rate" refers to the genotyping success rate, i.e., the minimum percentage of successfully genotyped SNPs.

Study				Sample QC			
Short name	Full name	Study design	Total sample size (*N*)	Call rate	Other exclusions	Sample in analysis (*N*)	References
ALSPAC	Avon Longitudinal Study of Parents and Children	Prospective pregnancy cohort	8,340	≥97%	1) Gender mismatches 2) Minimal or excessive heterozygosity 3) Cryptic relatedness (IBD > 0.1 and IBD < 0.8) 4) Non-European ancestry 5) Missing cognitive performance phenotype	5,517	(42)
ERF	Erasmus Rucphen Family study	Family-based	3,658	≥95%	1) Failing IBS checks 2) Sex chromosome checks 3) Ethnic outliers removed 4) Age < 45 years 5) Missing cognitive performance phenotype	1,076	(43)
GenR	Generation R	Birth-cohort	6,135	≥97.5%	1) Duplicate samples 2) Gender mismatch 3) Relatedness 4) Missing cognitive performance phenotype	3,701	(44)
GS	Generation Scotland	Family-based	10,000	≥98%	1) Sample call rate 0.95 2) SNPs diverging from HWE with a significance $p<1\times10^{-3}$ 3) SNPs with a MAF <0.01 4) Missing cognitive performance phenotype 5) Only siblings	1,081	(45)
HU	Harvard/Union Study	Population-based	415	≥93%	1) Ethnic outliers removed 2) Participants more than 6 SD away from any of the top 10 principal components	389	(46)

					3) Missing cognitive performance phenotype		
LBC1921	Lothian Birth Cohort 1921	Population-based birth-cohort	517	≥95%	1) Unresolved gender discrepancy 2) Relatedness 3) Non-Caucasian descent 4) Missing cognitive performance phenotype	464	(47)
LBC1936	Lothian Birth Cohort 1936	Population-based birth-cohort	1,005	≥95%	1) Unresolved gender discrepancy 2) Relatedness 3) Non-Caucasian descent 4) Missing cognitive performance phenotype	947	(48)
MCTFR	Minnesota Center For Twin and Family Research	Family-based	7,438	≥99%	1) >5000 uncalled SNPs 2) Low GenCall score 3) Extreme hetero- or homozygosity 4) Sample mix-up or unable to confirm known genetic relationships 5) Missing cognitive performance phenotype	3,367	(49)
QIMR	Brisbane Adolescent Twin Study, Queensland Institute of Medical Research	Population-based	3,899	≥95%	1) Non-European ancestry 2) Missing cognitive performance phenotype	1,752	(50)
Raine	Western Australian Pregnancy Cohort Study	Prospective pregnancy cohort	1,593	≥97%	1) Gender mismacht 2) Relatedness 3) Low heterozygosity 4) Missing cognitive performance phentoype	936	(51)
STR	Swedish Twin Registry	Family-based	9,836	≥97%	1) Sex-check (heterozygosity of X-chomosomes) 2) Deviations in heterozygosity of more then 5 SD from the population mean 3) Cryptic relatedness check 4) Missing cognitive performance phenotype	3,215	(52)
TEDS	Twins of Early Development Study	Family-based	3,747	Exact percentage unknown (done by	1) Low call rate 2) Heterozygosity outliers 3) Intensity outliers 4) Ancestry outliers	2,825	(53)

		external genotyping center)	5) Relatedness/duplicates 6) Gender mismatches 7) Samples were re-genotyped on a panel of 30 SNPs using Sequenom and were excluded because of low concordance (<90%). 8) Missing cognitive performance phenotype

Table S2. Information on genotyping methods, imputation, and assocation analysis.

Study	Genotyping platform	Genotyping calling algorithm	Imputation software	Imputation reference dataset	Association software
ALSPAC	Illumina HumanHap550	GenomeStudio	MACH	HapMap 2 CEU	Mach2QTL
ERF	Illumina 318K, Affymetrix 250K, Illumina 350K, Illumina 610K	GenCall & BRLMM	MACH/Minimac	1000Genomes I v3 (GIANT)	ProbABEL
GenR	Illumina 610K Quad, 660W Quad	GenomeStudio	MACH	HapMap2	PLINK
GS	Illumina HumanOmniExpressExome-8 v1.0	GenomeStudio	MACH	HapMap 2 CEU	N.A.
HU	Affymetrix 6.0	Birdseed	MACH	HapMap2	PLINK
LBC1921	Illumina Human610_Quadv1	GenomeStudio	MACH	HapMap 2 CEU	Mach2QTL
LBC1936	Illumina Human610_Quadv1	GenomeStudio	MACH	HapMap 2 CEU	Mach2QTL
MCTFR	Illumina 660W Quad	BeadStudio	Minimac	HapMap2 CEU	RFGLS (R)
QIMR	Illumina 610, Illumina 370, Illumina 317	BeadStudio	MACH	HapMap 2 CEU	Merlin
Raine	Illumina Human660W	BeadStudio	MACH	HapMap 2 CEU	Mach2QTL
STR	Illumina HumanOmniExpress-12v1_A	GenomeStudio	IMPUTE	HapMap2 CEU	Merlin-offline
TEDS	Affymetrix GeneChip 6.0	Affymetrix Genotyping Console	IMPUTE2	HapMap 2/3 CEU	SNPTEST

Table S3. Results for the theory-based candidate SNPs; SNPs are ordered according to their *p*-value in the cognitive performance meta-analysis. The chromosome and basepair position are from the NCBI genome annotation (build 36). The frequency of the coded allele is from the cognitive performance meta-analysis.

						Years of Education		Cognitive Performance	
SNP ID	Chromosome	Basepair	Coded allele	Non-coded allele	Frequency coded allele	Beta coeff. (standardized)	*p*-value	Beta coeff. (standardized)	*p*-value
rs1042713	5	148186633	a	g	0.380	-0.004	4.05×10^{-1}	0.029	2.65×10^{-3}
rs1800497	11	112776038	a	g	0.201	-0.004	5.16×10^{-1}	-0.025	2.95×10^{-2}
rs2830102	21	26456898	t	c	0.314	-0.005	2.62×10^{-1}	0.021	5.59×10^{-2}
rs1612902	19	56191007	t	c	0.566	0.008	7.60×10^{-2}	-0.020	5.75×10^{-2}
rs2274185	1	158587804	c	g	0.942	-0.001	8.94×10^{-1}	0.037	7.95×10^{-2}
rs2251621	8	31007504	a	g	0.041	0.010	3.83×10^{-1}	-0.052	9.09×10^{-2}
rs1799990	20	4628251	a	g	0.636	0.011	2.16×10^{-2}	0.015	1.44×10^{-1}
rs4680	22	18331271	a	g	0.522	-0.002	6.10×10^{-1}	0.013	1.69×10^{-1}
rs1800855	4	26100215	a	t	0.785	-0.007	2.07×10^{-1}	-0.016	2.35×10^{-1}
rs8191992	7	136351848	a	t	0.542	0.001	7.93×10^{-1}	-0.012	2.55×10^{-1}
rs237895	3	8782423	t	c	0.394	0.006	2.41×10^{-1}	-0.012	2.70×10^{-1}
rs714939	2	75688615	a	g	0.385	-0.006	1.56×10^{-1}	0.009	3.48×10^{-1}
rs821616	1	230211221	a	t	0.719	0.010	4.71×10^{-2}	0.008	4.35×10^{-1}
rs6489630	12	5474885	t	c	0.191	0.000	9.40×10^{-1}	0.009	4.72×10^{-1}
rs1130214	14	104330779	a	c	0.297	-	-	0.008	4.74×10^{-1}
rs2725385	8	31047688	t	c	0.291	-0.015	1.33×10^{-3}	-0.007	4.90×10^{-1}
rs2760118	6	24611569	t	c	0.349	-0.003	5.61×10^{-1}	0.005	6.03×10^{-1}
rs9536314	13	32526138	t	g	0.844	-0.009	1.41×10^{-1}	0.007	6.03×10^{-1}
rs363043	20	10174146	t	c	0.294	-0.002	6.33×10^{-1}	0.005	6.19×10^{-1}
rs17571	11	1739170	a	g	0.081	-0.015	5.80×10^{-2}	0.009	6.32×10^{-1}
rs760761	6	15759111	a	g	0.212	-0.003	5.56×10^{-1}	0.006	6.51×10^{-1}
rs12239747	1	158587689	a	g	0.939	-0.005	6.61×10^{-1}	0.002	9.11×10^{-1}
rs6265	11	27636492	t	c	0.186	0.010	7.65×10^{-2}	-0.001	9.48×10^{-1}
rs16944	2	113311338	a	g	0.347	-0.003	5.43×10^{-1}	0.000	9.71×10^{-1}

Table S4. Results for the education-associated candidate SNPs; SNPs are ordered according to their *p*-value in the cognitive performance meta-analysis. The chromosome and basepair position are from the NCBI genome annotation (build 36). The frequency of the coded allele is from the cognitive performance meta-analysis.

						Years of Education		Cognitive performance	
SNP ID	Chromosome	Basepair	Coded allele	Non-coded allele	Frequency coded allele	Beta coeff. (standardized)	*p*-value	Beta coeff. (standardized)	*p*-value
rs1487441	6	98660615	a	g	0.473	0.026	1.78×10^{-9}	0.036	1.24×10^{-4}
rs7923609	10	64803828	a	g	0.521	-0.021	1.06×10^{-6}	-0.034	2.58×10^{-4}
rs2721173	8	145715237	t	c	0.473	-0.020	8.61×10^{-6}	-0.034	2.88×10^{-4}
rs8049439	16	28745016	t	c	0.595	0.021	1.48×10^{-6}	0.027	4.36×10^{-3}
rs1606974	2	51727103	a	g	0.124	0.031	5.39×10^{-6}	0.042	5.93×10^{-3}
rs2970992	2	100688741	a	c	0.493	-0.020	8.27×10^{-6}	-0.025	7.03×10^{-3}
rs3127447	10	78923267	a	c	0.529	0.020	6.21×10^{-6}	0.024	9.95×10^{-3}
rs7847231	9	117248892	a	c	0.620	-0.020	6.73×10^{-6}	-0.024	1.20×10^{-2}
rs4658552	1	241479559	t	c	0.632	0.021	2.01×10^{-6}	0.023	1.61×10^{-2}
rs1892700	21	33938007	a	g	0.256	-0.023	2.96×10^{-6}	-0.024	2.39×10^{-2}
rs7980687	12	122388664	a	g	0.200	0.029	7.14×10^{-8}	0.028	2.66×10^{-2}
rs1187220	18	33605724	t	c	0.323	-0.024	3.48×10^{-7}	-0.027	3.47×10^{-2}
rs3783006	13	97909210	c	g	0.457	0.023	3.11×10^{-7}	0.022	3.84×10^{-2}
rs7309	2	161800886	a	g	0.491	-0.022	2.21×10^{-7}	-0.019	4.26×10^{-2}
rs10166311	2	162575859	a	g	0.326	0.023	9.50×10^{-7}	0.019	5.13×10^{-2}
rs3789044	1	202855724	a	g	0.219	0.028	5.44×10^{-8}	0.022	5.62×10^{-2}
rs2635047	18	42990334	t	c	0.483	0.020	5.76×10^{-6}	0.019	5.94×10^{-2}
rs17176043	14	36064553	a	g	0.946	0.043	7.17×10^{-6}	-0.045	5.98×10^{-2}
rs1198575	1	98334848	t	c	0.189	-0.026	2.37×10^{-6}	-0.025	7.17×10^{-2}
rs889956	2	57258338	a	g	0.397	-0.023	1.52×10^{-7}	-0.017	7.76×10^{-2}
rs7594192	2	199159337	a	g	0.250	0.026	1.28×10^{-7}	0.018	9.98×10^{-2}
rs3753275	1	8348487	t	c	0.824	-0.030	3.97×10^{-7}	-0.020	1.01×10^{-1}
rs9289301	3	128627683	c	g	0.155	0.031	7.77×10^{-7}	0.024	1.03×10^{-1}
rs9858213	3	49706865	t	g	0.288	0.028	4.85×10^{-9}	0.018	1.05×10^{-1}
rs11191193	10	103792398	a	g	0.653	0.023	5.65×10^{-7}	0.014	1.65×10^{-1}
rs6732189	2	161281027	a	g	0.526	-0.023	8.44×10^{-8}	0.013	1.66×10^{-1}
rs4073894	7	104254200	a	g	0.202	0.024	9.32×10^{-6}	0.017	1.73×10^{-1}
rs2066955	12	80614747	a	c	0.237	0.023	4.77×10^{-6}	0.015	1.87×10^{-1}
rs2966	6	33797498	t	c	0.452	0.022	3.60×10^{-7}	-0.012	1.89×10^{-1}
rs188133	15	45489734	a	g	0.683	-0.021	9.29×10^{-6}	-0.013	2.01×10^{-1}
rs11742741	5	24198698	a	t	0.515	-0.022	2.61×10^{-7}	-0.012	2.02×10^{-1}
rs10783779	12	54778147	t	g	0.607	-0.021	6.25×10^{-6}	-0.012	2.05×10^{-1}
rs4468007	9	123634160	t	c	0.554	0.021	3.38×10^{-6}	0.011	2.74×10^{-1}

rs9940536	16	77713418	t	c	0.321	0.022	3.47×10^{-6}	0.011	2.94×10^{-1}
rs3731896	2	219854646	t	c	0.174	0.029	5.21×10^{-6}	-0.013	3.06×10^{-1}
rs1970584	9	125150127	a	c	0.060	0.048	4.64×10^{-7}	-0.021	3.45×10^{-1}
rs6712515	2	100172946	t	c	0.471	-0.026	2.21×10^{-9}	-0.009	3.51×10^{-1}
rs1478110	9	1711478	t	c	0.480	-0.023	3.54×10^{-7}	-0.011	3.59×10^{-1}
rs1239771	18	75666608	t	c	0.218	0.024	9.54×10^{-6}	0.011	3.72×10^{-1}
rs12640626	4	176863266	a	g	0.570	0.022	7.63×10^{-7}	0.009	3.75×10^{-1}
rs2955259	4	171110419	a	g	0.569	0.024	7.04×10^{-8}	0.009	3.77×10^{-1}
rs2053831	14	84049789	a	g	0.776	0.023	8.35×10^{-6}	-0.010	3.94×10^{-1}
rs7788657	7	13888666	t	c	0.436	0.056	8.78×10^{-7}	0.018	4.86×10^{-1}
rs4451621	10	12471373	t	c	0.536	-0.023	9.73×10^{-7}	0.008	4.37×10^{-1}
rs1056667	6	26618543	t	c	0.628	0.023	5.25×10^{-7}	0.007	4.45×10^{-1}
rs10028773	4	120484707	c	g	0.675	0.020	7.45×10^{-6}	0.007	4.63×10^{-1}
rs1360382	9	23369719	a	g	0.042	-0.024	3.41×10^{-7}	-0.007	4.81×10^{-1}
rs17013497	1	207061559	t	c	0.135	0.030	6.78×10^{-6}	0.010	4.95×10^{-1}
rs6984449	8	19372239	a	g	0.601	0.022	1.40×10^{-6}	-0.006	5.09×10^{-1}
rs6882046	5	88004620	a	g	0.727	-0.024	8.63×10^{-7}	-0.006	5.57×10^{-1}
rs10519388	5	113879949	t	c	0.835	-0.029	5.21×10^{-7}	0.007	5.64×10^{-1}
rs362987	20	10225452	a	c	0.522	0.020	7.80×10^{-6}	0.005	6.19×10^{-1}
rs9537938	13	57551696	a	g	0.672	0.023	4.85×10^{-7}	-0.005	6.21×10^{-1}
rs7729356	5	107425114	a	c	0.341	0.021	3.53×10^{-6}	-0.004	6.55×10^{-1}
rs11590526	1	116229090	t	c	0.077	-0.039	8.50×10^{-6}	0.008	6.63×10^{-1}
rs1875714	8	68590101	t	c	0.628	0.022	2.07×10^{-6}	0.004	6.63×10^{-1}
rs12075	1	157441978	a	g	0.577	-0.022	1.33×10^{-6}	-0.004	6.64×10^{-1}
rs1105881	15	39859822	c	g	0.643	0.020	6.67×10^{-6}	0.004	6.92×10^{-1}
rs10904180	10	4127661	t	g	0.820	0.026	8.00×10^{-6}	0.005	7.18×10^{-1}
rs13401104	2	236770257	a	g	0.176	-0.032	2.74×10^{-8}	-0.004	7.67×10^{-1}
rs4818225	21	41551765	a	g	0.338	0.021	5.61×10^{-6}	0.003	7.79×10^{-1}
rs334147	2	127972527	t	g	0.929	-0.046	8.67×10^{-6}	-0.005	8.16×10^{-1}
rs6025281	20	54994407	t	c	0.566	-0.021	1.75×10^{-6}	-0.002	8.36×10^{-1}
rs10500871	11	20172332	t	c	0.322	-0.022	3.31×10^{-6}	-0.002	8.73×10^{-1}
rs1995082	16	75564938	t	g	0.865	-0.029	1.97×10^{-6}	-0.002	9.12×10^{-1}
rs247929	12	44581175	c	g	0.513	-0.020	8.36×10^{-6}	0.001	9.13×10^{-1}
rs12134600	1	72408584	a	c	0.116	0.038	6.18×10^{-8}	-0.001	9.38×10^{-1}
rs1550582	8	135611266	a	g	0.262	0.022	7.16×10^{-6}	-0.001	9.38×10^{-1}
rs2930713	9	7639442	t	g	0.523	0.021	2.47×10^{-6}	0.000	9.97×10^{-1}

Table S5. Winner's curse corrections (MLE and Bayesian) applied to Rietveld et al.'s (2013) SNPs associated with educational attainment at the genome-wide significance threshold ($p < 5\times10^{-8}$). Standard errors are reported in parentheses.

SNP	Discovery-stage estimates			Replication- stage estimates
	Naïve (Uncorrected)	MLE Corrected	Bayesian (diffuse) Corrected	
rs9320913	0.106 (0.018)	0.070	0.065	0.077 (0.034)
rs11584700	-0.014 (0.002)	-0.011	-0.009	-0.016 (0.005)
rs4851266	0.012 (0.002)	0.009	0.008	0.011 (0.004)

Table S6. Winner's curse corrections (MLE and Bayesian) applied to Rietveld et al.'s (1) SNPs associated with educational attainment at a suggestive significance threshold ($p < 10^{-6}$). The SNPs are listed in the same order as in (1) Table 1 (the first four in order of increasing *p*-value for association with years of schooling, and the last six in order of increasing *p*-value for association with college completion). SNPs rs9320913, rs11584700, and rs4851266 are also listed in Supplementary Table S5 above (though the corrected estimates here are different because the significance threshold is different). Standard errors are reported in parentheses.

SNP	Discovery-stage estimates			Replication- stage estimates
	Naïve (Uncorrected)	MLE Corrected	Bayesian (diffuse) Corrected	
rs9320913	0.106 (0.018)	0.096	0.087	0.077 (0.034)
rs3783006	0.096 (0.018)	0.035	0.050	0.056 (0.035)
rs8049439	0.090 (0.018)	0.008	0.039	0.065 (0.033)
rs13188378	-0.136 (0.027)	-0.011	-0.058	0.091 (0.067)
rs11584700	-0.014 (0.002)	-0.013	-0.012	-0.016 (0.005)
rs4851266	0.012 (0.002)	0.011	0.010	0.011 (0.004)
rs2054125	0.023 (0.004)	0.011	0.010	0.006 (0.008)
rs3227	0.011 (0.002)	0.008	0.007	0.002 (0.004)
rs4073894	0.012 (0.002)	0.008	0.006	0.000 (0.005)
rs12640626	0.010 (0.002)	0.001 0.096	0.005	0.000 (0.004)

Table S7. Winner's curse corrections (MLE, Bayesian, and empirical Bayes) applied to the cognitive-performance associations that pass the significance threshold ($p < .05/69$). Standard errors are reported in parentheses. Since the phenotypic variance has been normalized to 1, the estimated R^2 is calculated simply as the amount of phenotypic variance explained: $R^2 = 2m(1\text{-}m)\beta^2$, where m is the MAF and β is the effect size estimate.

SNP	Effect size estimates				Estimated R^2	
	Naïve (Uncorrected)	MLE Corrected	Bayesian (diffuse) Corrected	Empirical Bayes Corrected	Naïve (Uncorrected)	Empirical Bayes Corrected
rs1487441	0.036 (0.009)	0.022	0.023	0.023	0.064%	0.027%
rs7923609	-0.034 (0.009)	-0.013	-0.020	-0.020	0.058%	0.019%
rs2721173	-0.034 (0.009)	-0.008	-0.019	-0.018	0.056%	0.017%

Table S8. Posterior probability of true association as a function of effect size (R^2) and prior probability (π).

		Effect size (R^2)	
		$R^2 = 0.0002$ (power = .1186)	$R^2 = 0.0006$ (power = .6658)
Prior (π)	0.1%	14%	48%
	1%	62%	90%
	5%	90%	98%
	10%	95%	99%

Table S9. Results for the functional annotation analysis for the 14 *NSEA* SNPs and respective proxies at consderable LD ($r^2 > 0.5$).

SNP ID	Proxy SNP	LD	Coded Allele	Non-coded allele	Minor allele freqency	Gene name	Sequence change	Amino acid change
rs7923609	rs1935	0.75	c	g	0.47	*JMJD1C*	GA**G** ⇒ GA**C**	E [Glu] ⇒ D [Asp]
rs2721173	rs4251691	0.9	c	t	0.46	*RECQL4*	C**G**G ⇒ C**A**G	R [Arg] ⇒ Q [Gln]
	rs13277542	0.8	t	g	0.47	*LRRC14*	G**A**A ⇒ G**C**A	E [Glu] ⇒ A [Ala]
rs8049439	rs7498665	0.69	a	g	0.34	*SH2B1*	**A**CA ⇒ **G**CA	T [Thr] ⇒ A [Ala]
rs4658552	rs2275155	0.64	a	t	0.33	*SDCCAG8*	GA**A** ⇒ GA**T**	E [Glu] ⇒ D [Asp]
rs1892700	rs139852262	0.55	caatta	c	0.25	*DNAJC28*		Frameshift
	rs8971	0.58	t	c	0.25	*GART*	G**A**T ⇒ G**G**T	D [Asp] ⇒ G [Gly]
rs7980687	rs1060105	0.95	c	t	0.23	*SBNO1*	A**G**T ⇒ A**A**T	S [Ser] ⇒ N [Asn]

Table S10. Results for the gene expression *cis*-eQTL analysis in blood. SNP ID – nominally significant cognitive performance associated variant; FDR – false discovery rate; LD – linkage disequilibrium; ArrayID – Illumina probe identifier; * – denotes a probe not annotated; NSEA - *Nominally-Significant Education-Associated SNPs*: Best eQTL-SNP – the strongest eQTL SNP for a given probe.

		NSEA			*Best eQTL-SNP*					
SNP ID	Coded Allele	eQTL *p*-vaule	Zscore	FDR (5%)	SNP ID	eQTL *p*-vaule	Zscore	FDR (5%)	Gene name	ArrayID
rs7923609	a	3.4×10^{-5}	4.1	6.1×10^{-4}	rs10761725	4.1×10^{-7}	5.1	5.7×10^{-6}	*	1850242
rs2721173	t	2.1×10^{-27}	-24.0	$<<1.0\times10^{-7}$	rs6989368	7.2×10^{-132}	-24.4	$<<1.0\times10^{-7}$	*LRRC24*	2810687
		1.2×10^{-48}	-14.7	$<<1.0\times10^{-7}$	rs750472	1.6×10^{-56}	-15.8	$<<1.0\times10^{-7}$	*GPT/ PPP1R16A*	3140408
		3.4×10^{-27}	-10.8	$<<1.0\times10^{-7}$	rs3735840	9.8×10^{-198}	34.4	$<<1.0\times10^{-7}$	*VPS28*	1190110
		1.0×10^{-14}	7.7	$<<1.0\times10^{-7}$	rs3757966	7.5×10^{-15}	7.8	$<<1.0\times10^{-7}$	*MFSD3*	1510703
rs8049439	c	9.8×10^{-198}	57.7	$<<1.0\times10^{-7}$	rs8049439	9.8×10^{-198}	57.7	$<<1.0\times10^{-7}$	*TUFM*	6370097
		9.8×10^{-198}	35.6	$<<1.0\times10^{-7}$	rs8045689	$9.8^{-}\times10^{198}$	50.8	$<<1.0\times10^{-7}$	*SPNS1*	1230192
		2.1×10^{-49}	-14.8	$<<1.0\times10^{-7}$	rs480400	1.9×10^{-84}	19.5	$<<1.0\times10^{-7}$	*CCDC101*	1240113
		1.2×10^{-4}	3.8	2.0×10^{-3}	rs13331691	1.4×10^{-7}	5.3	2.5×10^{-6}	*SULT1A2/ SULT1A1*	7510711
		2.5×10^{-3}	3.0	0.03	rs4788115	1.6×10^{-5}	-4.3	2.8×10^{-4}	*LAT*	3610288
		2.9×10^{-3}	3.0	0.04	rs4788115	1.2×10^{-8}	-5.7	$<<1.0\times10^{-7}$	*LAT*	460259
rs4658552	c	3.1×10^{-17}	8.4	$<<1.0\times10^{-7}$	rs2275155	3.2×10^{-21}	9.5	$<<1.0\times10^{-7}$	*SDCCAG8*	460458
rs7980687	a	1.1×10^{-5}	-4.4	1.8×10^{-4}	rs1662	4.7×10^{-93}	20.5	$<<1.0\times10^{-7}$	*RILPL2*	1660286
		4.3×10^{-4}	3.2	6.5×10^{-3}	rs12366872	3.4×10^{-17}	8.4	$<<1.0\times10^{-7}$	*SETD8*	2350735
rs1892700	a	2.8×10^{-36}	12.4	$<<1.0\times10^{-7}$	rs2834217	9.8×10^{-198}	-34.8	$<<1.0\times10^{-7}$	*	4480647
		1.3×10^{-13}	-7.4	$<<1.0\times10^{-7}$	rs12626309	1.7×10^{-21}	-9.5	$<<1.0\times10^{-7}$	*GART*	20544
		4.8×10^{-10}	6.2	$<<1.0\times10^{-7}$	rs2251854	1.8×10^{-102}	-21.5	$<<1.0\times10^{-7}$	*ITSN1*	2507
		2.1×10^{-5}	4.3	3.7×10^{-4}	rs2834237	5.0×10^{-7}	5.0	6.5×10^{-6}	*GART*	3780435
rs3783006	c	6.0×10^{-6}	4.5	1.0×10^{-4}	rs4389009	$1.7^{-}\times10^{-40}$	-13.3	$<<1.0\times10^{-7}$	*STK24*	6180050
		1.4×10^{-3}	3.2	0.02	rs9513427	9.7×10^{-6}	4.4	1.7×10^{-4}	*STK24*	4480373
rs7309	a	5.8×10^{-10}	-6.2	$<<1.0\times10^{-7}$	rs1921310	1.8×10^{-13}	-7.4	$<<1.0\times10^{-7}$	*TANK*	2230113
		3.2×10^{-4}	-3.6	4.9×10^{-3}	rs11884495	2.0×10^{-4}	-3.7	0.003	*PSMD14*	2600025

Table S11. Results for the gene expression *cis*-eQTL analysis in brain tissues. SNP ID – nominally significant cognitive performance associated variant; FDR – false discovery rate; LD – linkage disequilibrium; DistanceArrayID – Affimetrix probe identifier; # – genes not considered as biological candidates in subsequent analysis due to distance > 250 kb from a *NSEA* SNP.

SNP ID	Proxy SNP	LD (r^2)	Distance (kb)	Brain tissue	eQTL *P*-vaule	Gene name	ArrayID
rs2721173	rs9071	1.00	6 077	Prefrontal cortex	1.3×10^{-89}	*LRRC14*	10025908411
	rs9071	1.00	6 077	Cerebellum	1.3×10^{-75}	*LRRC14*	10025908411
	rs9071	1.00	6 077	Visual cortex	1.5×10^{-62}	*LRRC14*	10025908411
	rs4532636	0.67	159 994	Prefrontal cortex	8.4×10^{-35}	*LRRC14*	10025908411
	rs4532636	0.67	159 994	Cerebellum	1.2×10^{-28}	*LRRC14*	10025908411
	rs4532636	0.67	159 994	Visual cortex	1.2×10^{-22}	*LRRC14*	10025908411
	rs748193	0.84	62 314	Cerebellum	4.3×10^{-7}	*LRRC24*	10023828992
	rs2721195	0.87	67 418	Cerebellum	4.8×10^{-6}	*LRRC24*	10031920304
	rs3757966	0.97	189	Prefrontal cortex	1.3×10^{-8}	*KIFC2*	10025905398
	rs3757936	0.67	159 994	Cerebellum	1.3×10^{-8}	*KIFC2*	10025905398
	rs2958492	0.65	174 698	Visual cortex	2.3×10^{-6}	*AF075035*	10025934744
rs8049439	rs4788102	0.97	35 883	Prefrontal cortex	1.7×10^{-13}	*EIF3C*	10025912109
	rs12928404	0.97	9 731	Prefrontal cortex	9.7×10^{-12}	*EIF3C*	10025912109
	rs4788102	0.97	35 883	Cerebellum	5.4×10^{-18}	*EIF3C*	10025912109
	rs12928404	0.97	9 731	Cerebellum	7.6×10^{-11}	*EIF3C*	10025912109
	rs4788102	0.97	35 883	Visual cortex	1.2×10^{-9}	*EIF3C*	10025912109
	rs12928404	0.97	9 731	Visual cortex	7.6×10^{-11}	*EIF3C*	10025912109
	rs6565259	0.68	61 278	Prefrontal cortex	8.0×10^{-10}	*LAT*	10023818276
	rs12928404	0.97	9 731	Prefrontal cortex	1.3×10^{-5}	*LAT*	10023818276
	rs1968752	0.80	205 930	Cerebellum	3.5×10^{-5}	*NUPR1*	10023813116
	rs12446550	0.76	294 134	Cerebellum	1.4×10^{-8}	*NFATC2IP*	10025913085
	rs8049439	–	–	Prefrontal cortex	2.3×10^{-5}	*TUFM*	10025905429
rs4658552	rs10926978	0.86	18 718	Prefrontal cortex	5.1×10^{-9}	*SDCCAG8*	10025912019
	rs2484639	0.54	49 431	Visual cortex	3.2×10^{-7}	*SDCCAG8*	10025912019
	rs10926975	0.56	15 154	Visual cortex	1.0×10^{-5}	*SDCCAG8*	10025912019
	rs10926975	0.56	15 154	Prefrontal cortex	1.0×10^{-5}	*SDCCAG8*	10025912019
rs7980687	rs7304782	0.57	103 267	Prefrontal cortex	1.1×10^{-8}	*SBNO1*	10025903955
	rs1727302	0.81	189 781	Prefrontal cortex	2.0×10^{-6}	*SBNO1*	10025903955

	rs655293	0.74	294 306	Cerebellum	5.6×10^{-10}	*C12ORF65*	10025904993
	rs1060105	0.94	164 920	Cerebellum	1.5×10^{-7}	*C12ORF65*	10025904993
	rs1060105	0.94	164 920	Visual cortex	5.8×10^{-7}	*C12ORF65*	10025904993
	rs7304782	0.69	103 267	Visual cortex	2.4×10^{-6}	*C12ORF65*	10025904993
	rs1790098	0.80	167 230	Prefrontal cortex	2.9×10^{-8}	*C12ORF65*	10025904993
	rs1060105	0.94	164 920	Prefrontal cortex	1.1×10^{-6}	*C12ORF65*	10025904993
	rs937564[#]	0.70	345 400	Cerebellum	1.5×10^{-7}	*MPHOSPH9*[#]	10025905642
rs1892700	rs9647066	0.84	13 801	Prefrontal cortex	1.3×10^{-6}	*TMEM50B*	10023807235
	rs8971	0.77	132 519	Cerebellum	7.7×10^{-5}	*GART*	10025903876
	rs2834213	0.66	223 227	Cerebellum	2.8×10^{-7}	*IFNGR2*	10025902355
rs3783006	rs9517337	0.59	70 438	Cerebellum	2.1×10^{-5}	*AK026896*	10025930847
	rs7338549	0.64	31 536	Visual cortex	2.6×10^{-5}	*AF339799*	10025928383

Table S12. Results of gene function prediction analysis in 80,000 gene expression profiles. Pathway terms originate from several databases: (1) Gene Ontology Biological Processes [GO-BioProc], (2) Gene Ontology Molecular Function [GO-MolFunc], (3) Gene Ontology Cellular Component [GO-CellComp], (4) REACTOME, and (5) KEGG. Table lists only genes with terms directly related to neuronal or central nervous system function – full predictions are available at – http://www.ssgac.org[3]. *P*-values refer to the correlation between the Gene principal component profile and the reconstituted Term principal component profile, uncorrected for multiple testing; all reported terms meet False Discovery Rate < 0.05. The Annotated column indicates if the gene has previously been listed as a member of that term (Y) or not (N). Results are sorted alphabetically by gene name.

Gene name	Database	Pathway term	Annotated	*P*-value
ATXN2L	GO-CellComp	npBAF complex	N	1.4×10^{-8}
ATXN2L	GO-CellComp	nBAF complex	N	3.0×10^{-7}
ATXN2L	GO-CellComp	chromatin remodeling complex	N	7.0×10^{-7}
ATXN2L	GO-CellComp	SWI/SNF-type complex	N	1.4×10^{-6}
ATXN2L	GO-CellComp	SWI/SNF complex	N	4.7×10^{-6}
CRYZL1	GO-BiolProc	synaptic vesicle endocytosis	N	9.1×10^{-9}
FARP1	GO-BiolProc	Axonogenesis	N	8.0×10^{-10}
FARP1	GO-BiolProc	axon guidance	N	2.0×10^{-9}
FARP1	GO-CellComp	Actomyosin	N	1.1×10^{-8}
FARP1	GO-CellComp	Synapse	N	2.0×10^{-8}
FARP1	KEGG	Axon guidance	N	5.6×10^{-4}
FARP1	REACTOME	Cell-extracellular matrix interactions	N	1.8×10^{-8}
FARP1	REACTOME	Axon guidance	N	5.9×10^{-8}
KCNMA1	GO-BiolProc	calcium ion transmembrane transport	N	2.8×10^{-12}
KCNMA1	GO-BiolProc	calcium ion transport	N	2.6×10^{-6}
KCNMA1	GO-BiolProc	synapse organization	N	3.9×10^{-6}
KCNMA1	GO-CellComp	Synapse	Y	1.4×10^{-6}
KCNMA1	GO-CellComp	synapse part	Y	2.8×10^{-6}
KCNMA1	GO-CellComp	Costamere	N	3.0×10^{-6}
KCNMA1	GO-CellComp	voltage-gated calcium channel complex	N	8.8×10^{-6}
KCNMA1	GO-CellComp	calcium channel complex	N	1.3×10^{-6}
KCNMA1	GO-CellComp	postsynaptic density	N	3.1×10^{-5}

[3] The link will be activated on the day of publication of this article. The materials that will be posted online are included as a separate appendix to the submitted manuscript.

KCNMA1	GO-CellComp	dendritic spine head	N	3.1×10^{-5}
KCNMA1	GO-CellComp	Dendrite	N	4.0×10^{-5}
KCNMA1	GO-CellComp	neuron projection terminus	Y	4.7×10^{-5}
KCNMA1	GO-MolFunc	calcium channel activity	N	2.5×10^{-9}
KCNMA1	GO-MolFunc	voltage-gated calcium channel activity	N	1.1×10^{-8}
KCNMA1	GO-MolFunc	cation channel activity	Y	1.6×10^{-8}
KCNMA1	GO-MolFunc	voltage-gated cation channel activity	Y	5.6×10^{-8}
KCNMA1	GO-MolFunc	gated channel activity	Y	5.6×10^{-7}
KCNMA1	GO-MolFunc	solute:cation antiporter activity	N	7.4×10^{-7}
KCNMA1	GO-MolFunc	ion channel activity	Y	1.2×10^{-6}
KCNMA1	GO-MolFunc	substrate-specific channel activity	Y	1.6×10^{-6}
KCNMA1	GO-MolFunc	passive transmembrane transporter activity	Y	3.3×10^{-6}
KCNMA1	GO-MolFunc	channel activity	Y	3.3×10^{-6}
KCNMA1	GO-MolFunc	cation:cation antiporter activity	N	5.1×10^{-6}
KCNMA1	GO-MolFunc	glutamate receptor binding	N	9.1×10^{-6}
KCNMA1	GO-MolFunc	voltage-gated channel activity	Y	1.7×10^{-6}
KCNMA1	GO-MolFunc	voltage-gated ion channel activity	Y	1.7×10^{-6}
KCNMA1	GO-MolFunc	calmodulin binding	N	2.1×10^{-5}
KCNMA1	GO-MolFunc	ion gated channel activity	Y	2.3×10^{-5}
KCNMA1	KEGG	Calcium signaling pathway	N	3.4×10^{-9}
KCNMA1	KEGG	Long-term potentiation	N	1.9×10^{-7}
KCNMA1	KEGG	Vascular smooth muscle contraction	Y	1.0×10^{-4}
KCNMA1	REACTOME	Voltage gated Potassium channels	N	2.1×10^{-9}
KCNMA1	REACTOME	Neuronal System	Y	5.7×10^{-9}
KCNMA1	REACTOME	Unblocking of NMDA receptor, glutamate binding and activation	N	1.1×10^{-7}
KCNMA1	REACTOME	Potassium Channels	Y	5.2×10^{-7}
KCNMA1	REACTOME	Depolarization of the Presynaptic Terminal Triggers the Opening of Calcium Channels	N	2.6×10^{-6}
KCNMA1	REACTOME	Reduction of cytosolic Ca++ levels	N	5.0×10^{-6}
KCNMA1	REACTOME	Smooth Muscle Contraction	N	5.5×10^{-6}
KCNMA1	REACTOME	Platelet calcium homeostasis	N	7.5×10^{-6}

KCNMA1	REACTOME	CREB phosphorylation through the activation of CaMKII	N	7.7×10^{-6}
KCNMA1	REACTOME	Transmission across Chemical Synapses	N	1.0×10^{-5}
KCNMA1	REACTOME	Ras activation uopn Ca2+ infux through NMDA receptor	N	1.7×10^{-5}
KCNMA1	REACTOME	Activation of NMDA receptor upon glutamate binding and postsynaptic events	N	2.3×10^{-5}
KCNMA1	REACTOME	Glutamate Binding, Activation of AMPA Receptors and Synaptic Plasticity	N	4.3×10^{-5}
KCNMA1	REACTOME	Trafficking of AMPA receptors	N	4.3×10^{-5}
KIFC2	GO-BiolProc	neurotransmitter secretion	N	2.3×10^{-9}
KIFC2	GO-BiolProc	regulation of synaptic transmission	N	8.7×10^{-9}
KIFC2	GO-BiolProc	regulation of alpha-amino-3-hydroxy-5-methyl-4-isoxazole	N	3.9×10^{-8}
KIFC2	GO-BiolProc	regulation of transmission of nerve impulse	N	4.4×10^{-8}
KIFC2	GO-BiolProc	regulation of neurological system process	N	9.5×10^{-8}
KIFC2	GO-BiolProc	synaptic vesicle transport	N	3.3×10^{-7}
KIFC2	GO-BiolProc	regulation of neurotransmitter levels	N	6.2×10^{-7}
KIFC2	GO-BiolProc	regulation of synaptic plasticity	N	8.3×10^{-7}
KIFC2	GO-BiolProc	synaptic vesicle exocytosis	N	9.0×10^{-8}
KIFC2	GO-BiolProc	glutamate secretion	N	1.0×10^{-6}
KIFC2	GO-BiolProc	generation of a signal involved in cell-cell signaling	N	2.3×10^{-6}
KIFC2	GO-CellComp	Dendrite	N	1.3×10^{-7}
KIFC2	GO-CellComp	dendritic spine head	N	1.7×10^{-7}
KIFC2	GO-CellComp	postsynaptic density	N	1.7×10^{-7}
KIFC2	GO-CellComp	Synaptosome	N	1.8×10^{-7}
KIFC2	GO-CellComp	dendritic spine	N	2.8×10^{-7}
KIFC2	GO-CellComp	neuron spine	N	2.8×10^{-7}
KIFC2	GO-CellComp	voltage-gated calcium channel complex	N	3.0×10^{-7}
KIFC2	GO-CellComp	synapse part	N	1.1×10^{-6}
KIFC2	GO-CellComp	Synapse	N	1.1×10^{-6}
KIFC2	GO-CellComp	ciliary rootlet	N	2.3×10^{-6}
KIFC2	GO-CellComp	cell body	N	1.4×10^{-5}
KIFC2	GO-CellComp	synaptic membrane	N	2.2×10^{-5}

KIFC2	GO-CellComp	calcium channel complex	N	2.2×10^{-5}
KIFC2	GO-MolFunc	voltage-gated calcium channel activity	N	1.5×10^{-5}
KIFC2	REACTOME	Ras activation uopn Ca2+ infux through NMDA receptor	N	6.8×10^{-9}
KIFC2	REACTOME	Depolarization of the Presynaptic Terminal Triggers the Opening of Calcium Channels	N	1.2×10^{-8}
KIFC2	REACTOME	CREB phosphorylation through the activation of CaMKII	N	9.7×10^{-8}
KIFC2	REACTOME	Transmission across Chemical Synapses	N	3.4×10^{-7}
KIFC2	REACTOME	GABA synthesis, release, reuptake and degradation	N	4.2×10^{-6}
KIFC2	REACTOME	Neuronal System	N	1.1×10^{-5}
KIFC2	REACTOME	Dopamine Neurotransmitter Release Cycle	N	2.3×10^{-5}
KIFC2	REACTOME	Serotonin Neurotransmitter Release Cycle	N	2.3×10^{-5}
KIFC2	REACTOME	Trafficking of AMPA receptors	N	2.9×10^{-5}
KIFC2	REACTOME	Glutamate Binding, Activation of AMPA Receptors and Synaptic Plasticity	N	2.9×10^{-5}
KIFC2	REACTOME	Post NMDA receptor activation events	N	3.0×10^{-5}
KIFC2	REACTOME	NCAM signaling for neurite out-growth	N	3.1×10^{-5}
KIFC2	REACTOME	Neurotransmitter Release Cycle	N	3.4×10^{-5}
KIFC2	REACTOME	CREB phosphorylation through the activation of Ras	N	3.4×10^{-5}
KIFC2	REACTOME	Glutamate Neurotransmitter Release Cycle	N	3.7×10^{-5}
NRXN1	GO-BiolProc	glutamate signaling pathway	N	2.6×10^{-19}
NRXN1	GO-BiolProc	neurotransmitter secretion	N	1.5×10^{-16}
NRXN1	GO-BiolProc	gamma-aminobutyric acid signaling pathway	N	5.6×10^{-16}
NRXN1	GO-BiolProc	synaptic vesicle exocytosis	N	7.5×10^{-15}
NRXN1	GO-BiolProc	regulation of neurotransmitter levels	N	3.6×10^{-14}
NRXN1	GO-BiolProc	regulation of synaptic transmission	Y	8.4×10^{-14}
NRXN1	GO-BiolProc	neurotransmitter transport	N	8.7×10^{-14}
NRXN1	GO-BiolProc	regulation of neurological system process	Y	2.9×10^{-14}
NRXN1	GO-BiolProc	regulation of transmission of nerve impulse	Y	8.0×10^{-14}
NRXN1	GO-BiolProc	neuron-neuron synaptic transmission	Y	1.1×10^{-12}
NRXN1	GO-BiolProc	glutamate secretion	N	1.1×10^{-12}
NRXN1	GO-BiolProc	synaptic vesicle transport	N	5.8×10^{-12}

NRXN1	GO-BiolProc	synaptic transmission, glutamatergic	Y	2.1×10^{-11}
NRXN1	GO-BiolProc	signal release	N	6.7×10^{-11}
NRXN1	GO-BiolProc	generation of a signal involved in cell-cell signaling	N	6.7×10^{-11}
NRXN1	GO-BiolProc	learning or memory	Y	2.5×10^{-10}
NRXN1	GO-BiolProc	cellular potassium ion transport	N	2.7×10^{-10}
NRXN1	GO-BiolProc	potassium ion transmembrane transport	N	2.7×10^{-10}
NRXN1	GO-BiolProc	Axonogenesis	Y	3.0×10^{-10}
NRXN1	GO-BiolProc	regulation of excitatory postsynaptic membrane potential	Y	4.1×10^{-10}
NRXN1	GO-CellComp	presynaptic membrane	Y	1.7×10^{-26}
NRXN1	GO-CellComp	Synapse	Y	2.5×10^{-23}
NRXN1	GO-CellComp	Axon	Y	5.2×10^{-23}
NRXN1	GO-CellComp	axon part	Y	2.2×10^{-21}
NRXN1	GO-CellComp	synapse part	Y	4.2×10^{-21}
NRXN1	GO-CellComp	synaptic membrane	Y	2.5×10^{-19}
NRXN1	GO-CellComp	ion channel complex	N	1.3×10^{-16}
NRXN1	GO-CellComp	outer membrane-bounded periplasmic space	N	1.4×10^{-16}
NRXN1	GO-CellComp	periplasmic space	N	1.4×10^{-16}
NRXN1	GO-CellComp	cation channel complex	N	1.0×10^{-15}
NRXN1	GO-CellComp	main axon	N	1.1×10^{-15}
NRXN1	GO-CellComp	Dendrite	N	1.6×10^{-15}
NRXN1	GO-CellComp	external encapsulating structure part	N	2.2×10^{-15}
NRXN1	GO-CellComp	cell envelope	N	2.2×10^{-15}
NRXN1	GO-CellComp	postsynaptic membrane	N	2.3×10^{-14}
NRXN1	GO-CellComp	synaptic vesicle membrane	N	1.7×10^{-13}
NRXN1	GO-CellComp	Axolemma	N	2.8×10^{-13}
NRXN1	GO-CellComp	terminal button	N	3.1×10^{-13}
NRXN1	GO-CellComp	external encapsulating structure	N	4.3×10^{-13}
NRXN1	GO-CellComp	voltage-gated sodium channel complex	N	$5.\times10^{-13}$
NRXN1	GO-MolFunc	glutamate receptor activity	N	2.8×10^{-25}
NRXN1	GO-MolFunc	gated channel activity	N	2.2×10^{-21}

NRXN1	GO-MolFunc	substrate-specific channel activity	N	2.4×10^{-19}
NRXN1	GO-MolFunc	GABA receptor activity	N	7.7×10^{-19}
NRXN1	GO-MolFunc	passive transmembrane transporter activity	N	7.0×10^{-19}
NRXN1	GO-MolFunc	extracellular ligand-gated ion channel activity	N	1.1×10^{-17}
NRXN1	GO-MolFunc	GABA-A receptor activity	N	6.8×10^{-17}
NRXN1	GO-MolFunc	voltage-gated channel activity	N	7.9×10^{-17}
NRXN1	GO-MolFunc	voltage-gated ion channel activity	N	7.9×10^{-17}
NRXN1	GO-MolFunc	ionotropic glutamate receptor activity	N	1.5×10^{-16}
NRXN1	GO-MolFunc	extracellular-glutamate-gated ion channel activity	N	1.7×10^{-16}
NRXN1	GO-MolFunc	ligand-gated channel activity	N	4.7×10^{-16}
NRXN1	GO-MolFunc	ligand-gated ion channel activity	N	4.7×10^{-16}
NRXN1	GO-MolFunc	voltage-gated cation channel activity	N	3.5×10^{-15}
NRXN1	GO-MolFunc	cation channel activity	N	5.2×10^{-12}
NRXN1	GO-MolFunc	voltage-gated sodium channel activity	N	5.6×10^{-12}
NRXN1	KEGG	Neuroactive ligand-receptor interaction	N	9.5×10^{-6}
NRXN1	KEGG	Axon guidance	N	2.1×10^{-5}
NRXN1	KEGG	ErbB signaling pathway	N	2.7×10^{-5}
NRXN1	KEGG	Long-term potentiation	N	3.3×10^{-5}
NRXN1	KEGG	Amyotrophic lateral sclerosis (ALS)	N	2.9×10^{-4}
NRXN1	KEGG	Long-term depression	N	6.2×10^{-4}
NRXN1	KEGG	Cell adhesion molecules (CAMs)	Y	9.8×10^{-4}
NRXN1	REACTOME	GABA A receptor activation	N	7.0×10^{-23}
NRXN1	REACTOME	Neuronal System	N	2.6×10^{-22}
NRXN1	REACTOME	Ligand-gated ion channel transport	N	4.0×10^{-22}
NRXN1	REACTOME	Transmission across Chemical Synapses	N	6.4×10^{-20}
NRXN1	REACTOME	Interaction between L1 and Ankyrins	N	1.6×10^{-18}
NRXN1	REACTOME	Neurotransmitter Receptor Binding And Downstream Transmission In The Postsynaptic Cell	N	1.1×10^{-17}
NRXN1	REACTOME	GABA receptor activation	N	6.7×10^{-17}
NRXN1	REACTOME	Class C/3 (Metabotropic glutamate/pheromone receptors)	N	2.5×10^{-16}
NRXN1	REACTOME	Unblocking of NMDA receptor, glutamate binding and activation	N	1.4×10^{-14}

NRXN1	REACTOME	Potassium Channels	N	5.4×10^{-14}
NRXN1	REACTOME	Ion channel transport	N	3.9×10^{-13}
NRXN1	REACTOME	Serotonin Neurotransmitter Release Cycle	N	7.6×10^{-13}
NRXN1	REACTOME	Dopamine Neurotransmitter Release Cycle	N	7.6×10^{-13}
NRXN1	REACTOME	Voltage gated Potassium channels	N	1.7×10^{-11}
NRXN1	REACTOME	L1CAM interactions	N	5.0×10^{-11}
NRXN1	REACTOME	GABA synthesis, release, reuptake and degradation	N	8.5×10^{-10}
NRXN1	REACTOME	Norepinephrine Neurotransmitter Release Cycle	N	1.7×10^{-9}
NRXN1	REACTOME	Activation of NMDA receptor upon glutamate binding and postsynaptic events	N	2.2×10^{-9}
NRXN1	REACTOME	Glutamate Neurotransmitter Release Cycle	N	5.7×10^{-8}
NRXN1	REACTOME	Ionotropic activity of Kainate Receptors	N	5.9×10^{-8}
PITPNM2	GO-CellComp	cation channel complex	N	1.7×10^{-5}
PITPNM2	GO-CellComp	asymmetric synapse	N	2.3×10^{-5}
PITPNM2	GO-MolFunc	diacylglycerol kinase activity	N	7.03×10^{-7}
PITPNM2	GO-MolFunc	cation channel activity	N	5.7×10^{-6}
PITPNM2	GO-MolFunc	voltage-gated cation channel activity	N	2.5×10^{-5}
PITPNM2	GO-MolFunc	GTPase regulator activity	N	3.3×10^{-5}
PITPNM2	GO-MolFunc	nucleoside-triphosphatase regulator activity	N	4.3×10^{-5}
PITPNM2	GO-MolFunc	ion channel activity	N	5.0×10^{-5}
PITPNM2	GO-MolFunc	gated channel activity	N	6.0×10^{-5}
PITPNM2	GO-MolFunc	calmodulin-dependent protein kinase activity	N	6.1×10^{-5}
PITPNM2	GO-MolFunc	substrate-specific channel activity	N	6.6×10^{-5}
PITPNM2	GO-MolFunc	voltage-gated channel activity	N	1.0×10^{-4}
PITPNM2	GO-MolFunc	voltage-gated ion channel activity	N	1.0×10^{-4}
PITPNM2	KEGG	Calcium signaling pathway	N	1.4×10^{-4}
PITPNM2	REACTOME	Voltage gated Potassium channels	N	1.3×10^{-6}
PITPNM2	REACTOME	Potassium Channels	N	1.4×10^{-6}
PITPNM2	REACTOME	Effects of PIP2 hydrolysis	N	2.1×10^{-6}
PITPNM2	REACTOME	Ras activation uopn Ca2+ infux through NMDA receptor	N	1.5×10^{-5}

PITPNM2	REACTOME	Neuronal System	N	2.2×10^{-5}
PITPNM2	REACTOME	PLC-gamma1 signalling	N	6.6×10^{-5}
PITPNM2	REACTOME	DAG and IP3 signaling	N	8.2×10^{-5}
PITPNM2	REACTOME	Depolarization of the Presynaptic Terminal Triggers the Opening of Calcium Channels	N	9.9×10^{-5}
POU3F2	GO-BiolProc	central nervous system neuron differentiation	N	2.9×10^{-28}
POU3F2	GO-BiolProc	forebrain generation of neurons	N	4.1×10^{-22}
POU3F2	GO-BiolProc	forebrain neuron differentiation	N	3.1×10^{-21}
POU3F2	GO-BiolProc	telencephalon development	Y	5.8×10^{-19}
POU3F2	GO-BiolProc	forebrain development	Y	5.3×10^{-19}
POU3F2	GO-BiolProc	negative regulation of gliogenesis	N	9.1×10^{-18}
POU3F2	GO-BiolProc	astrocyte differentiation	Y	1.0×10^{-17}
POU3F2	GO-BiolProc	negative regulation of glial cell differentiation	N	2.9×10^{-17}
POU3F2	GO-BiolProc	brain development	Y	1.6×10^{-16}
POU3F2	GO-BiolProc	central nervous system neuron development	N	2.7×10^{-16}
POU3F2	GO-BiolProc	glial cell differentiation	Y	4.6×10^{-16}
POU3F2	GO-BiolProc	regulation of neuron differentiation	Y	1.6×10^{-15}
POU3F2	GO-BiolProc	pallium development	Y	2.8×10^{-15}
POU3F2	GO-BiolProc	cerebral cortex development	Y	4.7×10^{-15}
POU3F2	GO-BiolProc	neuron fate commitment	N	1.2×10^{-14}
POU3F2	GO-BiolProc	regulation of neurogenesis	Y	1.3×10^{-14}
POU3F2	GO-BiolProc	central nervous system projection neuron axonogenesis	N	1.5×10^{-14}
POU3F2	GO-BiolProc	positive regulation of neural precursor cell proliferation	N	2.2×10^{-14}
POU3F2	GO-BiolProc	Gliogenesis	Y	2.8×10^{-14}
POU3F2	GO-BiolProc	cerebral cortex neuron differentiation	N	3.0×10^{-14}
POU3F2	GO-CellComp	neuron projection membrane	N	2.8×10^{-7}
POU3F2	GO-CellComp	Axolemma	N	9.9×10^{-7}
POU3F2	GO-CellComp	Dendrite	N	1.2×10^{-6}
POU3F2	GO-CellComp	external encapsulating structure part	N	2.6×10^{-6}
POU3F2	GO-CellComp	cell envelope	N	2.6×10^{-6}

POU3F2	GO-CellComp	periplasmic space	N	7.5×10^{-6}
POU3F2	GO-CellComp	outer membrane-bounded periplasmic space	N	7.5×10^{-6}
POU3F2	GO-MolFunc	ionotropic glutamate receptor activity	N	3.7×10^{-6}
POU3F2	GO-MolFunc	ephrin receptor activity	N	5.0×10^{-6}
POU3F2	REACTOME	CRMPs in Sema3A signaling	N	1.1×10^{-5}
POU3F2	REACTOME	Unblocking of NMDA receptor, glutamate binding and activation	N	1.3×10^{-5}
SCRT1	GO-BiolProc	potassium ion transport	N	9.3×10^{-12}
SCRT1	GO-BiolProc	visual learning	N	2.5×10^{-11}
SCRT1	GO-BiolProc	locomotory behavior	N	3.2×10^{-11}
SCRT1	GO-BiolProc	mating behavior	N	2.5×10^{-10}
SCRT1	GO-BiolProc	visual behavior	N	7.0×10^{-10}
SCRT1	GO-BiolProc	associative learning	N	1.1×10^{-9}
SCRT1	GO-BiolProc	Learning	N	1.3×10^{-9}
SCRT1	GO-BiolProc	regulation of neurotransmitter levels	N	1.4×10^{-9}
SCRT1	GO-BiolProc	ionotropic glutamate receptor signaling pathway	N	2.7×10^{-9}
SCRT1	GO-BiolProc	neurotransmitter secretion	N	2.9×10^{-9}
SCRT1	GO-BiolProc	neurotransmitter transport	N	7.5×10^{-9}
SCRT1	GO-BiolProc	adult locomotory behavior	N	8.1×10^{-9}
SCRT1	GO-BiolProc	response to tropane	N	1.3×10^{-8}
SCRT1	GO-BiolProc	response to cocaine	N	1.3×10^{-8}
SCRT1	GO-BiolProc	neuron-neuron synaptic transmission	N	1.3×10^{-8}
SCRT1	GO-BiolProc	neuromuscular process	N	2.8×10^{-8}
SCRT1	GO-BiolProc	reproductive behavior	N	4.3×10^{-8}
SCRT1	GO-BiolProc	regulation of postsynaptic membrane potential	N	5.4×10^{-8}
SCRT1	GO-BiolProc	membrane hyperpolarization	N	6.4×10^{-8}
SCRT1	GO-BiolProc	synaptic transmission, glutamatergic	N	1.0×10^{-7}
SCRT1	GO-CellComp	axon part	N	2.2×10^{-12}
SCRT1	GO-CellComp	main axon	N	1.1×10^{-10}
SCRT1	GO-CellComp	synapse part	N	1.2×10^{-8}

SCRT1	GO-CellComp	Axon	N	1.2×10^{-8}
SCRT1	GO-CellComp	voltage-gated potassium channel complex	N	1.5×10^{-8}
SCRT1	GO-CellComp	potassium channel complex	N	1.5×10^{-8}
SCRT1	GO-CellComp	cation channel complex	N	3.0×10^{-8}
SCRT1	GO-CellComp	Synapse	N	1.2×10^{-7}
SCRT1	GO-CellComp	neuron projection terminus	N	2.9×10^{-7}
SCRT1	GO-CellComp	neuronal cell body	N	3.0×10^{-7}
SCRT1	GO-CellComp	cell body	N	7.0×10^{-7}
SCRT1	GO-CellComp	axon terminus	N	1.4×10^{-6}
SCRT1	GO-CellComp	terminal button	N	2.8×10^{-6}
SCRT1	GO-CellComp	dendritic spine head	N	5.8×10^{-6}
SCRT1	GO-CellComp	postsynaptic density	N	5.8×10^{-6}
SCRT1	GO-CellComp	ion channel complex	N	7.2×10^{-6}
SCRT1	GO-CellComp	synaptic membrane	N	8.8×10^{-6}
SCRT1	GO-CellComp	synaptic vesicle membrane	N	9.2×10^{-6}
SCRT1	GO-CellComp	ionotropic glutamate receptor complex	N	9.9×10^{-6}
SCRT1	GO-CellComp	periplasmic space	N	3.4×10^{-5}
SCRT1	GO-MolFunc	potassium ion transmembrane transporter activity	N	4.5×10^{-10}
SCRT1	GO-MolFunc	potassium channel activity	N	3.4×10^{-9}
SCRT1	GO-MolFunc	dopamine binding	N	4.5×10^{-9}
SCRT1	GO-MolFunc	voltage-gated potassium channel activity	N	7.4×10^{-9}
SCRT1	GO-MolFunc	voltage-gated cation channel activity	N	2.6×10^{-8}
SCRT1	GO-MolFunc	voltage-gated ion channel activity	N	2.4×10^{-7}
SCRT1	GO-MolFunc	voltage-gated channel activity	N	2.4×10^{-7}
SCRT1	GO-MolFunc	cation channel activity	N	9.1×10^{-7}
SCRT1	GO-MolFunc	gated channel activity	N	1.8×10^{-6}
SCRT1	GO-MolFunc	delayed rectifier potassium channel activity	N	2.3×10^{-6}
SCRT1	GO-MolFunc	extracellular-glutamate-gated ion channel activity	N	4.7×10^{-6}
SCRT1	GO-MolFunc	inorganic cation transmembrane transporter activity	N	6.2×10^{-6}
SCRT1	GO-MolFunc	ionotropic glutamate receptor activity	N	1.8×10^{-5}

SCRT1	KEGG	Neuroactive ligand-receptor interaction	N	2.92E-06
SCRT1	KEGG	Calcium signaling pathway	N	6.67E-04
SCRT1	REACTOME	Voltage gated Potassium channels	N	7.6×10^{-12}
SCRT1	REACTOME	Neuronal System	N	6.8×10^{-11}
SCRT1	REACTOME	Potassium Channels	N	2.1×10^{-10}
SCRT1	REACTOME	Unblocking of NMDA receptor, glutamate binding and activation	N	1.7×10^{-6}
SCRT1	REACTOME	Transmission across Chemical Synapses	N	7.6×10^{-6}
SCRT1	REACTOME	CREB phosphorylation through the activation of CaMKII	N	8.0×10^{-6}
SCRT1	REACTOME	GABA synthesis, release, reuptake and degradation	N	3.5×10^{-5}
SCRT1	REACTOME	Trafficking of AMPA receptors	N	3.8×10^{-5}
SCRT1	REACTOME	Glutamate Binding, Activation of AMPA Receptors and Synaptic Plasticity	N	3.8×10^{-5}
SCRT1	REACTOME	Amine ligand-binding receptors	N	4.0×10^{-5}
SCRT1	REACTOME	Neurotransmitter Release Cycle	N	4.6×10^{-5}
SCRT1	REACTOME	Ras activation uopn Ca2+ infux through NMDA receptor	N	5.7×10^{-5}
SCRT1	REACTOME	Dopamine Neurotransmitter Release Cycle	N	7.0×10^{-5}
SCRT1	REACTOME	Serotonin Neurotransmitter Release Cycle	N	7.0×10^{-5}
TBR1	GO-BiolProc	behavioral defense response	N	1.8×10^{-32}
TBR1	GO-BiolProc	behavioral fear response	N	3.5×10^{-27}
TBR1	GO-BiolProc	fear response	N	6.6×10^{-25}
TBR1	GO-BiolProc	hippocampus development	N	2.8×10^{-23}
TBR1	GO-BiolProc	pallium development	N	8.8×10^{-23}
TBR1	GO-BiolProc	G-protein coupled acetylcholine receptor signaling pathway	N	5.3×10^{-22}
TBR1	GO-BiolProc	axonal fasciculation	N	2.0×10^{-21}
TBR1	GO-BiolProc	limbic system development	N	9.4×10^{-18}
TBR1	GO-BiolProc	neuron recognition	N	3.5×10^{-17}
TBR1	GO-BiolProc	telencephalon development	N	2.1×10^{-16}
TBR1	GO-BiolProc	multicellular organismal response to stress	N	2.0×10^{-14}
TBR1	GO-BiolProc	forebrain development	N	4.9×10^{-14}
TBR1	GO-BiolProc	cerebral cortex neuron differentiation	N	1.2×10^{-13}

TBR1	GO-BiolProc	cerebral cortex radially oriented cell migration	N	1.5×10^{-13}
TBR1	GO-BiolProc	potassium ion transport	N	1.9×10^{-13}
TBR1	GO-BiolProc	synaptic transmission, glutamatergic	N	5.2×10^{-13}
TBR1	GO-BiolProc	ionotropic glutamate receptor signaling pathway	N	3.2×10^{-12}
TBR1	GO-BiolProc	neuron-neuron synaptic transmission	N	8.3×10^{-12}
TBR1	GO-BiolProc	learning or memory	N	1.6×10^{-11}
TBR1	GO-BiolProc	regulation of synaptic plasticity	N	2.4×10^{-11}
TBR1	GO-CellComp	synapse part	N	1.3×10^{-15}
TBR1	GO-CellComp	synaptic membrane	N	5.1×10^{-15}
TBR1	GO-CellComp	cation channel complex	N	5.4×10^{-15}
TBR1	GO-CellComp	potassium channel complex	N	6.5×10^{-15}
TBR1	GO-CellComp	voltage-gated potassium channel complex	N	6.5×10^{-15}
TBR1	GO-CellComp	ion channel complex	N	1.4×10^{-14}
TBR1	GO-CellComp	presynaptic membrane	N	4.7×10^{-13}
TBR1	GO-CellComp	Synapse	N	3.6×10^{-12}
TBR1	GO-CellComp	postsynaptic membrane	N	6.2×10^{-10}
TBR1	GO-CellComp	Dendrite	N	7.3×10^{-10}
TBR1	GO-CellComp	asymmetric synapse	N	5.6×10^{-9}
TBR1	GO-CellComp	site of polarized growth	N	3.0×10^{-8}
TBR1	GO-CellComp	growth cone	N	3.5×10^{-8}
TBR1	GO-CellComp	synaptic vesicle membrane	N	7.1×10^{-8}
TBR1	GO-MolFunc	voltage-gated potassium channel activity	N	2.3×10^{-17}
TBR1	GO-MolFunc	potassium channel activity	N	2.6×10^{-17}
TBR1	GO-MolFunc	voltage-gated cation channel activity	N	7.5×10^{-17}
TBR1	GO-MolFunc	voltage-gated channel activity	N	1.9×10^{-15}
TBR1	GO-MolFunc	voltage-gated ion channel activity	N	1.9×10^{-15}
TBR1	GO-MolFunc	acidic amino acid transmembrane transporter activity	N	2.3×10^{-15}
TBR1	GO-MolFunc	L-glutamate transmembrane transporter activity	N	1.0×10^{-14}
TBR1	GO-MolFunc	potassium ion transmembrane transporter activity	N	6.4×10^{-13}
TBR1	GO-MolFunc	gated channel activity	N	3.8×10^{-12}

TBR1	GO-MolFunc	ion channel activity	N	1.2×10^{-10}
TBR1	GO-MolFunc	substrate-specific channel activity	N	1.5×10^{-10}
TBR1	GO-MolFunc	G-protein coupled amine receptor activity	N	1.9×10^{-19}
TBR1	GO-MolFunc	metal ion transmembrane transporter activity	N	6.3×10^{-10}
TBR1	GO-MolFunc	cation channel activity	N	8.2×10^{-10}
TBR1	GO-MolFunc	GABA receptor activity	N	9.1×10^{-10}
TBR1	GO-MolFunc	passive transmembrane transporter activity	N	1.4×10^{-9}
TBR1	GO-MolFunc	channel activity	N	1.4×10^{-9}
TBR1	GO-MolFunc	GABA-A receptor activity	N	2.6×10^{-9}
TBR1	KEGG	Calcium signaling pathway	N	4.1×10^{-6}
TBR1	KEGG	Neuroactive ligand-receptor interaction	N	7.7×10^{-5}
TBR1	REACTOME	Voltage gated Potassium channels	N	2.4×10^{-15}
TBR1	REACTOME	GABA A receptor activation	N	4.2×10^{-14}
TBR1	REACTOME	Potassium Channels	N	4.4×10^{-14}
TBR1	REACTOME	Neuronal System	N	5.6×10^{-14}
TBR1	REACTOME	Amine ligand-binding receptors	N	4.4×10^{-13}
TBR1	REACTOME	Glutamate Neurotransmitter Release Cycle	N	2.4×10^{-11}
TBR1	REACTOME	Ligand-gated ion channel transport	N	3.8×10^{-11}
TBR1	REACTOME	Transmission across Chemical Synapses	N	5.7×10^{-9}
TBR1	REACTOME	Sema3A PAK dependent Axon repulsion	N	1.6×10^{-8}

Table S13. Results of mouse phenotype prediction analysis in 80,000 gene expression profiles. Phenotypic annotations are obtained from the Mouse Genetics Initiative database (www.informatics.jax.org). Table lists only genes and phenotypic annotations directly related to neuronal or central nervous system function or morphology (marked with an asterix) – full predictions are available at – http://www.ssgac.org[4]. *P*-values refer to the correlation between the Gene principal component profile and the reconstituted phenotypic annotation principal component profile, uncorrected for multiple testing; all reported terms meet False Discovery Rate < 0.05. The Annotated column indicates if the gene has previously been linked to a specific mouse phenotype (Y) or not (N). Results are sorted alphabetically by gene name.

Gene name	Predicted mouse knock-out/-in phenotype	Annotated	*P*-value
AKT3	abnormal hippocampus pyramidal cell layer	N	1.7×10^{-13}
AKT3	small hippocampus	N	1.8×10^{-8}
AKT3	abnormal neocortex morphology	N	5.6×10^{-6}
AKT3	decreased neuron number	N	6.5×10^{-6}
AKT3	placental labyrinth hypoplasia	N	1.1×10^{-5}
AKT3	abnormal brain ventricle morphology	N	1.7×10^{-5}
AKT3	abnormal sensory capabilities/reflexes/nociception	N	1.7×10^{-4}
AKT3	abnormal hippocampus morphology	N	1.9×10^{-4}
AKT3	abnormal cerebellar foliation	N	1.9×10^{-4}
AKT3	abnormal postnatal subventricular zone morphology	N	2.5×10^{-4}
ARHGAP39	dilated lateral ventricles	N	3.2×10^{-5}
ARHGAP39	abnormal ventral spinal root morphology	N	$9{,}0\times10^{-5}$
ARHGAP39	abnormal hippocampus layer morphology	N	1.6×10^{-4}
ARHGAP39	dilated third ventricle	N	2.9×10^{-4}
ARHGAP39	abnormal neural crest cell migration	N	7.9×10^{-4}
ARHGAP39	decreased motor neuron number	N	9.0×10^{-4}
ATXN2L	dilated lateral ventricles	N	4.5×10^{-8}
ATXN2L	increased brain size	N	2.9×10^{-7}
ATXN2L	abnormal dendritic cell morphology	N	4.8×10^{-4}
ATXN2L	dilated third ventricle	N	6.3×10^{-4}
C12orf65	impaired olfaction	N	6.0×10^{-3}
C12orf65	abnormal nervous system physiology	N	7.5×10^{-3}
C12orf65	abnormal medulla oblongata morphology	N	8.2×10^{-3}

[4] The link will be activated on the day of publication of this article. The materials that will be posted online are included as a separate appendix to the submitted manuscript.

C12orf65	abnormal neural tube closure	N	1.4×10^{-2}
C12orf65	abnormal seizure response to electrical stimulation	N	1.6×10^{-2}
C12orf65	abnormal hippocampus CA1 region morphology	N	1.7×10^{-2}
C12orf65	absent distortion product otoacoustic emissions	N	1.8×10^{-2}
C12orf65	increased drinking behavior	N	1.8×10^{-2}
CELF4	abnormal CNS synaptic transmission	N	1.1×10^{-26}
CELF4	abnormal synaptic vesicle number	N	7.6×10^{-22}
CELF4	abnormal miniature excitatory postsynaptic currents	N	4.5×10^{-17}
CELF4	increased susceptibility to pharmacologically induced seizures	N	1.1×10^{-16}
CELF4	abnormal inhibitory postsynaptic currents	N	1.8×10^{-16}
CELF4	abnormal synaptic vesicle recycling	N	2.8×10^{-16}
CELF4	abnormal synaptic vesicle morphology	N	8.8×10^{-16}
CELF4	convulsive seizures	N	2.6×10^{-15}
CELF4	reduced long term potentiation	N	8.2×10^{-15}
CELF4	abnormal excitatory postsynaptic potential	N	2.2×10^{-14}
CELF4	increased synaptic depression	N	1.4×10^{-13}
CELF4	tonic-clonic seizures	Y	6.7×10^{-13}
CELF4	enhanced paired-pulse facilitation	N	7.8×10^{-13}
CELF4	abnormal excitatory postsynaptic currents	N	4.9×10^{-12}
CELF4	abnormal brain wave pattern	N	1.6×10^{-11}
CELF4	sporadic seizures	N	2.1×10^{-11}
CELF4	decreased paired-pulse facilitation	N	3.4×10^{-11}
CELF4	impaired coordination	N	5.7×10^{-11}
CELF4	abnormal conditioned taste aversion behaviour	N	9.7×10^{-11}
CRYZL1	abnormal synaptic vesicle recycling	N	2.1×10^{-4}
CYHR1	abnormal brain white matter morphology	N	4.7×10^{-8}
CYHR1	dilated third ventricle	N	5.1×10^{-5}
CYHR1	abnormal astrocyte morphology	N	1.5×10^{-4}
CYHR1	thick interventricular septum	N	6.7×10^{-4}

DEC1	hydroencephaly	N	3.2×10^{-3}
DEC1	abnormal startle reflex	N	5.6×10^{-3}
DEC1	impaired passive avoidance behavior	N	1.7×10^{-2}
DEC1	abnormal drinking behavior	N	2.2×10^{-2}
FOXH1	abnormal anterior visceral endoderm morphology	N	1.3×10^{-19}
FOXH1	abnormal neural fold formation	Y	1.4×10^{-14}
ITSN1	decreased brain size	N	2.8×10^{-7}
ITSN1	abnormal behavior	N	3.1×10^{-5}
ITSN1	microgliosis	N	4.1×10^{-5}
ITSN1	abnormal hippocampal commissure morphology	N	7.2×10^{-5}
ITSN1	ectopic Purkinje cell	N	1.3×10^{-4}
ITSN1	abnormal otic capsule morphology	N	1.5×10^{-4}
KCNMA1	decreased vasoconstriction	N	6.7×10^{-8}
KCNMA1	abnormal miniature excitatory postsynaptic currents	N	1.2×10^{-7}
KCNMA1	abnormal brain wave pattern	N	3.0×10^{-6}
KCNMA1	limb grasping	N	5.3×10^{-6}
KCNMA1	intracerebral hemorrhage	N	8.3×10^{-6}
KCNMA1	abnormal GABA-mediated receptor currents	N	9.2×10^{-6}
KCNMA1	abnormal synaptic plasticity	N	1.1×10^{-5}
KCNMA1	decreased aggression towards males	N	1.7×10^{-5}
KIFC2	abnormal miniature excitatory postsynaptic currents	N	6.4×10^{-7}
KIFC2	abnormal inhibitory postsynaptic currents	N	2.7×10^{-6}
KIFC2	abnormal spatial learning	N	3.8×10^{-6}
KIFC2	abnormal excitatory postsynaptic currents	N	5.5×10^{-6}
KIFC2	abnormal AMPA-mediated synaptic currents	N	5.6×10^{-6}
KIFC2	reduced long term depression	N	7.5×10^{-6}
KIFC2	abnormal hippocampal mossy fiber morphology	N	9.4×10^{-6}
KIFC2	abnormal long term depression	N	1.3×10^{-5}
KIFC2	enhanced long term potentiation	N	2.3×10^{-5}

KIFC2	enhanced paired-pulse facilitation	N	2.7×10^{-5}
KIFC2	abnormal synaptic vesicle morphology	N	4.5×10^{-5}
KIFC2	abnormal excitatory postsynaptic potential	N	5.2×10^{-5}
KIFC2	abnormal zygomatic bone morphology	N	8.3×10^{-5}
KIFC2	abnormal anxiety-related response	N	9.3×10^{-5}
KIFC2	abnormal synaptic vesicle recycling	N	9.9×10^{-5}
KIFC2	abnormal brain internal capsule morphology	N	1.7×10^{-4}
KIFC2	clonic seizures	N	2.0×10^{-4}
KIFC2	decreased susceptibility to pharmacologically induced seizures	N	2.1×10^{-4}
KIFC2	abnormal CNS synaptic transmission	N	2.1×10^{-4}
LRRC14	impaired coordination	N	2.6×10^{-5}
LRRC14	dilated third ventricle	N	1.2×10^{-3}
LRRC14	small cerebellum	N	1.3×10^{-3}
LRRC14	impaired contextual conditioning behavior	N	1.4×10^{-3}
LRRC14	impaired hearing	N	1.6×10^{-3}
LRRC14	abnormal axon outgrowth	N	1.7×10^{-3}
LRRC14	abnormal retinal apoptosis	N	2.3×10^{-3}
LRRC14	abnormal lateral ventricle morphology	N	3.2×10^{-3}
LRRC14	dilated lateral ventricles	N	3.5×10^{-3}
LRRC14	abnormal brain white matter morphology	N	4.1×10^{-3}
NRXN1	abnormal inhibitory postsynaptic currents	N	1.6×10^{-26}
NRXN1	abnormal CNS synaptic transmission	N	2.6×10^{-25}
NRXN1	abnormal GABA-mediated receptor currents	N	2.6×10^{-24}
NRXN1	abnormal excitatory postsynaptic currents	N	1.2×10^{-22}
NRXN1	hyperactivity	N	6.3×10^{-18}
NRXN1	abnormal synaptic transmission	N	1.4×10^{-17}
NRXN1	abnormal spatial learning	N	7.7×10^{-17}
NRXN1	abnormal synaptic vesicle number	N	3.6×10^{-16}
NRXN1	abnormal posture	N	6.4×10^{-16}
NRXN1	ataxia	N	1.4×10^{-14}

NRXN1	abnormal brain wave pattern	N	2.4×10^{-14}
NRXN1	seizures	N	6.8×10^{-14}
NRXN1	convulsive seizures	N	1.4×10^{-13}
NRXN1	abnormal nervous system electrophysiology	N	4.9×10^{-13}
NRXN1	abnormal spatial reference memory	N	4.9×10^{-13}
NRXN1	abnormal excitatory postsynaptic potential	N	8.1×10^{-13}
NRXN1	abnormal hippocampus morphology	N	1.2×10^{-12}
NRXN1	impaired coordination	N	1.4×10^{-12}
NRXN1	increased startle reflex	N	1.5×10^{-12}
NRXN1	abnormal social/conspecific interaction	N	3.9×10^{-12}
NUPR1	increased brain weight	N	1.7×10^{-7}
NUPR1	abnormal hippocampus layer morphology	N	6.7×10^{-6}
NUPR1	abnormal enteric neuron morphology	N	1.7×10^{-5}
PITPNM2	reduced long term depression	N	4.9×10^{-6}
PITPNM2	abnormal behavior	N	1.2×10^{-4}
PITPNM2	abnormal learning/ memory	N	2.3×10^{-4}
PITPNM2	impaired cued conditioning behavior	N	4.3×10^{-4}
PITPNM2	abnormal excitatory postsynaptic potential	N	5.2×10^{-4}
PITPNM2	impaired contextual conditioning behavior	N	6.6×10^{-4}
PITPNM2	abnormal calcium ion homeostasis	N	8.6×10^{-4}
POU3F2	abnormal brain commissure morphology	N	8.2×10^{-15}
POU3F2	enlarged third ventricle	N	1.2×10^{-14}
POU3F2	abnormal hippocampal mossy fiber morphology	N	2.2×10^{-13}
POU3F2	small olfactory bulb	N	7.7×10^{-12}
POU3F2	abnormal radial glial cell morphology	N	1.1×10^{-11}
POU3F2	abnormal cerebral cortex morphology	N	3.4×10^{-11}
POU3F2	abnormal axon guidance	N	3.5×10^{-10}
POU3F2	increased aggression towards mice	N	8.5×10^{-10}
POU3F2	abnormal corticospinal tract morphology	N	1.4×10^{-10}

POU3F2	decreased brain size	N	3.4×10^{-9}
POU3F2	abnormal hippocampus morphology	N	8.3×10^{-8}
POU3F2	abnormal embryonic/fetal subventricular zone morphology	N	1.0×10^{-8}
POU3F2	decreased corpus callosum size	N	1.6×10^{-8}
POU3F2	abnormal spinal cord interneuron morphology	N	1.8×10^{-8}
POU3F2	abnormal cerebellar foliation	N	1.9×10^{-8}
POU3F2	abnormal cerebrum morphology	N	3.7×10^{-8}
POU3F2	abnormal telencephalon development	N	4.2×10^{-8}
POU3F2	enlarged lateral ventricles	N	8.5×10^{-8}
REEP3	abnormal eating behavior	N	6.1×10^{-5}
REEP3	abnormal myelination	N	2.2×10^{-3}
REEP3	abnormal myelin sheath morphology	N	2.9×10^{-3}
REEP3	abnormal postural reflex	N	3.1×10^{-3}
REEP3	abnormal brain white matter morphology	N	3.2×10^{-3}
SCRT1	impaired conditioned place preference behavior	N	3.3×10^{-12}
SCRT1	abnormal spatial learning	N	8.6×10^{-12}
SCRT1	abnormal spike wave discharge	N	5.6×10^{-11}
SCRT1	impaired behavioral response to addictive substance	N	1.2×10^{-10}
SCRT1	increased exploration in new environment	N	1.6×10^{-10}
SCRT1	absence seizures	N	1.2×10^{-9}
SCRT1	abnormal nervous system electrophysiology	N	1.2×10^{-9}
SCRT1	enhanced coordination	N	1.8×10^{-9}
SCRT1	abnormal inhibitory postsynaptic currents	N	1.1×10^{-8}
SCRT1	decreased vertical activity	N	1.6×10^{-8}
SCRT1	abnormal behavioral response to xenobiotic	N	1.7×10^{-8}
SCRT1	sporadic seizures	N	2.1×10^{-8}
SCRT1	abnormal action potential	N	2.2×10^{-8}
SCRT1	abnormal excitatory postsynaptic currents	N	2.9×10^{-8}
SCRT1	decreased neurotransmitter release	N	2.9×10^{-8}
SCRT1	reduced long term depression	N	2.9×10^{-8}

SCRT1	ataxia	N	8.7×10^{-8}
SCRT1	abnormal brain wave pattern	N	2.3×10^{-7}
SCRT1	impaired swimming	N	3.2×10^{-7}
SCRT1	impaired coordination	N	4.0×10^{-7}
SNRNP35	abnormal brain morphology	N	7.1×10^{-4}
SNRNP35	abnormal action potential	N	1.5×10^{-4}
SNRNP35	astrocytosis	N	2.1×10^{-3}
SNRNP35	absent T cells	N	2.3×10^{-3}
SNRNP35	neurodegeneration	N	2.5×10^{-3}
SNRNP35	seminiferous tubule degeneration	N	2.8×10^{-3}
SNRNP35	abnormal miniature inhibitory postsynaptic currents	N	3.4×10^{-3}
SPNS1	astrocytosis	N	5.2×10^{-8}
SPNS1	Purkinje cell degeneration	N	7.8×10^{-6}
SPNS1	abnormal cued conditioning behavior	N	3.5×10^{-5}
SPNS1	abnormal Reichert's membrane morphology	N	2.2×10^{-4}
SPNS1	abnormal retinal ganglion layer morphology	N	2.8×10^{-4}
SPNS1	limb grasping	N	3.4×10^{-4}
SPNS1	myeloid hyperplasia	N	3.8×10^{-4}
SPNS1	gliosis	N	4.3×10^{-4}
SPNS1	abnormal anterior visceral endoderm morphology	N	9.2×10^{-4}
SPNS1	microgliosis	N	1.1×10^{-3}
TBR1	abnormal inhibitory postsynaptic currents	N	2.7×10^{-22}
TBR1	reduced long term depression	N	3.2×10^{-22}
TBR1	abnormal spatial learning	N	1.9×10^{-20}
TBR1	abnormal brain wave pattern	N	1.1×10^{-19}
TBR1	absent corpus callosum	N	4.7×10^{-18}
TBR1	sporadic seizures	N	4.7×10^{-16}
TBR1	increased startle reflex	N	4.8×10^{-16}
TBR1	abnormal cerebral cortex morphology	N	7.1×10^{-16}

TBR1	abnormal neocortex morphology	N	4.7×10^{-15}
TBR1	abnormal long term depression	N	7.9×10^{-15}
TBR1	hyperactivity	N	1.8×10^{-14}
TBR1	abnormal CNS synaptic transmission	N	4.3×10^{-14}
TBR1	increased anxiety-related response	N	4.4×10^{-13}
TBR1	abnormal GABA-mediated receptor currents	N	5.1×10^{-13}
TBR1	increased susceptibility to pharmacologically induced seizures	N	5.4×10^{-13}
TBR1	abnormal synaptic vesicle number	N	5.9×10^{-13}
TBR1	abnormal excitatory postsynaptic currents	N	2.2×10^{-12}
TBR1	abnormal thalamus morphology	N	3.2×10^{-12}
TBR1	abnormal telencephalon development	N	1.2×10^{-11}
TBR1	abnormal excitatory postsynaptic potential	N	1.7×10^{-8}

Table S14. Results of the tissue, organ and tissue type specific expression analysis in 80,000 gene expression profiles. The expression profiles were annotation into tissues, organs, or cell types using the MeSH database (http://www.nlm.nih.gov/mesh/). Table lists only genes in which show high expression in brain regions or specific nervous system cells – full predictions are available at http://www.ssgac.org[5]. Sample count specifies the number of expression profiles annotated with given annotation. AUC (*area under the curve*) gives the estimate how much of the variation on given gene expression profile is explained by a given tissue, organ or tissue type. *P*-values refer to enriched expression for a given gene in specific tissue, organ or tissue type compared to all other annotation terms. Results are sorted alphabetically by gene name.

Gene name	Tissue, organ or cell type	Sample count	AUC	*P*-value
AKT3	Prefrontal Cortex	46	0.98	6×10^{-30}
AKT3	Frontal Lobe	62	0.95	3×10^{-35}
AKT3	Visual Cortex	34	0.94	3×10^{-19}
AKT3	Occipital Lobe	42	0.94	5×10^{-23}
AKT3	Cerebral Cortex	276	0.94	3×10^{-14}
AKT3	Entorhinal Cortex	83	0.94	2×10^{-43}
AKT3	Temporal Lobe	91	0.94	5×10^{-47}
AKT3	Cerebellum	36	0.93	3×10^{-19}
AKT3	Hippocampus	55	0.93	7×10^{-28}
AKT3	Cerebrum	344	0.92	3×10^{-160}
AKT3	Parietal Lobe	17	0.91	5×10^{-9}
ARHGAP39	Hippocampus	55	0.88	5×10^{-22}
ARHGAP39	Visual Cortex	34	0.87	7×10^{-14}
ARHGAP39	Neural Stem Cells	11	0.87	3×10^{-5}
ARHGAP39	Occipital Lobe	42	0.86	5×10^{-16}
ARHGAP39	Parietal Lobe	17	0.86	3×10^{-7}
ARHGAP39	Hypothalamus	15	0.85	4×10^{-6}
ARHGAP39	Ganglia	11	0.83	2×10^{-4}
ARHGAP39	Cerebral Cortex	276	0.82	2×10^{-75}
ARHGAP39	Entorhinal Cortex	83	0.82	6×10^{-24}
ARHGAP39	Cerebrum	344	0.82	1×10^{-91}
ARHGAP39	Temporal Lobe	91	0.81	1×10^{-24}
ARHGAP39	Brain	1274	0.78	1×10^{-252}

[5] The link will be activated on the day of publication of this article. The materials that will be posted online are included as a separate appendix to the submitted manuscript.

ARHGAP39	Central Nervous System	1302	0.78	2×10^{-251}
C12orf65	Hypothalamus	15	0.68	1×10^{-2}
CRYZL1	Prefrontal Cortex	46	0.95	6×10^{-26}
CRYZL1	Frontal Lobe	62	0.86	1×10^{-22}
CRYZL1	Cerebellum	36	0.86	9×10^{-14}
CRYZL1	Substantia Nigra	22	0.73	2×10^{-4}
CYHR1	Hypothalamus	15	0.82	1×10^{-5}
CYHR1	Putamen	16	0.78	1×10^{-4}
CYHR1	Parotid Gland	19	0.73	4×10^{-4}
CYHR1	Occipital Lobe	42	0.71	2×10^{-6}
CYHR1	Visual Cortex	34	0.71	2×10^{-5}
CYHR1	Cerebellum	36	0.7	3×10^{-5}
CYHR1	Thalamus	16	0.7	7×10^{-3}
CYHR1	Astrocytes	12	0.69	2×10^{-2}
CYHR1	Hippocampus	55	0.67	8×10^{-6}
DEC1	Substantia Nigra	22	0.78	6×10^{-6}
DEC1	Thalamus	16	0.75	5×10^{-4}
DEC1	Mesencephalon	41	0.74	7×10^{-8}
DEC1	Hypothalamus	15	0.73	2×10^{-3}
DEC1	Subthalamic Nucleus	12	0.68	3×10^{-2}
FARP1	Neural Stem Cells	11	0.96	1×10^{-7}
FARP1	Astrocytes	12	0.84	4×10^{-5}
FOXH1	Substantia Nigra	22	0.86	4×10^{-9}
FOXH1	Subthalamic Nucleus	12	0.84	5×10^{-5}
FOXH1	Thalamus	16	0.82	8×10^{-6}
FOXH1	Mesencephalon	41	0.8	4×10^{-11}
FOXH1	Parietal Lobe	17	0.77	9×10^{-5}
FOXH1	Occipital Lobe	42	0.75	4×10^{-8}
FOXH1	Visual Cortex	34	0.74	9×10^{-7}

FOXH1	Hypothalamus	15	0.74	2×10^{-3}
ITSN1	Abdominal Fat	69	0.99	2×10^{-44}
ITSN1	Visual Cortex	34	0.98	4×10^{-22}
ITSN1	Motor Neurons	12	0.98	1×10^{-8}
ITSN1	Occipital Lobe	42	0.97	4×10^{-26}
ITSN1	Prefrontal Cortex	46	0.97	8×10^{-26}
ITSN1	Frontal Lobe	62	0.96	1×10^{-35}
ITSN1	Entorhinal Cortex	83	0.96	4×10^{-47}
ITSN1	Cerebral Cortex	276	0.96	1×10^{-150}
ITSN1	Temporal Lobe	91	0.95	7×10^{-51}
ITSN1	Hippocampus	55	0.95	7×10^{-31}
ITSN1	Spinal Cord	19	0.94	2×10^{-11}
ITSN1	Cerebrum	344	0.94	5×10^{-175}
ITSN1	Cicatrix	19	0.94	3×10^{-11}
ITSN1	Parietal Lobe	17	0.94	4×10^{-10}
ITSN1	Cerebellum	36	0.92	1×10^{-18}
JMJD1C	Cerebellum	36	0.91	4×10^{-17}
JMJD1C	Prefrontal Cortex	46	0.66	2×10^{-4}
KCNMA1	Visual Cortex	34	0.95	7×10^{-20}
KCNMA1	Occipital Lobe	42	0.94	4×10^{-23}
KCNMA1	Prefrontal Cortex	46	0.93	2×10^{-24}
KCNMA1	Entorhinal Cortex	83	0.93	7×10^{-42}
KCNMA1	Aortic Valve	10	0.93	2×10^{-6}
KCNMA1	Muscle, Smooth	248	0.92	1×10^{-115}
KCNMA1	Cerebral Cortex	276	0.92	2×10^{-125}
KCNMA1	Frontal Lobe	62	0.91	10×10^{-29}
KCNMA1	Hippocampus	55	0.9	6×10^{-25}
KIFC2	Putamen	16	0.99	9×10^{-12}
KIFC2	Frontal Lobe	62	0.98	3×10^{-39}

KIFC2	Parietal Lobe	17	0.98	9×10^{-12}
KIFC2	Prefrontal Cortex	46	0.98	4×10^{-29}
KIFC2	Cerebral Cortex	276	0.97	6×10^{-162}
KIFC2	Entorhinal Cortex	83	0.97	7×10^{-50}
KIFC2	Temporal Lobe	91	0.97	3×10^{-54}
KIFC2	Occipital Lobe	42	0.97	9×10^{-26}
KIFC2	Visual Cortex	34	0.97	6×10^{-21}
KIFC2	Hippocampus	55	0.96	6×10^{-32}
KIFC2	Cerebrum	344	0.93	4×10^{-168}
KIFC2	Hypothalamus	15	0.92	2×10^{-8}
KIFC2	Thalamus	16	0.88	1×10^{-7}
KIFC2	Brain	1274	0.82	1×10^{-300}
KIFC2	Neural Stem Cells	11	0.81	3×10^{-4}
KIFC2	Central Nervous System	1302	0.81	1×10^{-300}
KIFC2	Nervous System	1358	0.81	7×10^{-300}
KIFC2	Substantia Nigra	22	0.8	7×10^{-7}
MPHOSPH9	Visual Cortex	34	0.82	5×10^{-11}
MPHOSPH9	Cerebellum	36	0.78	3×10^{-9}
MPHOSPH9	Neural Stem Cells	11	0.74	6×10^{-3}
MPHOSPH9	Occipital Lobe	42	0.74	1×10^{-7}
NPAS2	Prefrontal Cortex	46	0.93	3×10^{-24}
NPAS2	Frontal Lobe	62	0.91	1×10^{-28}
NPAS2	Putamen	16	0.9	3×10^{-8}
NPAS2	Entorhinal Cortex	83	0.85	5×10^{-28}
NPAS2	Hippocampus	55	0.85	6×10^{-19}
NPAS2	Cerebral Cortex	276	0.84	3×10^{-86}
NRXN1	Prefrontal Cortex	46	1	2×10^{-31}
NRXN1	Cerebellum	36	0.99	2×10^{-24}
NRXN1	Cerebral Cortex	276	0.99	5×10^{-47}

NRXN1	Temporal Lobe	91	0.99	5×10^{-58}
NRXN1	Entorhinal Cortex	83	0.99	5×10^{-53}
NRXN1	Occipital Lobe	42	0.99	1×10^{-27}
NRXN1	Visual Cortex	34	0.98	1×10^{-22}
NRXN1	Parietal Lobe	17	0.98	5×10^{-12}
NRXN1	Ganglia	11	0.98	4×10^{-8}
NRXN1	Thalamus	16	0.97	6×10^{-11}
NRXN1	Cerebrum	344	0.97	4×10^{-195}
NRXN1	Mesencephalon	41	0.97	6×10^{-25}
NRXN1	Putamen	16	0.96	1×10^{-11}
NRXN1	Substantia Nigra	22	0.96	6×10^{-14}
NRXN1	Hypothalamus	15	0.96	6×10^{-10}
NRXN1	Motor Neurons	12	0.95	5×10^{-8}
NRXN1	Subthalamic Nucleus	12	0.95	8×10^{-8}
PITPNM2	Frontal Lobe	62	0.88	1×10^{-24}
PITPNM2	Hippocampus	55	0.87	9×10^{-22}
PITPNM2	Prefrontal Cortex	46	0.87	7×10^{-18}
PITPNM2	Putamen	16	0.81	1×10^{-5}
PITPNM2	Temporal Lobe	91	0.8	1×10^{-23}
PITPNM2	Cerebral Cortex	276	0.8	8×10^{-67}
PITPNM2	Entorhinal Cortex	83	0.8	8×10^{-21}
PITPNM2	Heart Ventricles	124	0.79	1×10^{-28}
PITPNM2	Hypothalamus	15	0.78	2×10^{-4}
PITPNM2	Cerebrum	344	0.75	3×10^{-56}
POU3F2	Neural Stem Cells	11	0.98	4×10^{-8}
POU3F2	Spinal Cord	19	0.97	9×10^{-13}
POU3F2	Substantia Nigra	22	0.97	2×10^{-14}
POU3F2	Visual Cortex	34	0.97	5×10^{-21}
POU3F2	Prefrontal Cortex	46	0.97	6×10^{-28}
POU3F2	Occipital Lobe	42	0.97	1×10^{-25}

POU3F2	Retinal Pigment Epithelium	12	0.97	2×10^{-8}
POU3F2	Motor Neurons	12	0.97	2×10^{-8}
POU3F2	Mesencephalon	41	0.96	8×10^{-25}
POU3F2	Parietal Lobe	17	0.96	4×10^{-11}
POU3F2	Frontal Lobe	62	0.96	4×10^{-36}
POU3F2	Cerebral Cortex	276	0.96	5×10^{-151}
POU3F2	Putamen	16	0.95	3×10^{-10}
POU3F2	Cerebrum	344	0.95	2×10^{-180}
POU3F2	Temporal Lobe	91	0.95	2×10^{-49}
POU3F2	Entorhinal Cortex	83	0.95	4×10^{-45}
POU3F2	Subthalamic Nucleus	12	0.95	9×10^{-8}
POU3F2	Hippocampus	55	0.94	4×10^{-30}
REEP3	Retinal Pigment Epithelium	12	0.96	4×10^{-8}
REEP3	Neural Stem Cells	11	0.84	7×10^{-5}
RILPL1	Subthalamic Nucleus	12	0.97	2×10^{-8}
RILPL1	Substantia Nigra	22	0.96	7×10^{-14}
RILPL1	Mesencephalon	41	0.96	5×10^{-24}
RILPL1	Thalamus	16	0.95	4×10^{-10}
RILPL1	Putamen	16	0.94	8×10^{-10}
RILPL1	Parietal Lobe	17	0.94	4×10^{-10}
RILPL1	Temporal Lobe	91	0.93	1×10^{-45}
RILPL1	Spinal Cord	19	0.93	9×10^{-11}
RILPL1	Entorhinal Cortex	83	0.93	4×10^{-41}
RILPL1	Neural Stem Cells	11	0.92	1×10^{-6}
RILPL1	Cerebral Cortex	276	0.92	4×10^{-129}
SBNO1	Cerebellum	36	0.87	9×10^{-15}
SBNO1	Granulocyte Precursor Cells	30	0.86	5×10^{-12}
SBNO1	Prefrontal Cortex	46	0.82	4×10^{-14}
SBNO1	Visual Cortex	34	0.8	8×10^{-10}

SBNO1	Motor Neurons	12	0.76	2×10^{-3}
SBNO1	Frontal Lobe	62	0.76	9×10^{-13}
SBNO1	Occipital Lobe	42	0.76	7×10^{-9}
SLC15A1	Thalamus	16	0.85	2×10^{-6}
SLC15A1	Putamen	16	0.82	1×10^{-5}
SLC15A1	Ganglia	11	0.8	5×10^{-4}
SLC15A1	Subthalamic Nucleus	12	0.74	4×10^{-3}
SLC15A1	Mesencephalon	41	0.69	2×10^{-5}
SLC15A1	Substantia Nigra	22	0.69	2×10^{-3}
SLC15A1	Hypothalamus	15	0.68	2×10^{-2}
SNRNP35	Visual Cortex	34	0.83	2×10^{-11}
SNRNP35	Occipital Lobe	42	0.81	2×10^{-12}
SNRNP35	Subthalamic Nucleus	12	0.76	2×10^{-3}
SNRNP35	Hypothalamus	15	0.75	7×10^{-4}
SULT1A2	Hypothalamus	15	0.83	9×10^{-6}
SULT1A2	Substantia Nigra	22	0.76	3×10^{-5}
SULT1A2	Ganglia	11	0.75	4×10^{-3}
TBR1	Prefrontal Cortex	46	0.99	1×10^{-30}
TBR1	Frontal Lobe	62	0.99	2×10^{-40}
TBR1	Hippocampus	55	0.92	4×10^{-27}
TBR1	Parietal Lobe	17	0.89	3×10^{-8}
TBR1	Cerebral Cortex	276	0.88	2×10^{-104}
TBR1	Temporal Lobe	91	0.86	1×10^{-32}
TBR1	Entorhinal Cortex	83	0.85	4×10^{-28}
TBR1	Subthalamic Nucleus	12	0.81	2×10^{-4}
TBR1	Cerebrum	344	0.79	3×10^{-78}
TBR1	Thalamus	16	0.78	1×10^{-4}
TBR1	Brain	1274	0.75	2×10^{-206}
TBR1	Central Nervous System	1302	0.75	7×10^{-200}

TMEM50B	Motor Neurons	12	0.89	4×10^{-6}
TMEM50B	Thalamus	16	0.87	3×10^{-7}
TMEM50B	Cerebellum	36	0.87	2×10^{-14}
TMEM50B	Neural Stem Cells	11	0.84	8×10^{-5}
TMEM50B	Ganglia	11	0.81	4×10^{-4}
TMEM50B	Spinal Cord	19	0.78	2×10^{-5}
TMEM50B	Neurons	37	0.76	7×10^{-8}
TUFM	Neural Stem Cells	11	0.88	1×10^{-5}
TUFM	Astrocytes	12	0.71	1×10^{-2}
VPS28	Neural Stem Cells	11	0.72	1×10^{-2}

Table S15. Implicated candidate genes in cognitive performance associated genomic loci. Table outlines the levels of supportive biological evidence across several annotation analysis – 1) functional SNP annotation (Supplementary Table S9); 2) promising eQTLs in blood (Supplementary Table S10) and brain (Supplementary Table S11); 3) showing relevant coexpression prediction results for reconstituted pathway terms (Supplementary Table S12), mouse phenotypes (Supplementary Table S13) and high site specific expression profiles (Supplementary Table S14). Two last colums give another layer of supportive evidence from literature – A) clustering into modules related to neuronal or central nervous system function (neuronal function; synaptic transmission, neurogenesis, neuropeptide hormone, nerve myelination) constructed using brain derived gene expression profiles (reported in (28)) and B) isolated from the proteasome of human neocortex postsynaptic density [hPSD] (reported in (34)). SNPs rs1487441 and rs1487441 are located in gene deserts, thus the nearest gene is considered for analysis. Only genes with at least one relevant annotation are listed. SNP ID – nominally significant cognitive performance associated variant; * – denotes a gene not annotated within the co-expression database;

SNP ID	Genes names	nsSNPs	Blood eQTL	Brain eQTL (Prefrontal cortex)	Brain eQTL (Visual cortex)	Brain eQTL (Cerebellum)	Prediction (Brain related functions)	Prediction (Mouse phenotypes)	Region specific expression (Brain)	Modules of neuronal function (Zhang et al)	Postsynaptic density proteome (Bayés et al)	Levels of Evidence
rs1487441	*POU3F2*						Y	Y	Y	Y		4
rs7923609	*JMJD1C*	Y					Y	Y	Y			4
	REEP3							Y	Y			2
rs2721173	*LRRC14*	Y		Y	Y	Y		Y				5
	RECQL4	Y										1
	LRRC24		Y				*na*	*na*	*na*			1
	MFSD3		Y									1
	ARHGAP39							Y	Y			2
	GPT		Y									1
	PPP1R16A		Y									1
	FOXH1							Y	Y			2
	KIFC2			Y			Y	Y	Y	Y		5
	CYHR1							Y	Y			2
	VPS28		Y						Y			2
	CPSF1									Y		1
	SCRT1						Y	Y		Y		3

rs8049439	*ATXN2L*						Y	Y				2
	TUFM		Y	Y					Y		Y	4
	SH2B1	Y										1
	EIF3CL			Y	Y	Y	*na*	*na*	*na*			3
	NFATC2IP					Y			Y	Y		3
	NUPR1					Y		Y				2
	SPNS1		Y					Y				2
	LAT		Y	Y								2
	SULT1A1		Y									1
	SULT1A2		Y						Y			2
	CCDC101		Y									1
rs1606974	*NRXN1*						Y	Y	Y	Y	Y	5
rs2970992	*NPAS2*					Y			Y			2
	NMS						*na*	*na*	*na*	Y		1
rs3127447	*KCNMA1*						Y	Y	Y	Y		4
rs7847231	*DEC1*							Y	Y			2
rs4658552	*SDCCAG8*	Y	Y	Y	Y							4
	AKT3							Y	Y			2
rs1892700	*CRYZL1*						Y	Y	Y			3
	ITSN1		Y					Y	Y	Y	Y	5
	GART	Y	Y			Y						3
	DNAJC28	Y		Y								2
	TMEM50B			Y		Y	Y		Y	Y		5
	IFNGR2					Y	Y					2
rs7980687	*SBNO1*	Y		Y		Y			Y			4
	SETD8		Y				Y					2
	RILPL2		Y									1
	C12orf65			Y	Y	Y		Y	Y			5
	MPHOSPH9								Y			1

	SNRNP35				Y	Y			2
	RILPL1					Y			1
	PITPNM2			Y	Y	Y			3
	TMED2						Y		1
rs1187220	*CELF4*			Y	Y	Y			3
rs3783006	*STK24*	Y							1
	FARP1			Y		Y		Y	3
	SLC15A1					Y			1
rs7309	*TANK*	Y							1
	PSMD14	Y							1
	TBR1			Y	Y	Y	Y		4

Table S16. Regression of cognitive performance on a polygenic score (*PGS*) in the GS, MCTFR, QIMR, and STR cohorts (coefficients for constructing the *PGS* are from the meta-analysis of cognitive performance, with the meta-analysis sample excluding the respective validation sample). Analyses for GS are based on 1,081 siblings from 476 independent families, analyses for MCTFR are based on 1,346 siblings from 673 independent families, analyses for QIMR are based on 1,426 individuals from 628 independent families, and analyses for STR are based on 810 DZ twins from 405 independent families. ΔR^2 is the incremental R^2 of adding the *PGS* to the regression. The family dummies explain 64.3% of the variance for GS, 72.8% for MCTFR, 68.4% for QIMR, and 77.4% for STR. Standard errors are clustered at the family level. The pooled estimates of are calculated using inverse-variance weighting.

Analysis		GS	MCTFR	QIMR	STR	Pooled
Without family dummies	Beta	0.05	0.05	0.06	0.07	0.06
	S.E.	0.04	0.03	0.03	0.04	0.02
	p-value	0.19	0.11	0.03	0.10	8.17×10^{-4}
	ΔR^2	0.0023	0.0022	0.0041	0.0044	-
With family dummies	Beta	-0.05	0.05	0.03	0.08	0.03
	S.E.	0.07	0.06	0.06	0.07	0.03
	p-value	0.41	0.36	0.61	0.26	0.36
	ΔR^2	0.0007	0.0007	0.0002	0.0015	-

Table S17. Simulation Results for Power of Within-Family Analysis

β [R^2]	Model	Mean($\hat{\beta}$)	Mean(Standard Error)	Power
0.045 [0.20%]	Without family dummies	0.044	0.017	78.2%
	With family dummies	0.043	0.027	31.2%
0.065 [0.42%]	Without family dummies	0.065	0.017	96.8%
	With family dummies	0.063	0.027	64.2%

Table S18. Results from polygenic-score analysis in the Health and Retirement Study. TWR = Total Word Recall, TMS = Total Mental Score, TC = Total Cognition. Standard errors are clustered per individual in the regression and standard errors of the regression coefficients are given in square brackets below the regression coefficients. The regressions for ΔTMS and ΔTC have the knots of the age spline at 70 and 80 and do not include person-wave observations with age < 60. * $p < 0.05$; ** $p < 0.01$. ΔR^2 denotes the increase in R^2 of a model with the score, and score interactions if applicable, compared to a model with only the age spline and sex.

	(1) TWR	(2) TWR	(3) TMS	(4) TMS	(5) TC	(6) TC	(7) ΔTWR	(8) ΔTWR	(9) ΔTMS	(10) ΔTMS	(11) ΔTC	(12) ΔTC
Score	0.040**	0.047**	0.062**	0.072**	0.057**	0.075**	-0.003	-0.005	-0.002	-0.008	-0.001	-0.006
	[0.007]	[0.010]	[0.010]	[0.012]	[0.009]	[0.012]	[0.002]	[0.004]	[0.004]	[0.006]	[0.004]	[0.007]
Age < 60	-0.006**	-0.006**	-0.006*	-0.006*	-0.007**	-0.007**	-0.002	-0.002				
	[0.002]	[0.002]	[0.003]	[0.003]	[0.002]	[0.002]	[0.001]	[0.001]				
Age 60-69	-0.037**	-0.037**	-0.004*	-0.004*	-0.031**	-0.031**	-0.006**	-0.006**	-0.013*	-0.013*	-0.023**	-0.023**
	[0.002]	[0.002]	[0.002]	[0.002]	[0.002]	[0.002]	[0.001]	[0.001]	[0.006]	[0.006]	[0.006]	[0.006]
Age 70-79	-0.051**	-0.051**	-0.018**	-0.018**	-0.047**	-0.047**	-0.005**	-0.005**	-0.007**	-0.007**	-0.006**	-0.006**
	[0.002]	[0.002]	[0.003]	[0.003]	[0.003]	[0.003]	[0.001]	[0.001]	[0.002]	[0.002]	[0.002]	[0.002]
Age ≥ 80	-0.056**	-0.056**	-0.053**	-0.053**	-0.066**	-0.067**	-0.006**	-0.006**	-0.019**	-0.019**	-0.015**	-0.015**
	[0.004]	[0.004]	[0.007]	[0.007]	[0.006]	[0.006]	[0.002]	[0.002]	[0.003]	[0.003]	[0.002]	[0.002]
Female	0.345**	0.344**	-0.169**	-0.169**	0.199**	0.198**	0.002	0.002	-0.018*	-0.018*	-0.011	-0.011
	[0.015]	[0.015]	[0.019]	[0.019]	[0.019]	[0.019]	[0.005]	[0.005]	[0.009]	[0.009]	[0.008]	[0.008]
Age 60-69 × score		0.000		-0.002		-0.002		0.000				
		[0.002]		[0.002]		[0.002]		[0.001]				
Age 70-79 × score		-0.001		0.002		0.000		0.001		0.002		0.002
		[0.003]		[0.003]		[0.003]		[0.001]		[0.001]		[0.001]
Age ≥ 80 × score		-0.008*		-0.004		-0.008		-0.004*		-0.003		-0.005*
		[0.004]		[0.006]		[0.005]		[0.002]		[0.002]		[0.002]
Constant	0.107	0.108	0.764**	0.764**	0.533**	0.534**	0.154*	0.155*	1.008**	1.006**	1.620**	1.619**
	[0.124]	[0.124]	[0.151]	[0.151]	[0.143]	[0.143]	[0.072]	[0.071]	[0.381]	[0.381]	[0.395]	[0.395]
N, person-wave	49,988	49,988	32,289	32,289	32,289	32,289	40,744	40,744	20,781	20,781	20,781	20,781
N, persons	8,652	8,652	8,539	8,539	8,539	8,539	8,543	8,543	5,248	5,248	5,248	5,248
R^2	0.164	0.164	0.038	0.038	0.135	0.135	0.002	0.002	0.005	0.005	0.000	0.000
ΔR^2	0.002	0.002	0.004	0.004	0.003	0.004	0.000	0.000	0.000	0.000	0.000	0.000

Table S19. Results from polygenic-score analysis in the Health and Retirement Study with years of education added as a control variable. TWR = Total Word Recall, TMS = Total Mental Score, TC = Total Cognition. Standard errors are clustered per individual in the regression and standard errors of the regression coefficients are given in square brackets below the regression coefficients. The regressions for ΔTMS and ΔTC have the knots of the age spline at 70 and 80 and do not include person-wave observations with age < 60. * $p < 0.05$; ** $p < 0.01$. ΔR^2 denotes the increase in R^2 of a model with the score, and score interactions if applicable, compared to a model with only the age spline and sex.

	(1) TWR	(2) TWR	(3) TMS	(4) TMS	(5) TC	(6) TC	(7) ΔTWR	(8) ΔTWR	(9) ΔTMS	(10) ΔTMS	(11) ΔTC	(12) ΔTC
Score	0.014*	0.022*	0.031**	0.043**	0.024**	0.045**	-0.002	-0.005	-0.003	-0.010	-0.002	-0.007
	[0.007]	[0.009]	[0.009]	[0.012]	[0.008]	[0.011]	[0.002]	[0.004]	[0.004]	[0.006]	[0.004]	[0.007]
Age < 60	-0.003	-0.003	-0.000	-0.000	-0.001	-0.001	-0.002	-0.002				
	[0.002]	[0.002]	[0.003]	[0.002]	[0.002]	[0.002]	[0.001]	[0.001]				
Age 60-69	-0.032**	-0.032**	-0.002	-0.002	-0.029**	-0.029**	-0.006**	-0.006**	-0.013*	-0.013*	-0.023**	-0.023**
	[0.002]	[0.002]	[0.002]	[0.002]	[0.002]	[0.002]	[0.001]	[0.001]	[0.006]	[0.006]	[0.006]	[0.006]
Age 70-79	-0.050**	-0.050**	-0.016**	-0.016**	-0.045**	-0.045**	-0.005**	-0.005**	-0.007**	-0.007**	-0.006**	-0.006**
	[0.002]	[0.002]	[0.003]	[0.003]	[0.003]	[0.003]	[0.001]	[0.001]	[0.002]	[0.002]	[0.002]	[0.002]
Age ≥ 80	-0.054**	-0.054**	-0.051**	-0.051**	-0.064**	-0.064**	-0.006**	-0.006**	-0.019**	-0.019**	-0.015**	-0.015**
	[0.004]	[0.004]	[0.007]	[0.006]	[0.006]	[0.005]	[0.002]	[0.002]	[0.003]	[0.003]	[0.002]	[0.002]
Female	0.392**	0.391**	-0.109**	-0.109**	0.261**	0.261**	0.002	0.002	-0.015	-0.015	-0.010	-0.010
	[0.014]	[0.014]	[0.018]	[0.018]	[0.017]	[0.017]	[0.005]	[0.005]	[0.009]	[0.009]	[0.008]	[0.008]
Years of education	0.101**	0.101**	0.120**	0.120**	0.127**	0.127**	0.000	0.000	0.004*	0.004*	0.001	0.001
	[0.003]	[0.003]	[0.004]	[0.004]	[0.004]	[0.004]	[0.001]	[0.001]	[0.002]	[0.002]	[0.002]	[0.002]
Age 60-69 × score		-0.000		-0.002		-0.002		0.000				
		[0.002]		[0.002]		[0.002]		[0.001]				
Age 70-79 × score		-0.002		0.002		-0.000		0.001		0.002		0.002
		[0.002]		[0.003]		[0.003]		[0.001]		[0.001]		[0.001]
Age ≥ 80 × score		-0.007		-0.004		-0.007		-0.004*		-0.003		-0.005*
		[0.004]		[0.006]		[0.005]		[0.002]		[0.002]		[0.002]
Constant	-1.513**	-1.512**	-1.270**	-1.270**	-1.622**	-1.621**	0.149*	0.149*	0.950*	0.948*	1.637**	1.636**
	[0.124]	[0.124]	[0.158]	[0.158]	[0.146]	[0.146]	[0.074]	[0.074]	[0.386]	[0.386]	[0.399]	[0.399]
N, person-wave	49,827	49,827	32,204	32,204	32,204	32,204	40,622	40,622	20,737	20,737	20,737	20,737
N, persons	8,615	8,615	8,504	8,504	8,504	8,504	8,506	8,506	5,235	5,235	5,235	5,235
R^2	0.225	0.225	0.128	0.128	0.236	0.236	0.002	0.002	0.005	0.005	0.005	0.005
ΔR^2	0.000	0.000	0.001	0.001	0.001	0.001	0.000	0.000	0.000	0.000	0.000	0.000

Table S20. Power of GWAS on cognitive performance vs. candidate-SNP method in our Cognitive Performance Sample (N = 24,189)

	Effect size of SNP on cognitive performance (in R^2)			
	0.02%	0.04%	0.06%	0.08%
GWAS ($\alpha = 5\times10^{-8}$)	0.06%	1%	5%	15%
Candidate-SNP (α = .00072)	12%	39%	67%	85%

Source: Authors' calculations using (22).

Table S21. Ex ante calculations of the expected number of true positive results, given alternative thresholds of including SNPs associated with educational attainment (EA) in the second stage on cognitive performance. Calculations are based on the actual sample sizes for EA in stage 1 (N = 106,703) and for cognitive performance in stage 2 (N = 24,189). The calculations assume that the effect of a SNP that is truly associated with EA only operates through cognitive performance and no other mediating factor. Under this assumption, the effect size of an EA-associated SNP would be attenuated by the imperfect correlation between EA and cognitive performance (see SI Appendix section 15). (1) and (2) are based on actual results of the stage 1 GWAS, after pruning SNPs for LD (the HapMap 2 CEU genotypes were used as reference panel; the physical threshold for clumping was 1000 kB, and the R^2 threshold for clumping was 0.01). Power in (3) and (7) was calculated using G*Power 3.1 (48, 49). Posterior beliefs in row (4) are calculated using Bayes' formula (21), with prior beliefs equal to 0.01%, power equal to (3), and α equal to the respective p-value threshold of the column. (5) results from dividing the family-wide significance level of 0.05 by (1). (6) results from dividing (2) by the assumed phenotypic correlation between EA and cognitive performance (0.6). (8) reports the expected number of true positives in the second stage by multiplying (1) × (4) × (7). (9) is calculated using Bayes' formula (21), with prior beliefs equal to (4), power equal to (7), and α equal to (5). Note that the available sample size for stage 2 and the assumed correlation between EA and cognitive performance only affect the absolute values in (8), whereas the p-value threshold that maximizes (8) depends only on the results of the first-stage GWAS.

		p-value threshold for including EA-associated SNPs in the second stage analyses on cognitive performance							
		5×10^{-8}	1×10^{-7}	1×10^{-6}	1×10^{-5}	1×10^{-4}	1×10^{-3}	1×10^{-2}	5×10^{-2}
Results of stage 1									
(1)	Number of EA-associated candidate SNPs	3	4	15	69	198	891	3,013	5,720
(2)	Avg R^2 of SNPs with EA	2.80×10^{-4}	2.73×10^{-4}	2.33×10^{-4}	1.98×10^{-4}	1.65×10^{-4}	1.25×10^{-4}	9.11×10^{-5}	7.05×10^{-5}
(3)	Ex-post power (two-sided) in first stage	55%	52%	52%	57%	62%	64%	71%	78%
(4)	Posterior belief that a candidate SNP from (1) is truly associated with EA	99.9%	99.8%	98.1%	85.1%	38.3%	6.0%	0.7%	0.2%
Ex-ante expectations for stage 2									
(5)	Bonferroni-adjusted p-value for second stage	1.67×10^{-2}	1.25×10^{-2}	3.33×10^{-3}	7.25×10^{-4}	2.53×10^{-4}	5.61×10^{-5}	1.66×10^{-5}	8.74×10^{-6}
(6)	Expected avg R^2 of SNPs in second stage given (2)	7.77×10^{-4}	7.59×10^{-4}	6.46×10^{-4}	5.51×10^{-4}	4.57×10^{-4}	3.47×10^{-4}	2.53×10^{-4}	1.96×10^{-4}
(7)	Expected power (two-sided) in second stage given (5) and (6)	97.4%	96.3%	84.6%	60.7%	36.9%	12.9%	3.3%	1.2%
(8)	Expected true positives second stage	3	4	12	36	28	7	7	0
(9)	Posterior belief (true|significant), using the p-value threshold of (5)	100%	100%	100%	100%	99.9%	99.5%	99.5%	75.8%

Additional Notes

1. Author contributions

Daniel Benjamin, David Cesarini, and Philipp Koellinger conceived and designed the study and organized the SSGAC consortium. Cornelius Rietveld performed the selection of education-associated SNPs and together with Gail Davies he also performed the quality control and meta-analyses of cohort-specific GWAS results. Anna Vinkhuyzen contributed to the interpretation of the meta-analysis results. The CHIC consortium was organized by George Davey Smith, Ian Deary, Robert Plomin and Peter Visscher. Beben Benyamin and Peter Visscher provided the CHIC meta-analysis results. Patrick Turley developed the correction of effect sizes for the winner's curse and the power calculations for the HRS polygenic score analyses. Christopher Chabris and Olga Rostapshova performed the selection of theory-based candidate SNPs. Daniel Benjamin conducted the Bayesian analysis of the credibility of the SNP associations. Cornelius Rietveld performed the polygenic score analyses in the HRS. Riccardo Marioni, Sarah Medland, Michael Miller, and Cornelius Rietveld performed the polygenic score analyses in the family samples. Tõnu Esko, Valur Emilsson, Rudolf Fehrmann, Lude Franke, Andrew Johnson, Juha Karjalainen and Tune Pers conducted the biological annotation. Daniel Benjamin, David Cesarini, Philipp Koellinger and Cornelius Rietveld wrote the first draft of the manuscript. Daniel Benjamin, David Cesarini, Tõnu Esko, Philipp Koellinger, Cornelius Rietveld and Patrick Turley all wrote substantial portions of the supplementary materials. Cornelius Rietveld prepared most of the tables and figures in the main text and supplementary materials. Christopher Chabris, Ian Deary, Robert Plomin, Vincent Jaddoe, Magnus Johannesson, David Laibson, Steven Pinker, Henning Tiemeier, Nicholas Timpson, Peter Visscher and Mary Ward critically reviewed and edited the manuscript.

2. Cohort-specific contributions

Cohort	Author	Overseeing (PI)	Genotyping	Phenotyping	Data analysis
ALSPAC	George Davey Smith	X			
	Nicholas Timpson		X	X	
	George McMahon				X
	Mary Ward				X
ERF	Sven van der Lee				X
	Carla Ibrahim-Verbaas				X
	Najaf Amin				X
	André Uitterlinden		X		
	Cornelia van Duijn	X	X	X	
GenR	Henning Tiemeier	X		X	
	Vincent Jaddoe	X	X		
	Christiaan De Leeuw				X
	Danielle Posthuma	X			X
	Frank Verhulst	X			
	Fernando Rivadeneira		X		
GS	Blair Smith			X	
	David Porteous		X	X	
	Caroline Hayward		X		
	Riccardo Marioni				X
HU	James Lee		X	X	X
	Steven Pinker	X			
	Christopher Chabris	X			
	David Laibson	X			
	Edward Glaeser	X			
LBC	Gail Davies		X		X
	David Liewald		X		X

	John Starr	X		X	
	Ian Deary	X		X	
MCTFR	Michael B. Miller		X	X	X
	Matt McGue	X			
	William G. Iacono	X			
	Jaime Derringer				X
QIMR	Sarah Medland				X
	Margaret Wright	X		X	
	Narelle Hansell			X	X
	Nicholas Martin	X	X		
STR	Patrik Magnusson		X	X	X
	Nancy Pedersen	X			
	Paul Lichtenstein	X			
	Magnus Johannesson	X		X	X
	Cornelius Rietveld				X
	David Cesarini				X
TEDS	Robert Plomin	X			
	Maciej Trzaskowski				X

3. Additional acknowledgements

The authors of this article are grateful to the Social Science Genetic Association Consortium (http://www.ssgac.org) for providing the meta-analysis data on educational attainment. In particular, we thank: Abdel Abdellaoui, Arpana Agrawal, Eva Albrecht, Behrooz Z. Alizadeh, Jüri Allik, John R. Attia, Stefania Bandinelli, John Barnard, François Bastardot, Sebastian E. Baumeister, Jonathan Beauchamp, Kelly S. Benke, David A. Bennett, Klaus Berger, Lawrence F. Bielak, Laura J. Bierut, Jeffrey A. Boatman, Dorret I. Boomsma, Patricia A. Boyle, Ute Bültmann, Harry Campbell, Lynn Cherkas, Mina K. Chung, Francesco Cucca, Mariza de Andrade, Philip L. De Jager, Jan-Emmanuel De Neve, George V. Dedoussis, Panos Deloukas, Maria Dimitriou, Gudny Eiriksdottir, Niina Eklund, Martin F. Elderson, Johan G. Eriksson, Daniel S. Evans, David M. Evans, Jessica D. Faul, Luigi Ferrucci, Krista Fischer, Melissa E. Garcia, Christian Gieger, Håkon K. Gjessing, Patrick J.F. Groenen, Henrik Grönberg, Vilmundur Gudnason, Sara Hägg, Per Hall, Jennifer R. Harris, Juliette M. Harris, Tamara B. Harris, Nicholas D. Hastie, Andrew C. Heath, Dena G. Hernandez, Wolgang Hoffmann, Adriaan Hofman, Albert Hofman, Rolf Holle, Elizabeth G. Holliday, Christina Holzapfel, Jouke-Jan Hottenga, Min A. Jhun, Thomas Illig, Erik Ingelsson, Bo Jacobsson, Marjo-Riitta Järvelin, Peter K. Joshi, Astanand Jugessur, Marika Kaakinen, Mika Kähönen, Stavroula Kanoni, Jaakkko Kaprio, Sharon L.R. Kardia, Robert M. Kirkpatrick, Ivana Kolcic, Matthew Kowgier, Kati Kristiansson, Robert F. Krueger, Zóltan Kutalik, Jari Lahti, Antti Latvala, Lenore J. Launer, Debbie A. Lawlor, Sang H. Lee, Terho Lethimäki, Jingmei Li, Peter K. Lichtner, Peng Lin, Penelope A. Lind, Yongmei Liu, Kurt Lohman, Marisa Loitfelder, Pamela A. Madden, Tomi E. Mäkinen, Pedro Marques Vidal, Nicolas W. Martin, Marco Masala, Osorio Meirelles, Andres Metspalu, Michelle N. Meyer, Andreas Mielck, Lili Milani, Grant W. Montgomery, Sutapa Mukherjee, Ronny Myhre, Marja-Liisa Nuotio, Dale R. Nyholt, Christopher J. Oldmeadow, Ben A. Oostra, Lyle J. Palmer, Aarno Palotie, Brenda Penninx, Markus Perola, Katja E. Petrovic, Wouter J. Peyrot, Patricia A. Peyser, Ozren Polašek, Martin Preisig, Lydia Quaye, Katri Räikkönen, Olli T. Raitakari, Anu Realo, Eva Reinmaa, John P. Rice, Susan M. Ring, Samuli Ripatti, Thais S. Rizzi, Igor Rudan, Aldo Rustichini, Veikko Salomaa, Antti-Pekka Sarin, David Schlessinger, Helena Schmidt, Reinhold Schmidt, Rodney J. Scott, Konstantin Shakhbazov, Albert V. Smith, Jennifer A. Smith, Harold Snieder, Beate St Pourcain, Jae Hoon Sul, Ida Surakka, Rauli Svento, Toshiko Tanaka, Antonio Terracciano, Alexander Teumer, A. Roy Thurik, Matthijs J.H.M. van der Loos, Frank J.A. van Rooij, David R. Van Wagoner, Erkki Vartiainen, Jorma Viikari, Veronique Vitart, Peter K. Vollenweider, Henry Völzke, Judith M. Vonk, Gérard Waeber, David R. Weir, Jürgen Wellmann, Harm-Jan Westra, H.-Erich Wichmann, Elisabeth Widen, Gonneke Willemsen, James F. Wilson, Alan F. Wright, Jian Yang, Lei Yu, Wei Zhao.

ALSPAC (**Avon Longitudinal Study of Parents and Children**) **–** We are extremely grateful to all the families who took part in this study, the midwives for their help in recruiting them, and the whole ALSPAC team, which includes interviewers, computer and laboratory technicians, clerical workers, research scientists, volunteers, managers, receptionists and nurses. The UK Medical Research Council and the Wellcome Trust (Grant ref: 092731) and the University of Bristol provide core support for ALSPAC. The MRC Integrative Epidemiology Unit is supported by the UK Medical Research Council and University of Bristol Integrative Epidemiology Unit MC_UU_12013/1-9.

ERF (Erasmus Rucphen Family Study) – The ERF study as a part of EUROSPAN (European Special Populations Research Network) was supported by European Commission FP6 STRP grant number 018947 (LSHG-CT-2006-01947) and also received funding from the European Community's Seventh Framework Programme (FP7/2007-2013)/grant agreement HEALTH-F4-2007-201413 by the European Commission under the programme "Quality of Life and Management of the Living Resources" of 5th Framework Programme (no. QLG2-CT-2002-01254). The ERF study was further supported by ENGAGE consortium and CMSB. High-throughput analysis of the ERF data was supported by joint grant from Netherlands Organisation for Scientific Research and the Russian Foundation for Basic Research (NWO-RFBR 047.017.043). We are grateful to all study participants and their relatives, general practitioners and neurologists for their contributions and to P. Veraart for her help in genealogy, J. Vergeer for the supervision of the laboratory work and P. Snijders for his help in data collection.

GenR (Generation R) – The Generation R Study is conducted by the Erasmus Medical Center, Rotterdam in close collaboration with the Erasmus University Rotterdam, the Municipal Health Service Rotterdam area, the Rotterdam Homecare Foundation and the Stichting Trombosedienst & Artsenlaboratorium Rijnmond (STAR), Rotterdam. The authors wish to thank the parents and children that participate in the Generation R Study. The Generation R Study is made possible by financial support from the Erasmus Medical Center, Rotterdam, the Erasmus University Rotterdam, and the Netherlands Organization for Health Research and Development (ZonMw grant numbers 10.000.1003); the present study was supported by an additional grant from the Sophia Foundation for Scientific Research (SSWO; grant 547, 2008) and a VIDI grant to HT from the Netherlands Organization for Scientific Research (NWO; grant number 017.106.370). DP gratefully acknowledges financial support from the Netherlands Organization for Scientific Research (NWO/MaGW VIDI 016-065-318 and NWO/NIHC 433-09-228). CdL gratefully acknowledges financial support from the Netherlands Organization for Scientific Research (NWO Complexity project 645.000.003).

GS (Generation Scotland) – Generation Scotland received core support from the Chief Scientist Office of the Scottish Government Health Directorates (CZD/16/6) and the Scottish Funding Council (HR03006). We are grateful to all the families who took part, the general practitioners and the Scottish School of Primary Care for their help in recruiting them, and the whole Generation Scotland team, which includes interviewers, computer and laboratory technicians, clerical workers, research scientists, volunteers, managers, receptionists, healthcare assistants and nurses. Genotyping of Generation Scotland was funded by the Medical Research Council UK and carried out at the Wellcome Trust Clinical Research Facility at the Western General Hospital, Edinburgh.

HRS (Health and Retirement Study) – HRS is supported by the National Institute on Aging (NIA U01AG009740). The genotyping was funded as a separate award from the National Institute on Aging (RC2 AG036495). Our genotyping was conducted by the NIH Center for Inherited Disease Research (CIDR) at Johns Hopkins University. Genotyping quality control and final preparation of the data were performed by the Genetics Coordinating Center at the University of Washington. HRS genotype data have been deposited in the NIH GWAS repository (dbGaP).

HU (Harvard/Union Study) – This study was supported by the authors' research funds and a grant from the National Institute on Aging to the National Bureau of Economic Research (T32-AG00186).

LBC 1921 and 1936 (Lothian Birth Cohorts of 1921 and 1936) – We thank the cohort participants and team members who contributed to these studies. Phenotype collection in the Lothian Birth Cohort 1921 was supported by the BBSRC, The Royal Society and The Chief Scientist Office of the Scottish Government. Phenotype collection in the Lothian Birth Cohort 1936 was supported by Age UK (The Disconnected Mind project). Genotyping of the cohorts was funded by the UK Biotechnology and Biological Sciences Research Council (BBSRC). The work was undertaken by The University of Edinburgh Centre for Cognitive Ageing and Cognitive Epidemiology, part of the cross council Lifelong Health and Wellbeing Initiative (MR/K026992/1). Funding from the BBSRC and Medical Research Council is gratefully acknowledged.

MCTFR (Minnesota Center for Twin and Family Research) – The Minnesota Center for Twin and Family Research (MCTFR) is supported by USPHS Grants from the National Institute on Alcohol Abuse and Alcoholism (AA09367 and AA11886), the National Institute on Drug Abuse (DA05147, DA13240, and DA024417), and the National Institute on Mental Health (MH066140). Jaime Derringer was supported by NIH grants DA029377 and MH016880.

STR (Swedish Twin Registry) – The Jan Wallander and Tom Hedelius Foundation, the Ragnar Söderberg Foundation, the Swedish Council for Working Life and Social Research, the Ministry for Higher Education, the Swedish Research Council (M-2005-1112), GenomEUtwin (EU/QLRT-2001-01254; QLG2-CT-2002-01254), NIH DK U01-066134, The Swedish Foundation for Strategic Research (SSF), the Heart and Lung foundation no. 20070481.

TEDS (Twins Early Development Study) – The Twins Early Development Study (TEDS) is supported by a program grant to RP from the UK Medical Research Council [G0901245 and previously G0500079], with additional support from the US National Institutes of Health [HD044454; HD059215]. Genome-wide genotyping was made possible by a grant from the Wellcome Trust to the Wellcome Trust Case Control Consortium 2 project [085475/B/08/Z; 085475/Z/08/Z].

References

1. Rietveld CA et al. (2013) GWAS of 126,559 individuals identifies genetic variants associated with educational attainment. *Science* 340:1467–1471.

2. Davies G et al. (2014) A genome-wide association study implicates the APOE locus in nonpathological cognitive ageing. *Mol Psychiatry* 19:76–87.

3. Harold D et al. (2009) Genome-wide association study identifies variants at CLU and PICALM associated with Alzheimer's disease. *Nat Genet* 41:1088–93.

4. Lambert J-C et al. (2013) Meta-analysis of 74,046 individuals identifies 11 new susceptibility loci for Alzheimer's disease. *Nat Genet* 45:1–9.

5. Schellenberg GD, Montine TJ (2012) The genetics and neuropathology of Alzheimer's disease. *Acta Neuropathol* 124:305–23.

6. Wisdom NM, Callahan JL, Hawkins KA (2011) The effects of apolipoprotein E on non-impaired cognitive functioning: A meta-analysis. *Neurobiol Aging* 32:63–74.

7. Benyamin B et al. (2014) Childhood intelligence is heritable, highly polygenic and associated with FNBP1L. *Mol Psychiatry* 19:253–258.

8. Liu F et al. (2010) The apolipoprotein E gene and its age-specific effects on cognitive function. *Neurobiol Aging* 31:1831–1833.

9. Smith BH et al. (2013) Cohort Profile: Generation Scotland: Scottish Family Health Study (GS:SFHS). The study, its participants and their potential for genetic research on health and illness. *Int J Epidemiol* 42:689–700.

10. Bors DA, Stokes TL (1998) Raven's advanced progressive matrices: Norms for first-year university students and the development of a short form. *Educ Psychol Meas* 58:382–398.

11. Carlstedt B (2000) *Cognitive Abilities: Aspects of Structure, Process and Measurement* (Acta Universitatis Gothoburgensis, Göteborg, Sweden).

12. Wechsler D (1992) *Wechsler intelligence scale for children* (Psychological Corporation, London). 3rd Ed.

13. Raven JC, Court JH, Raven J (1996) *Manual for Raven's Progressive Matrices and Vocabulary Scales* (Oxford University Press).

14. Devlin B, Roeder K (1999) Genomic control for association studies. *Biometrics* 55:997–1004.

15. Willer CJ, Li Y, Abecasis GR (2010) METAL: fast and efficient meta-analysis of genomewide association scans. *Bioinformatics* 26:2190–2191.

16. Ghosh A, Zou F, Wright FA (2008) Estimating odds ratios in genome scans: An approximate conditional likelihood approach. *Am J Hum Genet* 82:1064–1074.

17. Zöllner S, Pritchard JK (2007) Overcoming the winner's curse: Estimating penetrance parameters from case-control data. *Am J Hum Genet* 80:605–615.

18. Xu L, Craiu R V., Sun L (2011) Bayesian methods to overcome the winner's curse in genetic studies. *Ann Appl Stat* 5:201–231.

19. Goddard ME, Wray NR, Verbyla K, Visscher PM (2009) Estimating effects and making predictions from genome-wide marker data. *Stat Sci* 24:517–529.

20. Ioannidis JPA, Ioannidis (2005) Why most published research findings are false. *PLoS Med* 2:e124.

21. Benjamin DJ et al. (2012) The promises and pitfalls of genoeconomics. *Annu Rev Econom* 4:627–662.

22. Purcell S, Cherny SS, Sham PC (2003) Genetic Power Calculator : design of linkage and association genetic mapping studies of complex traits. *Bioinformatics* 19:149–150.

23. Davies G et al. (2011) Genome-wide association studies establish that human intelligence is highly heritable and polygenic. *Mol Psychiatry* 16:996–1005.

24. Chabris CF et al. (2012) Most reported genetic associations with general intelligence are probably false positives. *Psychol Sci* 23:1314–1323.

25. International T, Consortium H (2005) A haplotype map of the human genome. *Nature* 437:1299–320.

26. Casella G, Berger RL (2002) *Statistical Inference* (Duxbury Press, Pacific Grove)2nd editio.

27. Westra H-J et al. (2011) MixupMapper: correcting sample mix-ups in genome-wide datasets increases power to detect small genetic effects. *Bioinformatics* 27:2104–2111.

28. Zhang B et al. (2013) Integrated systems approach identifies genetic nodes and networks in late-onset Alzheimer's disease. *Cell* 153:707–20.

29. Cvejic A et al. (2013) SMIM1 underlies the Vel blood group and influences red blood cell traits. *Nat Genet* 45:542–545.

30. Edgar R (2002) Gene Expression Omnibus: NCBI gene expression and hybridization array data repository. *Nucleic Acids Res* 30:207–210.

31. Croft D et al. (2011) Reactome: a database of reactions, pathways and biological processes. *Nucleic Acids Res* 39:D691–697.

32. Raychaudhuri S et al. (2009) Identifying relationships among genomic disease regions: predicting genes at pathogenic SNP associations and rare deletions. *PLoS Genet* 5:e1000534.

33. Kanehisa M, Goto S, Sato Y, Furumichi M, Tanabe M (2012) KEGG for integration and interpretation of large-scale molecular data sets. *Nucleic Acids Res* 40:D109–14.

34. Bayés A et al. (2011) Characterization of the proteome, diseases and evolution of the human postsynaptic density. *Nat Neurosci* 14:19–21.

35. Liang K-Y, Zeger SL (1986) Longitudinal data analysis using generalized linear models. *Biometrika* 73:13–22.

36. Juster TF, Suzman R (1995) An overview of the Health and Retirement Study. *J Hum Resour* 20:7–56.

37. Purcell SM et al. (2009) Common polygenic variation contributes to risk of schizophrenia and bipolar disorder. *Nature* 460:748–752.

38. Lachman M, Spiro A (2002) Critique of Cognitive Measures in the Health Retirement Study (HRS) and the Asset and Health Dynamics among the Oldest Old (AHEAD) Study. Available at: http://www.researchgate.net/publication/242096659_Critique_of_Cognitive_Measures_in_the_Health_Retirement_Study_(HRS)_and_the_Asset_and_Health_Dynamics_among_the_Oldest_Old_(AHEAD)_Study/file/9c96052869f0bd6f6a.pdf.

39. McCarthy MI et al. (2008) Genome-wide association studies for complex traits: consensus, uncertainty and challenges. *Nat Rev Genet* 9:356–369.

40. Calvin C et al. (2012) Multivariate genetic analyses of cognition and academic achievement from two population samples of 174,000 and 166,000 school children. *Behav Genet* 42:699–710.

41. Deary IJ, Strand S, Smith P, Fernandes C (2007) Intelligence and educational achievement. *Intelligence* 35:13–21.

42. Fraser A et al. (2012) Cohort Profile: The Avon Longitudinal Study of Parents and Children: ALSPAC mothers cohort. *Int J Epidemiol* 42:97–110.

43. Sleegers K et al. (2007) Cerebrovascular risk factors do not contribute to genetic variance of cognitive function: The ERF study. *Neurobiol Aging* 28:735–741.

44. Tiemeier H et al. (2012) The Generation R Study: A review of design, findings to date, and a study of the 5-HTTLPR by environmental interaction from fetal life onward. *J Am Acad Child Adolesc Psychiatry* 51:1119–1135.e7.

45. Kerr SM et al. (2013) Pedigree and genotyping quality analyses of over 10,000 DNA samples from the Generation Scotland: Scottish Family Health Study. *BMC Med Genet* 14:38.

46. Chabris CF et al. (2013) Why is it hard to find genes that are associated with social science traits? Theoretical and empirical considerations. *Am J Public Health* 103:S152–S166.

47. Deary IJ, Whiteman MC, Starr JM, Whalley LJ, Fox HC (2004) The impact of childhood intelligence on later life: Following up the Scottish mental surveys of 1932 and 1947. *J Pers Soc Psychol* 86:130–147.

48. Deary I et al. (2007) The Lothian Birth Cohort 1936: a study to examine influences on cognitive ageing from age 11 to age 70 and beyond. *BMC Geriatr* 7:28.

49. Miller MB et al. (2012) The Minnesota Center for Twin and Family Research Genome-Wide Association Study. *Twin Res Hum Genet* 15:767.

50. Wright MJ, Martin NG (2004) Brisbane Adolescent Twin Study: Outline of study methods and research projects. *Aust J Psychol* 56:65–78.

51. Newnham JP, Evans SF, Michael CA, Stanley FJ, Landau LI (1993) Effects of frequent ultrasound during pregnancy: a randomised controlled trial. *Lancet* 342:887–891.

52. Magnusson PKE et al. (2013) The Swedish Twin Registry: Establishment of a Biobank and Other Recent Developments. *Twin Res Hum Genet* 16:317.

53. Oliver BR, Plomin R (2007) Twins' Early Development Study (TEDS): A Multivariate, Longitudinal Genetic Investigation of Language, Cognition and Behavior Problems from Childhood Through Adolescence. *Twin Res Hum Genet* 10:96–105.